Regulation of the cellular response to elevated temperatures by heat stress transcription factor HsfA7 in *Solanum lycopersicum*

Dissertation

zur Erlangung des Doktorgrades

der Naturwissenschaften

vorgelegt beim

Fachbereich Biowissenschaften (FB 15) der

Johann Wolfgang Goethe-Universität

in Frankfurt am Main

von

Anida Mesihovic

geboren in Ljubuski, Bosnien und Herzegowina

Frankfurt am Main 2018

(D30)

vom Fachbereich 15

der Johann Wolfgang Goethe-Universität als Dissertation angenommen.

Dekan: Prof. Dr. Sven Klimpel

Gutachter: Prof. Dr. Enrico Schleiff, Jun. Prof. Dr. Michaela Müller-McNicoll

Datum der Disputation:

Table of contents

1 Zusammenfassung

Pflanzen sind als sessile Organsimen während ihrer gesamten Lebenszeit fortwährend zahlreichen Umweltveränderungen ausgesetzt. Als eine der global wertvollsten Nutzpflanzen ist die Tomatenpflanze (*Solanum lycopersicum*) besonders stark von Temperaturschwankungen bedroht. Diese Tatsachen machen sich Wissenschaftler zu Nutze indem sie die Tomatenpflanze als Modellorganismus für Studien der Hitzestressantwort benutzen. Bekanntermaßen, besitzen alle Organismen eine gemeinsame molekulare Stressantwort, besser bekannt als Hitzestressantwort, die zumeist mit drastischen Veränderungen in der Genexpression und einer erhöhten Produktion von Hitzeschockproteinen (Hsps) einhergeht. Eine erhöhte Expression von Hsps führt in der Regel, aufgrund ihrer Funktion als Chaperone, zur Wahrung der Proteine vor einer stressbedingten Entfaltung und somit zum Überleben der Zelle. Hsps werden auf Transkriptions-Ebene durch sogenannte Hitzestresstranskriptionsfaktoren (Hsfs) reguliert. In Pflanzen gehören Hsfs einer großen Genfamilie an und bisherige Untersuchungen haben gezeigt, dass sie bemerkenswerte funktionale Diversifizierung besitzen.

In Tomatenpflanzen konnten zum einen anhand des funktionellen Zusammenspiels der drei Hsfs HsfA1a, HsfA2 und HsfB1 und zum anderen durch Wechselwirkungen dieser Hsfs mit Hsps gezeigt werden, dass sie wesentliche Aspekte der Hitzestressantwort regulieren. Als sogenannter Masterregulator der Hitzestressantwort in Tomaten gilt der Transkriptionsfaktor HsfA1a, der für die transkriptionelle Induktion anderer Hsfs und Hsps benötigt wird (Mishra et al., 2002). Die Transkriptionsfaktoren HsfA2 und HsfB1 werden zwar nicht unter physiologischen Bedingungen exprimiert aber bei Hitzestress-Exposition assistieren sie in den transkriptionellen Regulationsmechanismen und erhöhen somit die Genexpression durch funktionelle Interaktionen mit HsfA1a. Die Tomaten Hsf Genfamilie umfasst nichtsdestotrotz 27 Mitglieder unter denen 15 Klasse A Hsfs vorliegen. Überdies, haben phylogenetische Analysen in verschiedenen Pflanzenarten gezeigt, dass HsfA2 die größte Homologie zu HsfA6 und HsfA7 aufweist.

HsfA7 ist in vegetativen Geweben Hitzestress-induziert und das Protein konnte bereits bei schwach-erhöhten Temperaturen (~35C) detektiert werden, während HsfA2 nur unter höherer Hitzestress-Exposition (>40°C) vorliegt. Diese Tatsache weist darauf hin, dass eine Temperatur-abhängige Diversifikation vorliegt, darauf hindeutend, dass HsfA2 und HsfA7 bei Temperaturen um 40°C redundante Funktionen zu haben scheinen, wobei HsfA7 womöglich spezifisch bei einer Temperatur von 35°C agiert. Im Vergleich zu HsfA7 Transkriptleveln, die in der abgeschwächten Phase nach der Stressexposition vermindert vorliegen, akkumuliert das Protein weiterhin, was darauf schließen lässt, dass es Unterschiede in der Regulation der mRNA und Proteinstabilität während der Erholungsphase zu geben scheint. Weiterhin, wird gezeigt, dass HsfA7 bei nachkommenden Hitzestress Behandlungen ähnlich dem der erworbenen Thermotoleranz, stark induziert wird. In diesem Fall, akkumuliert das Protein bei dem nachfolgendem ausdauerndem Stress, welches dann graduell während der Erholungsphase abgebaut wird. Wie auch HsfA2, ist HsfA7 ein langlebiges Protein, dass selbst 24 Stunden nach dem Stress detektiert werden kann, was darauf hindeutet, dass HsfA7 womöglich in der

zellulären Antwort bei wiederholten Hitzestress-Zyklen und der erworbenen Thermotoleranz involviert ist.

Unter den Tomaten Hsfs, zeigt HsfA7 eine bemerkenswert komplexe Genstruktur mit drei Introns in der C-terminalen Region zuzüglich dem konservierten Intron, dass in der DNA-Bindedomäne (DBD) vorliegt. Die prä-mRNA wird Temperatur-abhängig C-Terminal alternativ gespleißt. Dieses führt zu zehn Transkript-Isoformen, die für die drei Protein-Isoformen kodieren: HsfA7-I, HsfA7-II und HsfA7-III. Die HsfA7-II/III kodierenden Transkripte werden durch effizientes Spleißen produziert und sind bei moderat erhöhten Temperaturen zwischen 27.5-37.5°C vorhanden, wie mittels RT-PCR und high-resolution RT-PCR gezeigt wurde. Die Beibehaltung des zweiten Introns und somit die Produktion von HsfA7-I ist graduell erhöht bei Temperaturen höher als 40°C.

HsfA7-I beinhaltet alle annotierten Domänen mitsamt des funktionalen Nuklearen Exportsignals (NES), während HsfA7-II und -III eine verkürzte NES und eine C-terminale Erweiterung aufgrund einer Leserasterverschiebung induziert durch alternativen Spleißens besitzen. HsfA7-II und -III haben die gleiche Aminosäuresequenz mit einer Ausnahme am C-Terminus. Anstelle eines Glyzins in Isoform II, befindet sich ein Aspartat-Serin Dipeptid in Isoform III. Die Lokalisation der Protein-Isoformen wurde anhand eines ektopischen GFP-Tags in Tomaten Mesophyll-Protoplasten unter Benutzung des Konfokalen-Laser-Scanning-Mikroskops (CLSM) untersucht. Aufgrund der Präsenz einer funktionalen NES vermag es HsfA7-I zwischen Nukleus und Cytosol hin und her zu pendeln, während HsfA7-II und HsfA7-III stark im Nukleus zurückgehalten werden, was auf die verkürzte NES zurückzuführen ist.

Bei Hitzestress-Behandlung wird ein Teil des neu synthetisierten HsfA2 in sogenannten Hitzestressgranula (HSGs) gelagert, was die zeitliche Speicherung von HsfA2 erlaubt und außerdem HsfA2 in einer inaktiven Form aufbewahrt (Nover et al., 1989; Scharf et al., 1998). Interaktionen mit cytosolischen Klasse CI und CII sHsps vermitteln die Rekrutierung und die Freilassung der HsfA2 aus den HSGs (Port et al., 2004). Im Gegensatz zu HsfA2, werden weder HsfA7-I noch HsfA7-II zu Hsp17.4-CII enthaltenden HSGs rekrutiert, wie Co-Transformationen von HsfA7 mit GFP-Tag und Hsp17.4-CII mit mCherry-Tag in Protoplasten gezeigt haben. Diese Ergebnisse deuten auf eine unterschiedliche Regulation in der Aktivität und Intrazellulären Verteilung von HsfA2 und HsfA7 hin.

HsfA2 bildet zusammen mit HsfA1a Heterooligomere aus um ein Co-Aktivator-Komplex zu bilden, genannt “Superaktivator-Komplex” (Chan-Schaminet et al., 2009). Der HsfA1a-HsfA2-Komplex aktiviert die Transkription von Downstream gelegenen Genen in einer synergistischen Weise. Unter Benutzung eines β-Glucuronidase (GUS) Reporter-Assays konnten wir zeigen, dass die Co-Transformation der einzelnen HsfA7-Isoformen mit entweder HsfA1a oder HsfA3 in Protoplasten zu synergistischen Aktivierungen verschiedener Hitzestress-induzierter (Hsp und Hsf) Promotoren geführt hat. Eine physikalische Interaktion zwischen HsfA7-I/II und HsfA1a sowie mit HsfA3 konnte mittels eines Bimolecular Fluorescence Complementation (BiFC) Assays nachgewiesen werden. Die putativen Heterooligomere hatten eine bevorzugt nukleare Lokalisation. Hinzukommend, resultierte die Co-Expression von HsfA3 mit den jeweiligen HsfA7-

Isoformen in der Bildung von charakteristischen nuklearen-Speckles. In Anbetracht der Tatsache, dass das Arabidopsis HsfA3 in der Salz- und Trockentoleranz involviert ist (Li 2013, Schramm 2008), können wir behaupten, dass HsfA3-HsfA7 Interaktionen ebenso für andere abiotischen Stressbedingungen zuständig sein könnte als Hitzestress.

Eine Deletion der HsfA7 Aktivierungsdomäne (AHA-Motif) der jeweiligen Isoformen beeinträchtigte zwar die Aktivität konnte sie aber nicht vollständig aufheben, wie ein GFP-Reporter-Assay in Mesophyll-Protoplasten zeigte. Weiterhin hatte die Deletion keinen Effekt über das Co-Aktivator Potenzial von HsfA7 wenn eine Co-Expression mit HsfA1a oder HsfA3 erfolgte. Hinzukommend, wurden Kernlokalisierungssignal (NLS)-Mutanten von HsfA7 generiert, die daraufhin nur noch eine cytosolische Lokalisierung aufwiesen. Interessanterweise, wurde bei Co-Transformationen von HsfA7 NLS-Mutanten mit HsfA1a die Co-Aktivator Funktion von HsfA7 aufgehoben und die transkriptionelle Aktivität entsprach der Aktivität von HsfA1a alleine. Darüber hinaus, wurde bei Co-Expression von HsfA3 mit der NLS-Mutante von HsfA7-I die Aktivität von HsfA3 nahezu vollständig aufgehoben. Wie mittels BiFC gezeigt wurde, kann die NLS-Mutante von HsfA7 mit HsfA1a und HsfA3 im Cytosol interagieren, jedoch konnten diese Hetero-oligomerischen Komplexe nicht in den Nukleus importiert werden, was darauf hinweist, dass eine funktionale NLS in HsfA7 eine Voraussetzung für den nuklearen Import von Hetero-Oligomeren ist.

Proteinabbau durch das Ubiquitin-Proteasom-System spielt eine wichtige Rolle in der Regulation der Transkription (Muratani and Tansey, 2003). Die Expression von HsfA7-I und HsfA7-II vom selben Plasmid-Rückgrat zeigte beim Immunoblotting Unterschiede in der Proteinsignalstärke. Um die Proteinstabilität einzuschätzen, wurden Plasmid-Konstrukte, die für beide Isoformen kodieren in Protoplasten exprimiert und anschließend die Translation durch Zugabe von Cycloheximid (CHX) gestoppt. Die Proteinlevels wurden sechs Stunden lang nach CHX-Behandlung bei 25°C und 39°C mittels Immunoblotting beobachtet. Unter Kontrollbedingungen, hatte HsfA7-II eine schnelle Umsatz-Rate mit einer Halbwertszeit von etwa 1.5 Stunden, während HsfA7-I sechs Stunden nach der Translationsinhibierung stabiler war und nur 20% Verminderung in den Proteinlevels zeigte. Die Hitzestress-Behandlung der Mesophyll-Protoplasten hat zu einer signifikanten Reduktion der Stabilität beider Isoformen geführt. Die schnelle Degradation von HsfA7-II kann das Fehlen eines Signals zu dieser entsprechenden Isoform in den Immunoblot Analysen von vegetativen Geweben behandelt mit verschiedenen Temperaturregimen, erklären.

Wir haben ebenfalls den Protein-Umsatz der NLS-Mutanten von den HsfA7-Isoformen während der sechsstündigen Behandlung mit CHX untersucht. Die NLS-Mutanten wurden während dieser Zeit nahezu keiner Degradation unterzogen, sodass geschlussfolgert werden kann, dass die Degradation von HsfA7 im Nukleus stattfindet. Aus diesem Grund, ist HsfA7-I stabiler als HsfA7-II, da es aufgrund seiner nukleozytoplasmatischen Transfers der Degradation im Nukleus entgehen kann, während HsfA7-II eine schnellere Umsatz-Rate, aufgrund der Nuklearen-Retention besitzt. Verschiedene Studien haben berichtet, dass es eine Korrelation zwischen Degradationsrate und Aktivierungsdomänen-Potential in Proteinen mit transkriptioneller Aktivität gibt (Molinari et al., 1999; Thuerauf et al., 2002; Sundqvist and Ericsson, 2003). Jedoch

hat eine Deletion des AHA-Motifs in HsfA7-I und HsfA7-II die Proteinstabilität nicht signifikant beeinflusst.

Zusätzlich, zeigen wir in MG132-behandelte Tomaten Zellkulturen, dass die Degradation von HsfA7, HsfA2 und HsfA1a durch das Ubiquitin-Proteasom-System vermittelt wird. HsfA1a akkumulierte signifikant unter Kontroll- und erhöhten Temperaturbehandlungen in MG132-behandelten Zellen und ist wie einst angenommen kein stabiles Protein, dennoch hat es einen sehr effizienten Protein-Umsatz. Überraschenderweise, konnten in der Zellkultur die HsfA7-II/III Proteine nachgewiesen werden, und dabei zeigen, dass dieses Protein im endogenen System produziert wird.

Um zu testen, ob die HsfA7-Stabilität durch Interaktionspartner beeinflusst wird, wurden konstante Mengen von Plasmiden, die für HsfA7-Isoformen kodieren mit gesteigerten Mengen von Plasmiden, die für HsfA1a und HsfA3 in Tomaten Protoplasten co-exprimiert. Beide Isoformen zeigen erhöhte Proteinlevels wenn sie mit HsfA1a oder HsfA3 titriert wurden, wobei der Effekt für HsfA7-II markanter war. Mittels RT-PCRs konnten wir ausschließen, dass der Effekt von Hitzestress und Co-Aktivator Co-Expression mit Veränderungen in den RNA-Levels verbunden ist.

Auf der anderen Seite, wenn wir konstante Mengen von HsfA1a oder HsfA3 mit steigenden Mengen der Plasmide kodierend für HsfA7-I oder HsfA7-II in Tomaten Protoplasten co-exprimiert haben, stimmten die steigenden Mengen von HsfA7 mit der graduellen Verringerung der Proteinlevels von HsfA1a und HsfA3 überein. Dieser Effekt wurde nicht beobachtet, als die NLS-Mutante von HsfA7 mit HsfA1a co-exprimiert wurde, anstatt mit dem Wildtyp-Protein. Aus diesem Grund, schließen wir daraus, dass die HsfA7-vermittelte erhöhte Degradation von HsfA1a einen nuklearen Co-Import der zwei Hsfs benötigt. Im Gegensatz, führt die Co-Expression von HsfA2 mit HsfA1a zur Stabilisierung des HsfA1a Protein. Weitere Experimente sind notwendig um zu analysieren wie die erhöhte Degradation oder Stabilisierung von HsfA1a durch HsfA7 oder HsfA2 reguliert wird.

In Anbetracht der Tatsache, dass HsfA2 und HsfA7 unter spezifischen Temperaturregimen co-existieren, führten wir ein “Konkurrenz-Assay” basierend auf der Aktivität von Hsfs in einem GUS-Reporter unter Benutzung der Co-Expression von HsfA2, der NLS Mutante von HsfA7-I und HsfA1a. Dabei zeigte sich, dass HsfA2 und HsfA7 um die Interaktion mit dem Masterregulator HsfA1a konkurrieren können um dabei gleichzeitig die Transkription von Hitzestress-induzierten Genen und den Protein-Umsatz von HsfA1a zu regulieren.

Um die Funktion von HsfA7 zu studieren wurden CRISPR/Cas9 knock-out (KO) Mutanten, sowie für den direkten Vergleich HsfA2 KO Mutanten, generiert. Die HsfA7 und HsfA2 KO Linien hatten keine phänotypischen Wachstumsveränderungen bei normalen Gewächshaus-Konditionen im Vergleich zu Wildtyp Pflanzen. Immunoblotting der Hitzegestressten Blattgeweben von Wildtyp und Mutanten-Linien bestätigten, dass HsfA7 die Protein-Abundanz des Masterregulators negativ beeinflusst. Hinzukommend, wurden *APX3*, *Hsa32*, *Hsp101* und *Hsp17.7A-CI* Transkripte in den HsfA7-KO Linien bei 35°C in höheren Levels exprimiert, was zeigt dass die Akkumulation von HsfA7 in einer schwächeren Induktion der Hitzestress-induzierten Gene resultiert. Durch

eine Komplementation der HsfA7 KO Tomaten Mesophyll Protoplasten mit den HsfA7-Isoformen unter Kontrolle des endogenen Promotors konnten wir bestätigen, dass die Induktion von *APX3* und *Hsa32* als Resultat des Fehlens von HsfA7 vorlag, welches durch die ektopische Expression von HsfA7 umgekehrt werden kann.

Keimlinge mit einem HsfA7 KO Hintergrund zeigten eine gesteigerte Thermotoleranz im Vergleich zu Wildtyp oder HsfA2 KO-Keimlingen, wie quantitative Hypokotyl-Elongationsraten unter verlängertem mildem Stress Behandlungen (35°C) zeigten. Die milde Behandlung bei 35°C wurde ausgewählt, da es eine moderat erhöhte Temperatur ist, die spezifisch für die Induktion von HsfA7 aber nicht HsfA2 ist. Andererseits, zeigten HsfA2-Keimlinge eine ähnliche Wachstumsrate wie der Wildtyp während dieses Temperaturregims. Die Tatsache, dass Keimlinge, die HsfA7 nicht produzieren eine verbesserte Leistung haben im Vergleich zum Wildtyp ist wahrscheinlich mit der Stabilisierung von HsfA1a verbunden.

Die Abundanz des endogenen HsfA2 und HsfA7 ist in einer Temperatur-abhängigen Weise reguliert. Daher ist es wahrscheinlich, dass bei graduell-erhöhten Temperaturen oder sogar mildem Hitzestress, HsfA7 überwiegend synthetisiert wird und als Co-Aktivator agiert und gleichzeitig die Abundanz von HsfA1a reguliert (und HsfA3 unter entsprechenden Bedingungen) indem es dessen Umsatzrate erhöht. Dadurch aktiviert die Zelle keine starke Hitzestressantwort und gewährleistet damit eine mittelmäßige Aktivität von HsfA1a. Wenn die Temperatur weiter steigt wird HsfA2 produziert, welches um die Interaktion mit HsfA1a konkurriert, den Masterregulator stabilisiert, eine stärkere Hitzestressantwort stimuliert und somit das Überleben und die Homöostase der Zelle sichert.

Wir schlagen hiermit ein neues regulatorisches Mechanismus vor, welches das Schicksal und die Aktivität von HsfA1a in einer Temperatur-abhängigen Weise durch zwei Interaktionspartner kontrolliert.

2 Abstract

Heat stress transcription factors (Hsfs) are required for transcriptional changes during heat stress (HS) thereby playing a crucial role in the heat stress response (HSR). The target genes of Hsfs include heat shock proteins (Hsps), other Hsfs and genes involved in protection of the cell from irreversible damages due to exposure to elevated temperatures. Among 27 Hsfs in *Solanum lycopersicum*, HsfA1a, HsfA2 and HsfB1 constitute a functional triad which regulates important aspects of the HSR. HsfA1a is constitutively expressed and described as the master regulator of stress response and thermotolerance. Activation of HsfA1a under elevated temperatures leads to the induction of HsfA2 and HsfB1 which further stimulate the transcription of HS-responsive genes by forming highly active complexes with HsfA1a. Despite the well-established role of these three Hsfs in tomato HSR, information about functional relevance of other Hsfs is currently missing.

The heat stress inducible HsfA7 belongs alongside with HsfA2 to a phylogenetically distinct clade. Thereby the two proteins share high homology and a functional redundancy has been assumed. However, HsfA7 function and contribution to stress responses have not been investigated into detail in any plant species.

Tomato HsfA7 protein accumulates already at moderately elevated temperatures (~35°C) while HsfA2 becomes dominant at higher temperatures (>40°C). HsfA7 pre-mRNA undergoes complex and temperature-dependent alternative splicing resulting in several transcripts that encode for three protein isoforms. HsfA7-I contains a functional nuclear export signal (NES) and shows nucleocytoplasmic shuttling while HsfA7-II and HsfA7-III have a truncated NES which leads to the strong nuclear retention of the protein. Differences in the nucleocytoplasmic equilibrium have a major impact on the stability of protein isoforms, as nuclear retention is associated with increased protein turnover. Consequently, HsfA7-I shows a higher stability and can be detected even after 24 hours of stress attenuation, while HsfA7-II is rapidly degraded. The degradation of these factors is mediated by the ubiquitin-proteasome pathway.

HsfA7 can physically interact with HsfA1a and HsfA3 and form co-activator (“superactivator”) complexes with a very high transcriptional activity as shown on different HS-inducible promoters. In order for the complex to be successfully transferred to the nucleus and confer its activity it needs a functional nuclear localization signal (NLS) of HsfA7. In contrast, the activator (AHA) motif of HsfA7 is not essential for its co-activator function. Interestingly, while interaction of HsfA7 with either HsfA3 or HsfA1a stabilizes HsfA7 isoforms, concomitantly this leads to an increased turnover of HsfA1a and HsfA3. In contrast, HsfA2 has a stabilizing effect on the master regulator HsfA1a.

Thus, HsfA7 knockout mutants generated by CRISPR/Cas9 gene editing, show increased HsfA1a levels and a stronger induction of HS-related genes at 35°C compared to wild-type plants and HsfA2 knockout mutants. Consequently, HsfA7 knockout seedlings exhibit increased thermotolerance as shown by the enhanced hypocotyl elongation under a prolonged mild stress treatment at 35°C.

In summary, these results highlight the importance of HsfA7 in regulation of cellular responses at elevated temperatures. Under moderately elevated temperatures, the accumulation of HsfA7 and its subsequent interaction with HsfA1a, leads to increased turnover of the latter, thereby ensuring a milder transcriptional activation of temperature-responsive genes like Hsps. In turn, in response to further elevated temperatures, HsfA2 becomes the dominant stress-induced Hsf. HsfA2 forms co-activator complexes with HsfA1a which in contrast to HsfA7, allows the stabilization of the master regulator, leading to the stronger expression of HS-responsive genes required for survival. Thereby, this study uncovers a new regulatory mechanism, where the temperature-dependent competitive interaction of HsfA2 and HsfA7 with HsfA1a control the fate of the master regulator and consequently the activity of temperature-responsive networks.

3 Abbreviations

aa	Amino acid
AF	Chlorophyll autofluorescence
AHA	Aromatic, hydrophobic, acidic (activator motif)
APX	Ascorbate peroxidase
AS	Alternative splicing
ATT	Acquired thermotolerance
BF	Bright field
BiFC	Bimolecular fluorescence complementation
BTT	Basal thermotolerance
CaMV	Cauliflower mosaic virus
Cas9	CRISPR-associated protein-9 nuclease
CHX	Cycloheximide
CLSM	Confocal laser scanning microscopy
CRISPR	Clustered regularly interspaced short palindromic repeats
CS	Co-supression
CTAD	Carboxyl-terminal activation domain
kDa	Kilo Dalton
DBD	DNA binding domain
DNA	Deoxyribonucleic acid
cDNA	Complementary DNA
DREB	Dehydration-responsive element binding protein
ES	Exon skipping
GFP	Green fluorescent protein
GUS	β-Glucuronidase
HAC1	Histone acetyltransferase of the CBP family 1
HA-tag	Hemagglutinin-tag
HR RT-PCR	High-resolution RT-PCR
HS	Heat stress
HSE	Heat stress element
Hsf	Heat stress transcription factor
HSG	Heat stress granule
Hsp	Heat shock protein
sHsp	Small heat shock protein
HSR	Heat stress response
IPCC	Intergovernmental panel on climate change
IR	Intron retention
KO	Knockout
LmB	Leptomycin B
Mc	Monoclonal
MAPK	Mitogen-activated protein kinase
MU	4-methylumbelliferone
MUG	4-methylumbelliferone β-glucuronide
NES	Nuclear export signal
mNES	Mutated nuclear export signal
NLS	Nuclear localization sequence
mNLS	Mutated nuclear localization sequence
NMD	Non-sense mediated decay
nptII	neomycin phosphotransferase II
OD *E.coli*	Optical density
OD Hsf	Oligomerization domain
OE	Overexpression
OEP7	Outer envelope membrane protein (7 kDa)
OL	Overlay
ORF	Open reading frame
PAGE	Polyacrilamide gel electrophoresis
PAM	Protospacer-adjacent motif
Pc	Polyclonal
PCD	Programmed cell death
PTC	Premature termination codon
QK	Quadruple knockout
qRT-PCR	Quantitative real-time PCR
RD	Repressor domain
RFU	Relative fluorescence unit
RNA	Ribonucleic acid
RNAi	RNA interference
mRNA	Messenger RNA
pre-mRNA	Precursor mRNA
sgRNA	Single guiding RNA
ROF	Rotamase FKBP
RT-PCR	Reverse transcription-PCR
RuBisCO	Ribulose-1,5-bisphosphate carboxylase/oxygenase
SD	Standard deviation
SDS	Sodium dodecyl sulfate
SE	Standard error
T-DNA	Transfer DNA
UTR	Untranslated region
WT	Wild type
YFP	Yellow fluorescent protein

4 Introduction

4.1 Climate change and food security

Plants are sensitive to environmental fluctuations and particularly to temperature changes beyond the limits of optimum for growth and development. Consequently, in the era of climate change and global warming, research on understanding the responses of plants to elevated temperatures is one of the top priorities for the scientific community. In this respect, ensuring high crop yield under more adverse conditions is one of the greatest challenges of this century (Mesihovic et al., 2016). Under all assessed emission scenarios the surface temperature is projected to rise over the 21st century (IPCC, 2014). Climate change is having immense impacts on all natural systems. The changes include, among others, severe precipitation events, floods, a decrease in low temperature extremes, an increase in high temperature extremes and heat waves (days in which the temperature is higher than the climatic normal by 5°C) which will increase in intensity, frequency and duration (IPCC, 2014). All these will have severe and in some cases irreversible impacts on people, society at large and ecosystems and therefore it is important to find efficient solutions to adapt to the ongoing environmental changes (IPCC, 2014; Lobell, 2014). Global temperature increases of ~4°C or more combined with increasing food demand will pose large risks to food security, both globally and regionally (Meehl et al., 2007; Karl, 2009; IPCC, 2014).

Many studies have shown negative effects of temperature extremes on crop yield (Hatfield et al., 2011; Lobell et al., 2011; Hatfield and Prueger, 2015). During the 21st century, increased temperatures are likely to cause yield losses between 2.5 and 10% across various agronomically important plants (Hatfield et al., 2011). In order to assess the impact of future climate changes on agricultural productivity and natural systems in general it is important to understand the plant response and underlying molecular regulatory mechanisms (Gray and Brady, 2016). Recent population projections of the United Nations showed that the population will not stop growing during this century and the world population (now 7.6 billion) will most likely increase to 9.6-12.3 billion in 2100 (Gerland et al., 2014). It is obvious that food security requires improved crop varieties with higher yield potential and better performance under less favourable conditions. In order to do so, traditional breeding techniques as well as modern biotechnological approaches need to be utilized (Khush, 2001).

4.1.1 Physiological responses to elevated temperatures

Each plant species has a defined range of maximum and minimum temperatures within which growth occurs and an optimum temperature at which growth progresses at its fastest rate (Hatfield et al., 2011). Elevated temperatures lead to adverse alterations in plant growth, development and yield. The first developmental stage to be affected is the seed germination capacity where heat can cause reduced germination, or inhibit seedling growth (Hasanuzzaman et al., 2013). Heat can lead to reduction of the size of a whole plant, leaf damage, senescence and abscission, which ultimately diminishes biomass. It can also cause fruit discoloration and abscission and shorten the grain filling period (Wahid et al., 2007; Hasanuzzaman et al., 2013).

Furthermore, increased temperatures can negatively affect chloroplast structures, the amount of photosynthetic pigments, activity of photosystem II and stomatal closure (Sharkey, 2005; Chen et al., 2012).

Elevated temperatures have different impacts on different organs, tissues and cell types and, accordingly, the response to stress varies among tissues and developmental stages (Gray and Brady, 2016). The plant productivity can be affected when temperatures fall below or rise above specific thresholds at critical times during development (Hatfield and Prueger, 2015). Vegetative development usually has a higher optimum temperature than the reproductive which occurs during a narrow window of plant development and is dependent on the particular species (Zinn et al., 2010; Hedhly, 2011; Hatfield and Prueger, 2015). Reproductive development has been described as the most thermosensitive particularly due to the vulnerability of the male gametophyte which can result in low pollen viability and germination capacity, and consequently fertilization, grain and fruit setting and production (Peet et al., 1998; Zinn et al., 2010; Mesihovic et al., 2016).

Pollen development starts with the formation of pollen mother cells and differentiation of anther tissues (tapetum and stomium) (McCormick, 2004; Honys et al., 2006; Borg et al., 2009). Diploid pollen mother cells undergo microsporogenesis or meiotic cell division which results in formation of haploid microspores (tetrads). Tetrads are released into unicellular microspores which enlarge during microgametogenesis and subsequently the microspore undergoes two mitotic cell divisions to form two gametes embedded in the vegetative pollen. Although male gametophytes are susceptible to increased temperatures across their whole developmental cycle, the meiotic stage has been characterized as the most sensitive (Ahmed et al., 1992; Peet et al., 1998; Prasad et al., 2000; Sato et al., 2002; Fragkostefanakis et al., 2016). Although the mechanistic details of this phenomenon remain to be elucidated, exposure to a short period of highly increased temperature or chronic exposure to mild elevated temperatures can affect pollen fitness. In general, the decrease in pollen viability and/or germination capacity is followed by a significant decrease in fruit set (Iwahori 1966; Abdul-baki, 1992; Sato et al., 2000). Although the basic features of temperature responses are common between the reproductive and vegetative tissues, it is very likely that qualitative and quantitative discrepancies contribute to their thermotolerance capacity (Frank et al., 2009; Fragkostefanakis et al., 2016).

4.2 The plant heat stress response

Since plants are bound to one place for their lifetime and continuously exposed to changing environmental conditions they need to activate complex processes which will help them to survive and cope with environmental cues including abiotic stresses (Mittler et al., 2012). Heat stress (HS) can cause metabolic imbalance by affecting the stability of proteins, membranes, RNA species and cytoskeleton structures, and by altering the efficiency of enzymatic reactions (Richter et al., 2010; Mittler et al., 2012). All this can lead to a disturbance in important cellular processes like RNA processing and translation. Many cellular and morphological effects of heat

are related to an imbalance in protein homeostasis including *de novo* protein synthesis, folding, intracellular targeting, function and degradation (Richter et al., 2010; Scharf et al., 2012).

In most cases plants are simultaneously exposed to various stresses, like for example heat and drought which are likely to occur at the same time (Rizhsky, 2002). Since cellular processes are tightly regulated most stresses are also accompanied with accumulation of reactive oxygen species (ROS) which can damage chlorophyll, protein, DNA, lipids and other molecules, having detrimental effects on cellular metabolism (Bokszczanin, 2013).

As a consequence of damage accumulation, plants can activate programmed cell death (PCD) in specific cells or tissues, a process that can lead to the shedding of leaves, flower and fruit abortion, or even death of the entire plant (Qu et al., 2009; Blanvillain et al., 2011). Alternatively, in response to heat, plants modify their metabolism in order to prevent damages to ensure acclimation (Mittler et al., 2012). The heat stress response (HSR) is a highly conserved mechanism among all living organisms leading to reprogramming of gene expression to adapt and protect homeostasis in response to elevated temperatures (Fragkostefanakis et al., 2015a).

4.2.1 How plants sense elevated temperatures

Plants are believed to sense heat through different pathways. High temperatures can lead to an increase of membrane fluidity, which in turn leads to opening of calcium channels and trigger influx of calcium in the cell that can regulate different signalling pathways (Murata and Los, 1997; Saidi et al., 2009; Saidi et al., 2010). This leads to the activation of transcriptional activators and repressors and induction of a HSR. For example, there are indications that Ca^{2+}-dependent activation of a mitogen-activated protein kinase (MAPK) is a component of the heat signalling pathway, likely involved in the activation of heat stress transcription factors (Hsfs) (Saidi et al., 2009). Imbalances in metabolic activities caused by HS lead to accumulation of toxic by-products, like ROS, which can also mediate the stress signal by activating downstream pathways via MBF1c, certain Hsfs or MAPKs and by opening additional calcium channels at the plasma membrane (Mittler et al., 2004). Some studies suggest that a decrease in histone occupancy induced by heat might also function as a mean of temperature sensing (Erkina et al., 2008; Kumar and Wigge, 2010). For example, H2A.Z could regulate gene expression by affecting DNA accessibility and wrapping DNA more tightly. Nucleosomes containing the alternative histone H2A.Z are essential for correctly perceiving elevated temperatures and H2A.Z nucleosome occupancy has been shown to decrease with increasing temperature which indicates the existence of a temperature sensing mechanism through DNA-nucleosome fluctuations (Kumar and Wigge, 2010). In addition, conditions which lead to accumulation of unfolded proteins can activate the unfolded protein response (UPR) in the endoplasmic reticulum (ER) and the cytosolic protein response (CPR) in the cytosol (Sugio et al., 2009; Walter and Ron, 2011). A consequence of the ER UPR is the proteolytic cleavage and release of bZIP transcription factors from the ER membrane (Moreno and Orellana, 2011). These can then translocate to the nucleus and activate transcription of genes encoding for ER chaperones. The CPR, on the other hand, is regulated by Hsfs (Sugio et al., 2009).

Similar subsets of genes are activated by the different sensors, but the relation between the different sensing pathways and their exact hierarchical order are unknown (Mittler et al., 2012). This is the established view of how each cell independently represents a sensory unit with its own system of stress sensing. When exposed to heat, cells in culture, unicellular organisms, and cells in a multicellular organism can all trigger a heat shock response autonomously (Åkerfelt et al., 2010). However, it has been proposed that multicellular organisms sense stress differently to isolated cells and it is important to acknowledge that there are most probably several levels of regulation in multicellular organisms. Metazoans, for example, utilize communication between tissues to transfer signals from cells proximal to proteotoxic stress conditions to prime distal cells against the upcoming adverse conditions (van Oosten-Hawle et al., 2013; Kawasaki et al., 2016). If and how the signals are integrated and transferred between different tissues and organs in the whole plant organism remains elusive.

4.2.2 The cellular heat stress response

The HSR has been defined as a response to elevated temperatures which disturb metabolic and structural integrity of the cell and thereby impair protein homeostasis (Bokszczanin, 2013). This in turn leads to cellular reprogramming on transcriptome, proteome and metabolome level to ensure stress adaptation, recovery and survival (Bita and Gerats, 2013). Although the HSR is characterized by a rapid and transient transcription program, the expression kinetics of individual HS-inducible genes are diverse (Richter et al., 2010). While early responding genes correspond to processes needed to rapidly counteract heat consequences, genes induced at later stages are more important for adaptation and recovery from stress (Richter et al., 2010). In addition to HS induced transcription there are other levels of regulation during and after HS exposure which include pre-mRNA splicing, mRNA localization and stability, translational control and post-translational modifications (Gidalevitz et al., 2011). To further support and enhance the protection, a selective repression of genes involved in various metabolic processes is initiated (Yángüez et al., 2013; Kantidze et al., 2015). Nevertheless, the most strikingly upregulated genes in response to high temperatures across all species are heat shock proteins (Hsps). They act as molecular chaperones, co-chaperones, prevent protein misfolding and aggregation, and assist in protein translocation and degradation to ensure protein homeostasis. This includes members of the HSP100, HSP90, HSP70, HSP60 and the small HSP (sHSP) gene families (Vierling, 1991; Wang et al., 2004).

4.2.3 Heat shock proteins

Chaperones are constantly needed for *de novo* protein folding and refolding of non-native polypeptides and thereby many genes encoding for proteins with chaperone activity are constitutively expressed in the cell (Gragerov et al., 1991). All chaperones except sHsps can bind and hydrolyze ATP which controls the affinity of the chaperone for its substrate (Waters et al., 1996; Richter et al., 2010). Hsp70 is stimulated by its co-chaperone DnaJ/Hsp40 to hydrolyse ATP, which is the key step that closes its substrate-binding cavity and thus allows stable binding of substrate proteins (Laufen et al., 1999).

Protein folding and maintenance under physiological conditions is mainly mediated by the constitutively expressed Hsp70, Hsp90 and Hsp60 chaperone family, while some members of the Hsp70 and Hsp90 family are upregulated in response to different environmental stresses to increase the chaperone capacity of the cell (Krishna and Gloor, 2001; Sung, 2001). The Hsp60 protein family is not directly involved in the HSR, however, they are essential for folding of newly synthesized and translocated proteins in the cytosol, mitochondria and chloroplasts (Hemmingsen et al., 1988; Gutsche et al., 1999; Wang et al., 2004). For example, chaperones play an important role in the import and assembly of ribulose-1,5-bisphosphate carboxylase/oxygenase (Rubisco) into chloroplasts as well as in assembly of proteins imported into the mitochondrial matrix into oligomeric complexes (Cheng et al., 1989; Lubben et al., 1989).

Hsp100/Clp chaperones are often constitutively expressed in plants, but their expression is developmentally regulated and is induced by different environmental stresses (Wang et al., 2004). Hsp100/Clps work together with the the Hsp70/DnaJ system on protein disaggregation and clearance of potentially harmful peptides (Agarwal et al., 2001; Seyffer et al., 2012). A recent study showed that *A.thalina* HSP101 is required for the efficient release of mRNAs encoding for ribosomal proteins from stress granules, which is important for rapid restoration of the translation machinery upon stress attenuation (Merret et al., 2017).

The sHsps efficiently bind non-native proteins to keep them in a folding competent state and represent a first line of defence which is supported by their rapid accumulation upon stress exposure. The vast majority of sHsps are dramatically induced at transcript level during HS or other stresses while some are expressed under non-stress conditions in specific developmental stages, such as in developing pollen (Waters et al., 1996; Giorno et al., 2010; Chaturvedi et al., 2013). Interaction with sHsps keeps denatured proteins from irreversible aggregation under stressful conditions in all cellular compartments (Waters et al., 1996; Kotak et al., 2007a; Basha et al., 2012). Their common feature is the conserved α-crystalline domain and most sHsps form oligomers which is required for chaperone activity (Giese and Vierling, 2002). Through interactions with ATP-dependent chaperones like Hsp70 and Hsp100 they can assist protein refolding (Mogk et al., 2003; Nakamoto and Vígh, 2007; Eyles and Gierasch, 2010). Class CI and CII sHsps have both been found to associate with specific translation factors in cytosolic stress granules of *A. thaliana* seedlings (McLoughlin et al., 2016). The function of sHsp was related to the protection of these factors during HS and enhancement of their recovery to the soluble cell fraction after HS, which was also dependent on Hsp101.

Many studies in various species have demonstrated that overexpression of Hsps can lead to increased HS tolerance. For example, overexpression of Hsp70 in many organisms correlated with enhanced thermotolerance, but also defective growth or other phenotypic alterations, suggesting the importance of a tight regulation of this protein in the cellular context (Feder et al., 1996; Nollen et al., 1999; Sung and Guy, 2003). On the other hand, overexpression of the HS inducible Hsp101 conferred an improved tolerance to heat treatments in *Arabidopsis thaliana*, tobacco and rice (*Oryza sativa*) without causing growth alterations, while suppression of Hsp101 in *A. thaliana* led to a decrease in the ability of the plant to acquire thermotolerance (Queitsch,

2000; Katiyar-Agarwal S, Agarwal M, 2003; Chang et al., 2007). Furthermore, a positive feedback loop between Hsp101 and HEAT STRESS-ASSOCIATED 32-KD PROTEIN (Hsa32) at the post-transcriptional level has been found to prolong the effect of heat acclimation in rice and *A. thaliana* seedlings (Wu et al., 2013; Lin et al., 2014) and to play an important role in basal thermotolerance of rice seeds (Lin et al., 2014). Ectopic overexpression of sHsps from different species has also been shown to enhance thermotolerance in Arabidopsis, while some studies could demonstrate that increased protein levels of certain sHsps could lead to enhanced salt and drought tolerance (Sun et al., 2001; Rhoads et al., 2005; Sato and Yokoya, 2008; Jiang et al., 2009; Zhou et al., 2012). Interestingly, the chloroplast localized sHsp in tomato and tobacco was shown to be involved in protection of photosystem II under stress conditions (Neta-Sharir, 2005; Guo et al., 2007).

4.2.4 Other proteins induced by heat stress

Other genes upregulated in response to increased temperatures at transcript level are related to various processes like calcium, phytohormone, sugar and lipid signaling and metabolism, protein phosphorylation, RNA metabolism, translation, primary and secondary metabolisms and transcription regulation (Mittler et al., 2012). Furthermore, proteomic studies have shown that ubiquitins, dehydrins, late embryogenesis abundant (LEA) proteins and oxidative stress related proteins like thioredoxin, glutathione S-transferase and dehydroascorbate reductase are often detected during stress response, as well as ASCORBATE PEROXIDASE (APX) 2 and 3 (Ortiz and Cardemil, 2001; Ferreira et al., 2006; Schramm et al., 2006; Lee et al., 2007; Wahid and Close, 2007; Fragkostefanakis et al., 2016). These proteins might play a role in protein degradation, protection of cellular components from oxidative damage and dehydration. Enzymes involved in the tri-carboxylic-acid (TCA) cycle and the pentose phosphate pathway were also up-regulated in response to HS which could lead to the enhancement of the energy capacity of the cell (Lee et al., 2007). Levels of proteins responsible for starch degradation and synthesis like β-amylase and glucose-1-phosphate adenyltransferase were differentially regulated at elevated temperature conditions (Majoul et al., 2003). Because HS can greatly influence photosynthesis rate, function of plastids can also be affected (Camejo et al., 2006; Zhang et al., 2008). Different studies have shown that the elongation factor EF-Tu which exhibits increased expression upon HS, has a potential chaperone function and protects stromal proteins from aggregation (Bhadula et al., 2001; Ristic et al., 2004).

All these findings demonstrate that in addition to increased Hsp synthesis, cells try to adjust their metabolic pathways by increasing or suppressing expression of specific proteins, and thereby amplifying the potential and ability of the cell to minimize damages induced by unfavourable conditions and survive.

4.3 Thermotolerance and stress memory

Like all other organisms plants can survive increased temperatures to a certain extent. The ability of plants to successfully respond to an episode of HS exposure is referred to as basal

thermorolerance (BTT). On the other hand, acquired thermotolerance (ATT) is accomplished if plants are exposed to elevated but non-lethal temperatures prior to a severe stress which would be lethal in the absence of the preconditioning heat treatment (Larkindale and Vierling, 2007; Bokszczanin, 2013). The reason for this is that the exposure to a mild priming treatment leads to the accumulation of transcription factors, molecular chaperones and signalling molecules together with sustained alterations of metabolites and a readjustment of the overall metabolic state (Mittler et al., 2012; Pick et al., 2012). Experimentally, ATT can be induced by either exposing plants to a moderate HS followed by a recovery for a few hours or a gradual increase in temperature which is followed by exposure to a second, severe HS (Larkindale and Vierling, 2007; Mesihovic et al., 2016). How plants react to these conditions is evaluated by measuring the growth rate, survival rate, or expression levels of HS-genes which are known to be markers of the HSR. Interestingly, while some genes are only involved in BTT like MBF1c and the ROS catalase, other genes including specific Hsfs and Hsp101 are important for both responses. Instead, Hsa32 and HsfA2 mutants of *A. thaliana* were compromised only if a long recovery period (>24h) was applied after the priming stress treatment (Queitsch, 2000; Charng, 2006; Suzuki et al., 2008; Vanderauwera et al., 2011).

In the recent years, chromatin modifications, nucleosome positioning and DNA methylation have been recognized as an important part of HS adaptation (Crisp et al., 2016; Lämke and Bäurle, 2017). In order to survive repeated stresses, priming stress cue is directly followed by a period of stress memory which can last a few days or a few weeks and allow the plant to respond faster and stronger to subsequent environmental challenges. HS memory is associated with hyper-induction of gene expression upon HS recurrence which is related to the accumulation of histone H3 lysine 4 di- and trimethylation at memory-related loci (Lamke et al., 2016). In *A. thaliana*, HsfA2 binds to these loci transiently and is required for the transcriptional memory, but not the initial HSR (Lamke et al., 2016). FORGETTER1 (FGT1) associates with promoter regions of actively expressed genes in *A. thaliana*, thereby modulating nucleosome occupancy and mediating stress-induced chromatin memory (Brzezinka et al., 2016). However, a key regulatory step governing whether memories are formed or forgotten and reset is the period of stress recovery (Crisp et al., 2016).

Additionally, there is some evidence that priming can persist between generations which is referred to as transgenerational memory (Boyko and Kovalchuk, 2011; Crisp et al., 2016; Lämke and Bäurle, 2017). A possible mechanistic basis of such stress memory could be alterations of chromatin states, DNA methylation or a paused RNA polymerase II (Pol II) (Mirouze and Paszkowski, 2011; Avramova, 2015).

4.4 Heat stress transcription factors

There are many signalling pathways and transcription factors that regulate the response to elevated temperatures and contribute to survival under HS. Hsfs are among the most important regulators of transcriptional reprogramming under increased temperatures. They are at the end of the signal transduction pathways activated in response to heat and are crucial for mediating

the transcriptional induction of HS inducible genes (Nover et al., 1996; Kotak et al., 2007a; Scharf et al., 2012). These include mainly Hsps but also genes implicated in various processes like protection of structural components jeopardized by the accumulation of detrimental molecules (e.g. ROS) (Driedonks et al., 2015).

4.4.1 Domain composition

Hsfs have a modular structure similar to other proteins involved in regulating transcription and the domain composition of Hsfs is conserved throughout the eukaryotic kingdom (Kotak et al., 2007a; Scharf et al., 2012). The basic domain composition of five tomato Hsfs is represented in Figure 1. The DNA binding domain (DBD) is located at the N-terminus of all Hsfs. Structural analyses have shown that it is composed of three α-helixes (H1, H2 and H3) and a four stranded antiparallel β-sheet (Harrison et al., 1994; Neudegger et al., 2016). The helix-turn-helix motif formed by H2 and H3 is important for precise and selective interaction with DNA. The promoter motifs recognized by Hsfs are called heat stress elements (HSEs). These are defined as repetitive patterns of palindromic motifs 5'AGAAnnTTCT3' which are located upstream of the TATA box. The G and C nucleotides are essential for HSEs to be functional and usually more than two HSE motifs are required for efficient Hsf binding (Santoro et al., 1998; Guo et al., 2008). However, there are other elements affecting the recognition and binding of Hsfs to HSEs like histone modifications and overall chromatin structure (Guertin and Lis, 2010).

The oligomerization domain (OD) is located C-terminal of the DBD, separated from it by a flexible linker, and is composed of a heptad pattern of hydrophobic amino acid residues (HR-A/B) which leads to the formation of a coiled-coil domain involved in protein interactions (Peteranderl et al., 1999). Hsfs are divided into three evolutionary conserved classes (A, B and C) based on the length of the linker inserted between the HR-A and B region. While class A Hsfs have an insertion of additional 21 and class C Hsfs of additional 7 amino acids, class B Hsfs have a compact OD with insertion of 6 residues similar to all non-plant Hsfs (Nover et al., 1996; Scharf et al., 2012).

The nuclear localization signal (NLS) is formed by monopartite or bipartite clusters of basic amino acid residues while the nuclear export signal (NES) is mostly leucine-rich and located at the C-terminus of many Hsfs. If both, NLS and NES are present, the factor is dynamically shuttling between nucleus and cytosol (Scharf et al., 1998). The nucleocytoplasmic equilibrium is dependent on the strength of NLS and NES but possibly on other factors as well, including conformational changes, post-translational modifications or interactions with other proteins (Heerklotz et al., 2001; Kotak et al., 2004).

The C-terminal activation domains (CTADs) of most class A Hsfs harbour one or two so-called AHA motifs consisting of aromatic, large hydrophobic and acidic amino acid residues. Only in HsfA3 the activation domain is comprised of a characteristic pattern of tryptophane residues while HsfA8 lacks an AHA motif and is therefore inactive (Bharti et al., 2000; Döring et al., 2000; Kotak et al., 2004). The characteristic feature of class B Hsfs is the -LFGV- repressor motif

(Czarnecka-Verner et al., 2004; Ikeda and Ohme-Takagi, 2009). Class C Hsfs do not possess an activation or repressor domain and their function remains unclear (Scharf et al., 2012).

Plants possess multiple Hsf-encoding genes. The Arabidopsis genome encodes for 21, rice 25, tomato 27, and soybean 52 Hsfs (Scharf et al., 2012). In addition, most Hsf-types are present in monocots and eudicots. The current understanding of the molecular mechanisms underlying Hsf function is mostly based on analyses of tomato and *A. thaliana* Hsfs. However, our knowledge about the spatio-temporal expression and activity of various Hsfs is still limited.

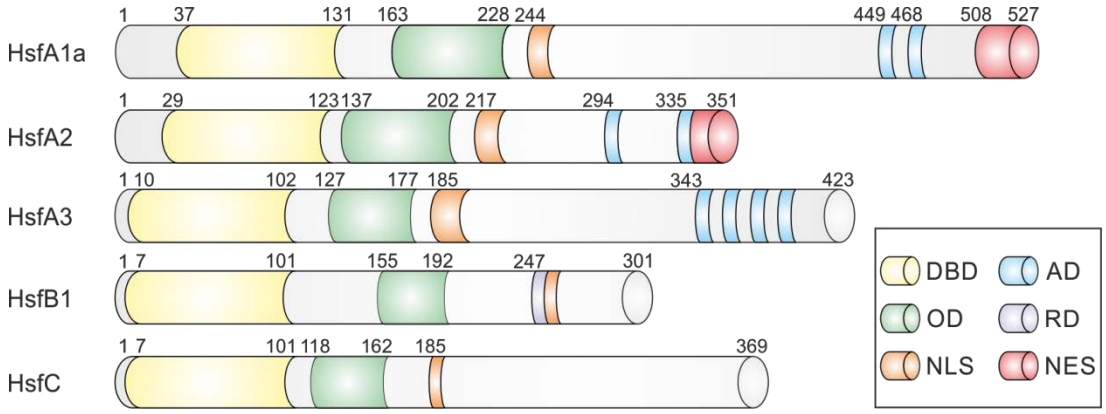

Figure 1. Hsf domain composition.
An overview of the domain composition of tomato HsfA1a, A2, A3, B1 and HsfC. DBD, DNA binding domain; OD, oligomerization domain (HR-A/B); NLS, nuclear localization signal; AD, activation domain (AHA motif); RD, repressor domain (R/KLFGV motif); NES, nuclear export signal. The domain overview of HsfA1a, A2, B1 and C1 was adapted from Scharf et al. (2012) while for HsfA3 the domain composition represents the M86 protein form which was most abundant in tomato according to Bharti et al. (2000).

4.4.2 Hsf involvement in temperature and other abiotic stresses

4.4.2.1 HsfA1 is the master regulator of heat stress response

Class A Hsfs have been characterized as main transcriptional activators which are responsible for induction of HS genes including other Hsfs. In tomato, among four HsfA1 genes, HsfA1a was defined as the master regulator of thermotolerance (Mishra et al., 2002). This was shown in experiments using transgenic plants exhibiting a co-suppression of HsfA1a expression (*A1CS*) which had drastically reduced thermotolerance when exposed to elevated temperatures even though the overall plant growth and development were not impaired under control conditions (Mishra et al., 2002). The reason behind this is that the HS-induced expression of HsfA2, HsfB1 and chaperones was almost completely diminished due to HsfA1a suppression. In contrast to this finding, *A. thaliana* does not have a single master regulator but all four of the class A Hsfs contribute to thermotolerance and HS-responsive gene expression (Liu et al., 2011; Yoshida et al., 2011). Furthermore, the *hsfa1a/b/d/e* quadruple knockout (KO) mutant plants were not only showing an impaired HSR, but also defects in growth and development suggesting that beyond the well-established role in HSR, the basal activity of some Hsfs is important for physiological processes. However, the *hsfa1a/b/d* triple KO mutants did not have developmental defects and

exhibited a severe thermosensitive phenotype even at a mild HS exposure of 27°C (Yoshida et al., 2011; Liu and Charng, 2013). The reason for this peculiarity in single and shared master regulator function between tomato and *A. thaliana* might be explained by the fact that the RNAi effect in the tomato co-suppression plants might have targeted all the HsfA1s (Scharf et al., 2012). However, this needs further investigation.

4.4.2.2 HsfA2 is important for acquired thermotolerance

Although HsfA2 is structurally similar to HsfA1a it is only induced in response to HS and belongs to the most prominent Hsfs in tomato, *A. thaliana* and rice. It accumulates at high levels in plants exposed to prolonged heat and recovery conditions after HS exposure (Scharf et al., 1998; Charng et al., 2006; Nishizawa et al., 2006; Schramm et al., 2008). Interestingly, ectopic expression of HsfA2 could complement the defects of the *hsfa1a/b/d/e* quadruple KO mutant regarding tolerance to different HS regimes and to hydrogen peroxide even though HS-genes were showing differential regulation by these factors (Liu and Charng, 2013). Analysis of tomato plants with suppressed HsfA2 levels revealed that HsfA2 is involved in the regulation of Hsp expression in a tissue-specific manner. Young seedlings of HsfA2 knock-down plants were not sensitive to a single heat exposure (BTT), however, HsfA2 was necessary for young seedlings to acquire thermotolerance (Fragkostefanakis et al., 2016). Interestingly, pollen viability and germination rate upon HS exposure were also significantly affected by HsfA2 suppression because HsfA2 is essential for the high expression of Hsps during pollen development (Fragkostefanakis et al., 2016).

Similarly, *A. thaliana* HsfA2 was important for extension of ATT, as shown by a hypocotyl elongation assay (Charng et al., 2006). This was related to a reduction of transcript levels of highly heat-inducible genes and lower protein levels of Hsa32 and class CI sHsps in the mutant compared to wild-type plants. Interestingly, both *A. thaliana* and tomato HsfA2 were shown to be important for the regulation of other stress-related genes like APX members, GALACTINOL SYNTHASE 1 (GOLS1), Hsa32 and MBF1c (Charng et al., 2006; Nishizawa et al., 2006; Schramm et al., 2006; Nishizawa-Yokoi et al., 2009; Fragkostefanakis et al., 2015b). These findings suggest involvement of HsfA2 in regulating stress related genes beyond Hsps. Furthermore, *A. thaliana* HsfA2 KO plants were sensitive to light and oxidative stress and anoxia, whereas HsfA2 overexpression plants had an increased thermotolerance and resistance to other stresses like salinity, oxidative stress and anoxia (Nishizawa et al., 2006; Ogawa et al., 2007; Zhang et al., 2009).

4.4.2.3 HsfA6 and HsfA7 members

According to the evolutionary relationship of Hsfs from nine plant species obtained by alignment of the N-proximal parts containing the DBD and OD region of 250 Hsfs, HsfA2/A6/A7 have the highest amino acid sequence similarity and the closest phylogenetic relationship (Nover et al., 2001; Scharf et al., 2012). Several studies extensively studied the role HsfA2 in transgenic plants; however, limited studies are available which investigate the importance of HsfA6 and HsfA7.

In tomato, it was shown that transcript abundance of HsfA6b and HsfA7 were enhanced more strongly in heat stressed anthers of HsfA2 knock-down plants compared to wild-type plants (Fragkostefanakis et al., 2016). This indicates the existence of a feedback regulatory mechanism between HsfA2, HsfA6b and HsfA7. A similar increase in expression upon loss of HsfA2 was not observed in leaves, indicating that such mechanisms might be tissue or even cell specific (Fragkostefanakis et al., 2016). According to transcriptome studies HsfA7 was shown to be one of the most significantly upregulated Hsfs upon a HS treatment (Busch et al., 2005; Charng et al., 2006; Cortijo et al., 2017) and it was proposed to play an important role in the cytosolic protein response (CPR) (Sugio et al., 2009). An *A. thaliana* HsfA7a KO mutant had a decreased viability upon a gradual acclimation temperature treatment and an ATT treatment (Larkindale and Vierling, 2007). This indicates that it is one of the Hsfs which contribute to heat acclimation in *A thaliana*. However, even though a close phylogenetic relationship exists, the loss of HsfA2 could not be compensated by the presence of HsfA7a/A7b in *A. thaliana* (Charng et al., 2006). Furthermore, the HsfA7 KO lines did not show a drastic thermotolerance defect comparable to the loss of HsfA2 (Charng et al., 2006). This points out, that although similarities exist, these Hsfs may not have simply redundant functions (Nover et al., 2001). Overexpression of the rice HsfA7 (*Os*HsfA7) in *A. thaliana* plants resulted in increased expression of GolS2 and some Hsps like Hsp101 upon HS exposure. The transgenic plants also had an improved thermotolerance upon a harsh temperature treatment (Liu et al., 2009). Furthermore, when *Os*HsfA7 was overexpressed in the rice background this resulted in increased drought and salinity stress resistance (Liu et al., 2013a).

A. thaliana HsfA6b was recently shown to act as a downstream regulator of the ABA-mediated stress response and participate in ABA-mediated salt and drought resistance while thermotolerance tests showed that HsfA6b is required for thermotolerance acquisition (Huang et al., 2016). This suggests that ABA-signalling plays an important role in the complexity of the HSR. Overexpression of HsfA6f in wheat resulted in improved thermotolerance by the stronger upregulation of several Hsps, as well as previously unknown Hsf target genes such as Golgi-antiapoptotic protein (GAAP) and the large isoform of Rubisco activase (Xue et al., 2015).

4.4.2.4 Other Hsf members

A. thaliana HsfA3 is induced in response to drought and heat and this is directly transcriptionally regulated by DEHYDRATION-RESPONSIVE ELEMENT BINDING PROTEIN (DREB2A) which is a transcription factor mediating expression of genes mainly involved in drought stress (Sakuma, 2006; Schramm et al., 2008). Overexpression of DREB2A can lead to induction of HsfA3 expression and other HS-inducible genes and an increased thermotolerance, while DREB2A KO mutants had a reduced thermotolerance (Sakuma, 2006).

HsfA4a was shown to play a key role in ROS sensing (Davletova, 2005). *A. thaliana* plants expressing a dominant negative mutant of HsfA4a had an impaired response to oxidative (H_2O_2) stress (Davletova, 2005).

HsfB1 and HsfB2b were not found to be directly involved in the regulation of the onset of the HSR (Kumar et al., 2009). However, in *hsfB1*/*hsfB2b* double KO plants Pdf genes were identified

as the major targets of an Hsf-dependent negative regulation. These genes are involved in immunity against infection by necrotrophic microorganisms, which implicates the interplay of Hsfs in the regulation of biotic stress responses (Kumar et al., 2009). On the other hand, Ikeda et al. (2011) showed that HsfB1 and HsfB2b suppress the HSR under non-stress conditions as shown by reduction of HsfA2, HsfA7a and HsfB2b transcript levels under control conditions and in the attenuation period (Ikeda et al., 2011). In addition, HsfB1 and HsfB2b were also important for the establishment of ATT in *Arabidopsis thaliana* (Ikeda et al., 2011).

Taken together, all these findings highlight the involvement of Hsfs in stress signalling cascades other than the ones activated in response to heat and there is a remarkable functional specificity of the different Hsfs participating in a certain abiotic stress response. It is also important to emphasize that knockouts of Hsfs are required in order to study and evaluate their involvement in regulation of HS-gene expression. Many studies mentioned above have shown that, when analysed in detail, a remarkable functional diversification can be found. However, there are not always obvious phenotypes, most probably due to functional redundancy among Hsfs (Scharf et al., 2012).

4.4.3 Hsfs are involved in developmental processes

Although the activity of many Hsfs has been related to HSR, in several cases Hsf mutants show phenotypic alterations related to specific developmental processes. HsfA9 has been identified as a specialized Hsf having a unique role during development, but not environmental stresses. It is exclusively expressed during seed maturation and is involved in embryogenesis and seed maturation in *A. thaliana* and sunflower (*Helianthus annuus*) (Diaz-Martin, 2005; Kotak et al., 2007b). HsfA9 cooperates with other transcription factors like ABSCISIC ACID-INSENSITIVE 3 (ABI3) in Arabidopsis and DREB2 in sunflower (Almoguera et al., 2002; Kotak et al., 2007b). In developing seeds of *A. thaliana* the expression of HsfA9 is regulated by ABI3 (Kotak et al., 2007b). Overexpression of sunflower HsfA9 alone or together with DREB2 enhanced the accumulation of Hsps and improved seed longevity in tobacco seeds (Prieto-Dapena et al., 2006; Almoguera et al., 2009). Furthermore, HsfA9 has been proposed as a molecular link between auxin responses and sHsp expression in seeds (Carranco et al., 2010). Another study suggested a link between seed maturation and early photomorphogenesis mediated by HsfA9 since overexpression of HsfA9 in tobacco accelerated the initial photosynthetic development of seedlings (Prieto-Dapena et al., 2017). Since HsfA9 is not present in monocots, it is still unknown whether another Hsf has a similar function in embryogenesis (Scharf et al., 2012).

It has been speculated that mature and germinating tomato pollen do not have a proper HSR and therefore cannot synthesize Hsps at adequate amounts, but rather utilize the Hsps produced in younger pollen (Duck and Folk, 1994). In a recent study the proteome of different developmental stages of tomato pollen was analysed and earlier developmental stages corresponding to pollen mother cells and tetrads were found to have higher levels of several Hsps and other stress related proteins compared to more advanced stages (Chaturvedi et al., 2013). This was referred to as “developmental priming” and indicated that the cells are prepared for a fast response against a potential upcoming stress. An alternative explanation

would be that molecular chaperones are induced to prevent proteins from misfolding (due to the increasing flux of nascent proteins) and remain in the cells during and after cellular divisions. Another study has shown that HsfA2 and Hsp17-CII are expressed during anther development under control conditions and further induced under short and prolonged HS conditions (Giorno et al., 2010). In addition, a stress tolerant cultivar had higher basal expression levels of HsfA2 and several Hsps in non-stressed microspores compared to a heat sensitive cultivar (Frank et al., 2009). Fragkostefanakis et al. (2016) demonstrated by analysing transgenic tomato HsfA2 knock-down plants that HsfA2 is directly involved in the developmental regulation of several HS-related genes in early stages of pollen development under control conditions. Other genes, like Hsp101, Hsp90-3, Hsp70-9 and MBF1c were not affected by HsfA2 suppression. In addition, HsfA1a was required for the expression of all analysed Hsps, showing a wider role of the master regulator functions which is not only restricted to stress response, but also to developmental programs. Furthermore, the same study showed that anthers from non-stressed plants released a lower number of pollen grains. This was attributed to the fact that several cell wall-modifying proteins were significantly downregulated by HsfA2 suppression (Fragkostefanakis et al., 2016).

Che et al. (2002) reported that expression of the HsfA2 gene increases during the process of callus formation and growth. In another study, HsfA2 has been shown to be involved in cell proliferation since HsfA2 overexpression plants had accelerated callus growth in root explants in comparison to the wild type (Che, 2006; Ogawa et al., 2007). No obvious difference in callus growth was observed between the wild-type and HsfA2 dominant negative mutant line, so the authors concluded that other class A Hsfs may be involved in callus formation and growth from root explants. In contrast to this, transient overexpression of *A. thaliana* HsfB1 and HsfB2b in tobacco leaves induced cell death, which means that their tight regulation is needed for normal growth and development as high levels of these factors can lead to defects resulting in cell death (Zhu et al., 2012).

*Os*HsfA7 overexpressing transgenic rice seedlings showed a different root morphology compared to wild-type rice. The *Os*HsfA7 overexpression seedlings exhibited longer young roots, including primary and adventitious roots, but shorter and less lateral roots and root hair (Liu et al., 2013a). This indicates that rice HsfA7 might have an important function in root growth and development.

These findings further strengthen the specific functions of different Hsfs which are not only restricted to stress conditions but also developmental cues. In some cases the tight regulation of Hsf levels is playing an important role for normal cell proliferation and cell survival. Unravelling the transcriptional regulation of Hsfs and thereby Hsp expression in tomato pollen and anther development is surely an important step in understanding and improving pollen thermotolerance and fruit set. The possible involvement of other Hsfs as potential transcriptional regulators in other developmental processes remains elusive.

4.4.4 The functional triad of HsfA1a, HsfA2, HsfB1 in tomato

In tomato, HsfA1a, HsfB1 and HsfA2 have been described as the central Hsf triad, forming a regulatory network which is crucial for the fine regulation of transcription in response to elevated temperatures. The major findings used to describe the current model on HSR regulation in tomato, are based on analyses of transgenic plants as well as on observations from transient expression assays in mesophyll protoplasts (Mishra et al., 2002; Chan-Schaminet et al., 2009; Hahn et al., 2011; Fragkostefanakis et al., 2016).

HsfA1a is a constitutively expressed Hsf and it is maintained inactive at physiological conditions by interaction with high molecular weight chaperones (Hahn et al., 2011). It is responsible for the transcriptional regulation of HsfA2 and HsfB1 under HS conditions and is the master regulator of HSR in tomato (Mishra et al., 2002). Based on its protein abundance under HS conditions, HsfA2 has been described as the major Hsf in stressed cells (Scharf et al., 1998; Schramm et al., 2006). In tomato, this is also related to the fact that HsfA2 heterooligomerizes with HsfA1a to form a co-activator complex referred to as “superactivator” complex (Chan-Schaminet et al., 2009). The HsfA1a-HsfA2 complex activates the transcription of downstream genes in a synergistic manner.

Due to efficient nuclear export, HsfA2 is mostly found in the cytosol when expressed alone (Lyck et al., 1997; Scharf et al., 1998). Deletion of the NES (eight C-terminal amino acid residues) results in a nuclear localization of the protein and subsequently to a higher activator potential (Lyck et al., 1997; Heerklotz et al., 2001). The C-terminal domain of HsfA2 has been discussed to be a putative HR-C region responsible for intra-molecular shielding of the NLS, which is probably mediated through interaction with the HR-A/B (Heerklotz et al., 2001). This effect is common for mammalian HSFs where it is related to suppression of spontaneous HSF trimerization (Rabindran et al., 1993). However, up to now, such a mode of regulation has not been proven for plant Hsfs. When HsfA2 is either co-expressed with HsfA1a or the cells are exposed to HS the balance of HsfA2 intracellular distribution is shifted towards the nucleus (Scharf et al., 1998; Heerklotz et al., 2001). This points to a heterooligomerization with HsfA1a which was confirmed using co-immunoprecipitation and crosslinking assays (Scharf et al., 1998; Chan-Schaminet et al., 2009). The HsfA1a-assisted nuclear import of HsfA2 depends on a direct physical interaction between the two proteins and therefore, the “superactivator complex” formation can be partially attributed to the effect of HsfA1a efficiently retaining HsfA2 in the nucleus which makes it a HS-induced enhancer of thermotolerance (Scharf et al., 1998). The accumulation and high protein stability of HsfA2 upon HS exposure is connected to its reversible recruitment to heat stress granules (HSGs). These have been described as 40-nm-diameter ribonucleoprotein (RNP) aggregates in the cytoplasm which serve as a storage of denatured proteins and are detectable in all plant tissues with sufficiently high levels of sHsps (Nover et al., 1983; Nover et al., 1989; Scharf et al., 1998). In summary, HsfA2 is part of and interacting with a network of proteins including HsfA1a and sHsps which influence its activity and intracellular distribution (Baniwal et al., 2004).

Since class B Hsfs lack the activator motifs and have a repressor motif they have been mostly shown to be involved in the attenuation of stress response and repression of class A Hsf activity

(Bharti, 2004; Ikeda et al., 2011). However, tomato HsfB1 acts as a co-activator of HsfA1a (Bharti, 2004; Hahn et al., 2011). The two Hsfs form an enhanceosome-like complex which recruits histone acetyl transferase (HAC1), a plant orthologue of the CREB binding protein (CBP). If the promoter has an appropriate architecture binding of the complex can achieve a synergistic activation of the reporter expression (Bharti, 2004).

The interplay of the functional triad (HsfA1a, HsfA2, and HsfB1) and Hsps in tomato is thought to regulate important aspects of the HSR which are summarized in Figure 2.

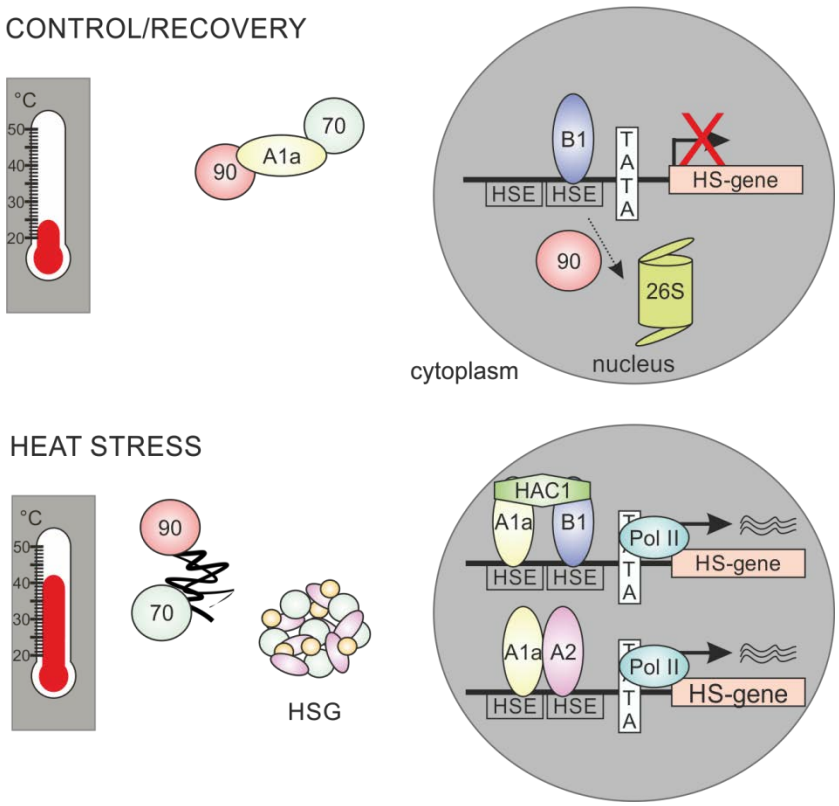

Figure 2. The functional triad of HsfA1a, HsfA2 and HsfB1 and their interplay with chaperones.
At control conditions the constitutively expressed HsfA1a (A1a) is kept inactive by interactions with Hsp70 (70) and Hsp90 (90) chaperones. Protein levels of HsfB1 (B1) are kept low by degradation, which involves Hsp90. Upon HS exposure, chaperones are recruited to unfolded proteins. HsfA1a and HsfB1 recruit histone acetyl transferase HAC1 and immediately cooperate to activate transcription of downstream HS-related genes. Long-term HS leads to an accumulation of high levels of chaperones and HsfA2 (A2). HsfA2 forms hetero-oligomeric "superactivator" complexes with HsfA1a which additionally boost HS-gene transcription. In addition, part of the newly synthesized chaperones (Hsp70 and Hsp17-CI in orange) and HsfA2 are assembled into high molecular weight protein aggregates called heat stress granules (HSGs). In the attenuation or recovery phase, the transcription of HS-genes is abolished. HsfA1a interacts with chaperones, while HsfB1 is targeted for degradation by the nuclear ubiquitin proteasome system in an Hsp90-dependent manner. The model was adapted from Hahn et al. (2011) and details about regulation of HsfB1 degradation from Röth et al. (2017).

4.5 Regulation of plant Hsf activity

Hsf activity can be regulated at the transcriptional, post-transcriptional and post-translational levels and all these processes together ultimately regulate the abundance and functionality of

RNA and proteins. The involvement in HSR and developmental networks requires tight regulation of Hsf activity prior, during and after stress occurs which is essential to ensure proper development before, survival during and recovery after stress. In addition to transcriptional and post-transcriptional regulation, Hsfs have been shown to interact with Hsps and other proteins which can additionally influence Hsf oligomerization capacity, transcriptional activation activity and stability. Even though there are many insights in the different layers of regulation of metazoan Hsfs, still there are a limited number of studies available on regulation of plant Hsfs.

4.5.1 Alternative splicing

In the recent years it has become clear that in addition to transcriptional regulation alternative splicing (AS) is an important process leading to a dynamic regulation and increased complexity of the transcriptome and proteome (Reddy et al., 2013). Furthermore, since AS mostly occurs co-transcriptionally it is dependent on chromatin structure and modifications in addition to RNA structure and splicing regulators (Braunschweig et al., 2013). AS occurs due to alternate 5´-donor and/or 3´-acceptor splice site selection by the spliceosome which can lead to the production of two or more mature mRNAs. The four main modes of AS are described as intron retention (IR), exon skipping (ES), alternative acceptor (AA) and alternative donor (AD) site splicing (Reddy, 2007). In contrast to metazoans where the predominant mode of AS is exon skipping (ES), in Arabidopsis and other plants intron retention (IR) is the most frequently occurring AS event (reviewed in Reddy et al., 2013). A consequence of AS can either be the generation of protein isoforms with similar, different or opposing properties, or a change in the transcript stability, transport, localization or translation efficiency (Reddy et al., 2013). Omics studies of AS in various tissues in response to different stresses have shown that AS is also differentially regulated among the different cell types, which provides the plant the ability to cope with stressors and adapt to the environmental changes (Kazan, 2003; Staiger and Brown, 2013; Filichkin et al., 2015).

A. thaliana HsfA2 pre-mRNA is alternatively spliced (Sugio et al., 2009; Liu et al., 2013b). At 37°C a 31 bp mini-exon from within the conserved intron in the DBD is retained in the transcript of *HsfA2-II* which leads to formation of a premature termination codon (PTC). Consequently, *HsfA2-II* RNA is targeted for nonsense-mediated decay (NMD) (Sugio et al., 2009). In this direction AS of HsfA2 in *A. thaliana* serves as a mechanism for post-transcriptional regulation of functional HsfA2 levels. A 42°C stress can activate a cryptic 5' splice site in the HsfA2 intron which leads to generation of an *HsfA2-III* transcript in addition to *HsfA2-II* (Liu et al., 2013b). It encodes for a truncated HsfA2 protein isoform which has a leucine-rich motif at the C-terminus and the ability to bind to HSEs in the HsfA2 promoter thereby activating its own transcription (Liu et al., 2013b). This splicing event is regulated by the splicing factor SF1 which mediates the HSR by contributing to differential production of *HsfA2-I* and *HsfA2-III*. However, a further increase in temperature (45°C) leads to a change in ratio of the two isoforms and only *HsfA2-III* can be detected. The same study showed that a HS-induced retention of intron 1 occurs in *A. thaliana* HsfA4c, HsfA7b, HsfB1 and HsfB2a. A splicing event and regulation of transcript abundance by NMD was also observed in *Medicago sativa* Hsf1 (He et al., 2008).

At specific temperatures, the conserved intron 1 in *Solanum lycopersicum* HsfA2 is alternatively spliced which leads to inclusion of a mini-exon into mature transcripts which were shown to be targeted for NMD (Hu, PhD thesis). However, in contrast to *A. thaliana*, tomato HsfA2 contains a second intron in the 3' end of the gene. AS of this intron leads to production of several *HsfA2* transcript isoforms encoding for two functional proteins, namely HsfA2-I and HsfA2-II which have different properties (Hu, PhD thesis). HsfA2-I is a stable protein involved in long-term responses and ATT, while HsfA2-II is short-lived and supports HsfA1a in the stimulation of target genes in the onset of the response.

Temperature-dependent AS has been shown to be involved in the regulation of expression and activity of other stress-inducible transcription factors like DREB2B and bZIP28 (Matsukura et al., 2010; Liu et al., 2013b). Recently, U5-snRNP-interacting protein STABILIZED1 (STA1) has been shown to play a role in pre-mRNA splicing of a wide range of HS-inducible genes including HsfA3 and Hsa32 in *A.thaliana* (Kim et al., 2017). In addition, the circadian clock network responds to temperature transitions which is linked to AS and small changes of 4°C in ambient or non-stressful temperatures can have significant effects on AS events (James et al., 2012; Streitner et al., 2013).

4.5.2 Post-translational modifications

Unlike in the case of human HSFs which have been shown to be regulated by basal and hyperphosphorylation, acetylation and sumoylation (Xu et al., 2012) there is not much known about post-translational modifications in plant Hsfs. A few heat activated MAPKs have been identified in plants (Sinha et al., 2011). Application of HS led to a rapid and transient activation of a MAPK in tomato and tobacco cells in a calcium-dependent manner (Link et al., 2002; Suri and Dhindsa, 2008). Furthermore, the tomato MAPK was able to specifically phosphorylate HsfA3 while inhibition of the heat-activated MAPK in tobacco cells led to inhibition of heat-induced accumulation of Hsp70 (Link et al., 2002; Suri and Dhindsa, 2008). In *A. thaliana*, there is evidence that activation of MAPK6 results in specific phosphorylation of HsfA2 which in turn affects its intracellular localization and protein stability (Evrard et al., 2013). *A.thaliana* HsfA1d has also been proposed to be activated by tyrosine phosphorylation (Ohama et al., 2015). In addition, Cohen-Peer et al. (2010) have shown that HsfA2 is SUMOylated by SUMO1 during the recovery period after HS exposure, and subsequently, the modified HsfA2 form remains in an inactive state in the nucleus of *A. thaliana*. After a second exposure to HS, HsfA2 is deSUMOylated and regains its activity.

4.5.3 Hsf-Hsp interactions

There are some similarities in the molecular mechanisms of Hsf activation in plant and mammalian cells. For example, under normal conditions HsfA1 is kept inactive in complex with Hsp90/Hsp70 chaperones. Upon HS and activation of the CPR the chaperones are recruited to protect proteins from denaturation while HsfA1 is released and activated (Kim and Schöffl, 2002; Yamada et al., 2007; Meiri et al., 2009; Meiri and Breiman, 2009; Hahn et al., 2011). In *A. thaliana* HsfA1d a temperature-dependent repression (TDR) domain was identified and found to

be a negative regulatory domain repressing its activity through interaction with Hsp 70 and Hsp90 (Ohama et al., 2015). Hsp70 dissociates from HsfA1d in response to HS, however, the mechanistic details of this event are unknown.

Hsp90 facilitates DNA binding of HsfB1 and its degradation (Hahn et al., 2011) In addition, inhibition of Hsp90 function led to accumulation and stabilization of HsfA2 transcripts, which resulted in accumulation of HsfA2 protein (Hahn et al., 2011). *A.thaliana* HsfA2 activity is regulated by interaction with Hsp90 and its specific co-chaperones ROF1 and ROF2, which are peptidyl prolyl isomerases belonging to the class of immunophilins (Aviezer-Hagai et al., 2007). *At*HsfA2 interacts with HSP90.1 and is responsible for translocation of the ROF1–HSP90.1–HsfA2 complex to the nucleus which enables the cell continuous sHsp expression during the recovery period, while it is proposed that ROF2 is involved in negative feedback regulation of HsfA2 (Meiri et al., 2009; Meiri and Breiman, 2009). Furthermore, as described above, tomato HsfA2 was found to co-localize in HSGs together with Hsp17-CII and is released from these structures upon repeated cycles of HS or recovery conditions which is possibly mediated by class CI sHsps and Hsp101/Hsp70 chaperones (Scharf et al., 1998; Port et al., 2004). In this way HsfA2 activity, solubility and intracellular localization is controlled by interaction with sHsps (Port et al., 2004; Tripp et al., 2009). In *A. thaliana,* Hsp101 has also been shown to restore solubility of aggregated sHsps after HS (Lee et al., 2005).

4.5.4 Protein turnover

The ubiquitin-proteasome-mediated proteolysis is an essential pathway responsible for the degradation of most intracellular proteins. Degradation of a protein by this system involves two steps: covalent attachment of multiple ubiquitin molecules to the target and degradation of the tagged protein by the 26S proteasome (Ciechanover, 1998). Many transcription factors are needed at specific time points during development or as a response to environmental stimuli. Upon decay of the signal, these factors need to be efficiently cleared from the cell which is crucial for efficient regulation of gene expression and protecting cellular homeostasis (Kodadek et al., 2006). Therefore, it has been proposed that there is a direct link between activator potential, ubiquitination and proteasome activity. In some cases, activity of transcription factors is tightly coupled to their proteolytic destruction, thereby allowing transcriptional activation only by ongoing synthesis of the activator (reviewed in Muratani and Tansey, 2003). In some cases the ubiquitin-proteasome-dependent degradation of a transcription factor is needed for full activity (Kodadek et al., 2006). For example, the transcription coactivator NPR1 in *A. thaliana* is constantly degraded in the nuclei by the ubiquitin-proteasome system to suppress plant immune responses in the absence of pathogen challenge (Spoel et al., 2009). Additionally, turnover of the phosphorylated NPR1 is required for efficient induction of target genes (Spoel et al., 2009). Interestingly, in many unstable transcription factors there is an overlap between the transcriptional activation domain and the degradation signal (degron) sequence (Muratani and Tansey, 2003).

In tomato, it has been proposed that Hsf degradation is mediated by the ubiquitin-proteasome pathway (Hahn et al., 2011). Recently, Röth et al. (2017) were able to show that the turnover of

*Sl*HsfB1 is dependent on its function as a transcriptional repressor. Addition of the repressor motif to a truncated HsfA2 protein placed the hybrid protein under the same regulatory regime.

Studies have shown that the rate of degradation of transcriptional activators correlates with their activation domain potency. Mutations in the DNA-binding or activation domain which abolish the DNA binding or transactivation function increased the protein half-life and made the protein resistant to degradation by the proteasome (Molinari et al., 1999; Thuerauf et al., 2002; Sundqvist and Ericsson, 2003). In case of a transcription factor carrying the VP16 transcriptional activation domain it was proposed that ubiquitination regulates the function of transcriptional activator domains by serving as a dual signal for activation and destruction (Salghetti, 2001). So far, it has not been investigated whether class A Hsfs undergo a similar regulatory mechanism for clearance. Whether the transcriptional activator function is a prerequisite for proteolysis of class A Hsfs remains unknown. Studying the involvement of ubiquitination and the proteasome in the process of transcription is important since these mechanisms are enabling the cells to rapidly respond and adapt to environmental changes by tightly controlling the levels of gene expression (Kodadek et al., 2006).

4.6 The metazoan Hsf system

In contrast to the multiplicity of Hsfs in plants, other organisms have fewer Hsfs. The *Saccharomyces cerevisiae* genome contains only a single HSF which is not only important for the HSR but also required for survival at normal growth temperatures since HSF1 depletion is lethal (Wiederrecht et al., 1988). Interestingly, tomato HsfA1 and HsfA2 can functionally replace the *S.cerevisiae* HSF1 (Boscheinen et al., 1997). On the other hand, in *C. elegans* and *Drosophila melanogaster* deletion of the HSF leads to developmental defects since most HSF binding sites are not contained in HS genes, but in genes encoding for processes related to development and reproduction (Jedlicka et al., 1997; Li et al., 2016).

HSF1 is the master regulator and together with HSF2 it mediates the stress induced transcriptional activation of mammalian genes. Metazoan HSF1 targets the transcriptional activation of genes encoding for proteins like molecular chaperones and components of the protein degradation machinery which are crucial for protection against proteotoxicity (Pirkkala et al., 2001; Åkerfelt et al., 2010; Li et al., 2017). Furthermore, HSF1 directs transcriptional programs in development and metabolism, PCD, carcinogenesis and the meiotic cell cycle which are different from the classical HSR and can influence cellular functions in aging and disease. In this respect, HSF1 regulates subsets of genes different to the ones of acute HS (Jedlicka et al., 1997; Le Masson et al., 2011). Although the alternative transcriptional programs regulated by HSF1 share common features, including expression of a small set of chaperones and metabolic regulators there are other, condition-specific targets. A recent study reported that HSF1 is involved in Poly (ADP-ribose) polymerase 1 (PARP1) redistribution, protecting cells from DNA damage by promoting DNA repair, and mammary tumorigenesis (Fujimoto et al., 2017). At the organismal level, HSF1 is subjected to cell non-autonomous regulation by neuronal, insulin/GF-1, germline stem cell and transcellular chaperone signalling (Li et al., 2017). HSF1 is also

differentially regulated in response to cellular NAD^+/NADH, AMP/ATP and amino acid levels which makes the HSR dependent on protein biogenesis and energy availability (Li et al., 2017). HSF1 and HSF2 have essential functions in oogenesis and spermatogenesis, while HSF3 and HSF4 have more specialized functions in stress response and development (Fujimoto et al., 2004; Akerfelt et al., 2008).

HSF1 is regulated by protein-protein interactions and post-translational modifications. Upon stress exposure chaperones dissociate from HSF1 allowing it to form DNA binding-competent trimers that can translocate to the nucleus which is promoted or inhibited by protein kinases (Shi et al., 1998; Holmberg, 2001). HSF1 DNA-binding ability can be impaired by acetylation which leads to attenuation of the HSR (Westerheide et al., 2009). Furthermore, the activity of HSF1 is regulated by co-activators, repressors and protein degradation which is stimulated by phosphorylation (Åkerfelt et al., 2010; Li et al., 2017). The HR-C region located adjacent to the C-terminus, which is conserved among the vertebrate Hsfs but not in plants and *S. cerevisiae*, has been found to have a role in suppression of trimerization (Wu, 1995; Pirkkala et al., 2001). Furthermore HSF1, HSF2 and HSF4 undergo alternative splicing as an additional regulatory level for control of expression. The functionally distinct HSF isoforms are differentially regulated in a tissue- and temperature- dependent manner (Goodson et al., 1995; Tanabe et al., 1999; Neueder et al., 2014). For example, HSF4a acts as an inhibitor of the constitutive expression of HS-related genes while HSF4b acts as a transcriptional activator (Tanabe et al., 1999). Upon HS, HSF1 and HSF2 co-localize and accumulate in nuclear stress bodies (NSBs) where they bind to a subclass of satellite II repeats and induce their transcription (Biamonti and Vourc'h, 2010). However, the function of those transcripts remains unknown.

4.7 Objectives of the study

A previous study on the role of HsfA2 in tomato, gave insights into the HsfA2-dependent regulatory network in vegetative and male reproductive tissues (Fragkostefanakis et al., 2016). In the same study, *HsfA6b* and *HsfA7* accumulated at higher levels in the HsfA2 knock-down background compared to the wild type. As a phylogenetic analysis in several plant species has shown that HsfA2 shares the highest sequence similarity with HsfA6 and HsfA7 proteins, the possibility of redundancy among these Hsfs was assumed.

There is no study available on the regulation, properties or function of tomato HsfA7 up to now. Consequently, the aim of my study was to characterize into detail HsfA7 in terms of activity and function in tomato plants. For this purpose, I aimed to get more insights into the expression properties of HsfA7 and to investigate its transcript and protein profiles in the context of different temperature conditions. Next, my aim was to characterize the protein in terms of localization, activity and protein stability. As the activity and fate of Hsfs are regulated by interactions with other members of the family, I examined the interaction HsfA7 with other major Hsfs and its importance in transcriptional regulation and relevance in the HSR. During my study, I obtained insights into the proteasomal degradation of HsfA7 as well as HsfA2 and the

master regulator HsfA1a. In this context, I examined the basis of HsfA7 protein turnover in the context of the Hsf activity cycle.

In parallel, in order to gain a more detailed picture of the functional importance of HsfA7 and its potential redundant and specific functions in relation to HsfA2, my objective was to generate HsfA7 and HsfA2 KO mutants using the CRISPR/Cas9 method. In comparative studies, the mutants were exposed to different temperatures and their response at the molecular and physiological level was monitored. This allowed the expansion of current knowledge about Hsf networks and highlights the importance of alternative splicing and protein turnover for the cellular responses to elevated temperatures. Overall, my results show that HsfA7 is important for the fine regulation of the temperature-responsive networks.

5 Materials and methods

5.1 Transformation of chemically competent *Escherichia coli*

100 µl of chemically competent *E. coli* DH5α cells (Dagert and Ehrlich, 1979) were thawed on ice and mixed with 100 µl of transformation buffer (100 mM $CaCl_2$; 50 mM $MgCl_2$) and plasmid DNA. The sample was incubated on ice for 20 min after which a heat shock was performed at 42°C for 90 s in a water bath. Cells were chilled on ice for 5 min followed by addition of 500 µl LB medium (Luria-Bertani, 10 g l^{-1} tryptone; 5 g l^{-1} yeast extract; 10 g l^{-1} NaCl) and incubation at 37°C for 1 hour with shaking at 750 rpm. Transformed cells were pelleted at 5,000 rpm and room temperature for 5 min and the pellet was resuspended in a small amount of medium, plated on LB plates (LB medium with 15 g l^{-1} agar) with the appropriate antibiotic and incubated overnight at 37°C.

5.2 Transformation of *Agrobacterium tumefaciens*

A 250 µl aliquot of competent *Agrobacterium tumefaciens* strain GV3101 was thawed on ice and mixed with ~5 ng plasmid DNA. The sample was kept on ice for 5 min and transferred to liquid nitrogen for another 5 min. Subsequently, the sample was incubated for 5 min at 37°C. After addition of 500 µl LB medium, the samples were placed in a heat block for 2 hours at 28°C and 750 rpm. Cells were collected at 8000 rpm for 1 min and spread on a LB plate with gentamicin (100 µg ml^{-1}) and kanamycin (50 µg ml^{-1}) as selection marker of the resistance gene neomycin phosphotransferase (nptII) carried by the plasmid construct. Plates were incubated for 2 days at 28°C.

5.3 Agrobacterium-mediated plant transformation

For Agrobacterium-mediated plant transformation a protocol adapted by Dr. Thomas Berberich (BiK-F, Frankfurt am Main) was used (McCormick, 1991). Competent *Agrobacterium tumefaciens* strain GV3101 was transformed with the constructs of interest and pre-cultures of 3 ml LB medium supplemented with 50 µg ml^{-1} kanamycin and 100 µg ml^{-1} gentamicin were inoculated and grown overnight at 28°C at 120 rpm in an incubator (Infors HT, Minitron). On the next day, 10 µl of the pre-culture was added to 20 ml of LB medium supplemented with Kan and 200 µM acetosyringone (prepared fresh in DMSO) and grown till OD600 reached 0.5. Cotyledons of 25 plants (for each plasmid constructs) grown under sterile conditions were sectioned into 4 pieces with a sterile surgical scalpel and incubated with the Agrobacterium suspension in a petri dish for 10 min. In the next step, the explants were dried on sterile filter paper and transferred to co-cultivation plates with the adaxial side down (4.4 g l^{-1} MS medium; 0.8% Agar; 2% glucose; 1mM MES; 0.75 µg ml^{-1} trans-zeatin in 1 M NaOH; 1 µg ml^{-1} indole-3 acetic-acid, IAA in EtOH; pH 5.7) and incubated at 25°C in dark. After 2 days the cotyledons were transferred onto shoot induction medium (same composition as co-cultivation medium only without acetosyringone) supplemented with 300 µg ml^{-1} cefotaxime and 100 µg ml^{-1} Kan, and moved to 80 µE, 16 hours

light conditions. Note: Due to overgrowth of Agrobacterium around the explants cefotaxime was later replaced with 300 µg ml^{-1} Timentin™ (ticarcillin disodium/clavunalate potassium, Duchefa). Explants were transferred to fresh medium every 2 weeks until shoots were formed. After 2 weeks explants which formed small shoots were transferred to shoot elongation medium (4.4 g l^{-1} MS medium; 0.8% Agar; 2% glucose; 1mM MES; 0.1 µg ml^{-1} trans-zeatin; 0.05 µg ml^{-1} IAA; 100 µg ml^{-1} Kan; 300 µg ml^{-1} Timentin™). Once the shoots reached 3-4 cm in height, these were detached from the explants and placed into rooting medium (4.4 g l^{-1} MS medium; 0.8% Agar; 2% glucose; 1mM MES; 0.2 µg ml^{-1} Indole-3-butyric acid, IBA; 400 µg ml^{-1} carbenicillin). When the regenerated plants (T_0 generation) developed roots they were transferred to soil and moved to the greenhouse.

5.4 Plant material

Wild-type tomato plants used in this study were *Solanum lycopersicum* cv. Moneymaker. HsfA2 (Solyc08g062960) and HsfA7 (Solyc09g065660) KO plants were generated using the CRISPR/Cas9 technology. Transformation of *Solanum lycopersicum* cv. Moneymaker cotyledon discs was performed as described above. The T-DNA cassette in the pICSL002208 (Table 1) plant transformation vector contained between left and right border as follows: a single guiding RNA (sgRNA) under the control of the *Arabidopsis thaliana* U6 small nuclear RNA (snRNA) promoter, *Streptococcus pyogenes* Cas9 controlled by the CaMV 35S promoter and kanamycin resistance gene neomycin phosphotransferase II (nptII) controlled by the CaMV 35S for selection based on kanamycin resistance. All plants were grown in a greenhouse at a temperature of 25°C day/20°C night and 16 hours day/8 hours night cycle (control conditions).

Plants for protoplast preparation were grown on gelrite-solidified Murashige and Skoog (MS) medium (Murashige and Skoog, 1962) supplemented with 20 g l^{-1} sucrose (25°C day/23°C night, 16 hours day/8 hours night).

The tomato cell culture (GCR237) was obtained from the RIKEN BRC Experimental Plant Division (Japan). It was established from *Solanum lycopersicum* cv. Craigella seedlings in MS medium supplemented with 2 mg l^{-1} 1-naphtalenacetic acid, 0.2 mg l^{-1} 2,4-dichlorophenoxy acetic acid and 0.2 mg l^{-1} zeatin (Ishibashi et al., 2007). The cell culture was maintained a 25°C and 120 rpm (GFL 3033 incubator) in dark. The culture was propagated weekly by transferring to freshly prepared MS medium.

5.5 Temperature treatments

Various HS treatments were performed on wild-type and transgenic plants according to the experimental setup as described by Fragkostefanakis et al. (2016). HS treatments were done either by exposing whole plants to HS in a climate chamber (120 µmol m^{-2} s^{-1} light intensity similar to greenhouse conditions) or by incubation of detached, young leaves in petri dishes on wet towels in a water bath with increased water temperatures. Control samples were either

kept at 25°C in a climate chamber or a water bath. Seedlings were treated in petri dishes in similar manner like detached leaves.

Tomato cell culture was treated at the indicated temperatures in a water-filled shaker at 120 rpm (GFL 1092). Control samples were kept during the same time in the shaker for cell culture maintenance at 25°C. In case of the proteasome inhibitor treatment MG132 (in DMSO) was added to a final concentration of 50 µM, followed by exposure of the cell culture to HS conditions. Control samples were treated with the same volume of DMSO.

In all cases samples were harvested at desired time points, frozen in liquid nitrogen and kept at -80°C until further processing.

5.6 Seedling thermotolerance assay

The relative hypocotyl elongation assay used in this study in order to quantitatively assess thermotolerance of tomato seedlings was based on the assay described for *Arabidopsis thaliana* seedlings (Queitsch, 2000). Seeds of wild-type and KO lines were surface sterilized by a 15% sodium hypochlorite wash for 1 min, followed by a 70% ethanol wash for 1 min and 4 consecutive 1 min washes with sterile water. Afterwards, seeds were placed on a wet paper towel in a petri dish and allowed to germinate for 4 days in dark at 25°C. At least ten of the etiolated seedlings were then exposed to the described temperature conditions by placing the sealed petri dish in a water bath with a controlled temperature. Another set of seedlings was kept during the same time at 25°C as control. Seedlings were photographed at different time points and hypocotyl length was measured using ImageJ.

5.7 Genomic DNA extraction

Leaf tissue (50-100 mg) was frozen in liquid nitrogen and homogenized using a TissueLyser MM300 (Qiagen/Retsch) 2 times for 30 sec at a frequency of 30 s^{-1}. 1300 µl of extraction buffer (100 mM Tris-HCl pH 6.0; 700mM NaCl; 50 mM EDTA pH 8.0) was added to the ground tissue and incubated for 15 min at 65°C. Afterwards, samples were let to cool at room temperature for 1 min and 650 µl chloroform/isoamyl alcohol (24:1) was added followed by gentle shaking for 5 min. Samples were centrifuged at 14,000 rpm for 2 min at room temperature, and the upper phase was transferred to a new tube and treated with 10 µl of RNase A (10 µg $µl^{-1}$; Roth) at 37°C for 10 min. Subsequently, 700 µl isopropanol was added and samples were let to precipitate for 10-15 min at room temperature. gDNA was pelleted by centrifugation at 14,000 rpm for 15 min followed by washing with 70% ethanol. The gDNA pellet was dried at 42°C for 10 min, resuspended in 100 µl ddH_2O and incubated for another 10 min at 65°C to dissolve the pellet. gDNA samples were stored at 4°C.

5.8 Plasmid construct generation

Plasmid constructs which were used in this study but generated previously and generated for this study are listed in Supplemental tables 2 and 3. The constructs were prepared using conventional cloning procedures, such as Golden gate cloning, quickchange site-directed mutagenesis and PCR-mediated deletion of plasmid constructs. PCR products were either cut out of an agarose gel and purified using an E.Z.N.A Gel Extraction Kit (OMEGA Bio-Tek Inc., Doraville, GA, USA) or precipitated using 0.1 vol. of 3 M sodium acetate (pH 5.2) and 2.5 vol. 96% EtOH at -20°C. Restriction enzymes used were from ThermoFisher. Oligonucleotides and restriction sites used for vector construction are listed in Supplemental table 3.

5.9 Quickchange site-directed mutagenesis

Quickchange mutagenesis PCR was used to perform an exchange of one or a few amino acids in the plasmid construct. To induce a desired mutation an oligonucleotide (Sigma-Aldrich) containing the exchanged nucleotides was designed and phosphorylated with T4-polynucleotide kinase (PNK) according to the manufacturer's protocol (ThermoFisher) at 37°C for 30 min, followed by an incubation at 70°C for 15 min. Afterwards a PCR reaction was performed with 10 ng plasmid DNA which served as template, 5 pmol phosphorylated primer, 0.625 mM NAD^+ and 5 U Ampligase (Biozym), Pfu buffer and Pfu polymerase in a 20 µl reaction. A similar reaction was prepared except for the phosphorylated primer and served as a negative control. The temperature used for annealing was chosen according to the primer melting temperature for each reaction. Elongation time was adjusted to the plasmid size (1 min/0.5kb for Pfu polymerase) and 28 cycles were employed. Subsequently, 0.5 µl DpnI (ThermoFisher) was added to the PCR reactions and incubated overnight at 37°C in order to digest the template plasmid. On the next day another 0.5 µl DpnI were added for 2 hours followed by transformation of the reactions into chemically competent *E.coli* DH5α cells. Resulting clones were sequenced and analysed for presence of the mutation using CloneManager software.

5.10 PCR-mediated deletions in plasmid constructs

Deletion of the activator (AHA) motif of HsfA7 in plasmid DNA was performed by *in vivo* recombination of homologous ends in *E. coli* as described previously (Hansson et al., 2008). In short, the primer A was designed as a reverse complement of 16-20 bp upstream of the plasmid sequence to be deleted and an additional 16-20 bp of the downstream sequence. Primer B was designed in the same manner but corresponding to the complementary plasmid strand. A 50 µl PCR reaction was prepared with 50 ng template plasmid DNA, 0.2 mM dNTP mix, 1 µM primer A and B and Pfu polymerase. The temperature used for annealing was 56 °C, elongation time was adjusted to the size of the final plasmid product and 28 PCR cycles were performed. DpnI digestion was done in the same way as described for the mutagenesis PCR in order to digest unwanted plasmid DNA template. Positive clones were identified by sequencing and alignment of the resulting sequence to the template using CloneManager.

5.11 Cloning of CRISPR/Cas9 plasmid constructs for plant transformation

Final plasmid constructs for CRISPR/Cas9-mediated plant genome editing were obtained through a modular cloning system based on the Golden Gate cloning technology (Engler et al., 2009). Type IIS restriction enzymes were used to assemble multiple DNA fragments in a particular order (Weber et al., 2011). The cloning was performed like described on The Sainsbury Laboratory SynBio website (http://synbio.tsl.ac.uk). In short, the target for Cas9 (or sgRNA) was selected with help of the CRISPR-PLANT (https://www.genome.arizona.edu/crispr/) online tool (Table 1). In the next step, the sgRNA of interest was introduced into the sgRNA scaffold by PCR on the pICSL01009::AtU6p (Addgene Plasmid #46968) plasmid which served as a template. The *Arabidopsis thaliana* U6 promoter and resulting sgRNA PCR product (132 bp) were cloned into the Level 1 acceptor pICH47732 from the MoClo Toolkit (Addgene Kit #1000000044) (Engler et al., 2014) in an "one pot digestion-ligation (dig-lig)" reaction. The reaction included: 150 ng acceptor plasmid (pICH47732), sgRNA and *At*U6p as inserts in a 2:1 molar ratio insert:acceptor, 1.5 µl BSA (1 mg ml^{-1}) 1.5 µl T4 ligase buffer, 200 U T4 DNA Ligase (ThermoFisher) and 5 U *BsaI* (ThermoFisher) in a total volume of 20 µl. The PCR cycler was set to initial 20 sec at 37°C followed by 3 min at 37°C and 4 min at 16°C which were repeated 26 times and in the end 5 min at 50°C followed by 5 min at 80°C. The PCR reactions were transformed into *E. coli* and plated on LB medium (40 µl of 2% X-gal in DMSO and 40 µl of 0.1 M IPTG were spread on LB plates for blue/white selection). After miniprep, digestion and sequencing positive colonies were selected and these were used for the last cloning step. In there, the AtU6p-sgRNA module assembled in the previous step into the pICH47732 plasmid and an endlinker from plasmid pICH41722 (MoClo Toolkit) served both as inserts for the final cloning step. The final (Level 2) vector pICSL002208 was kindly provided by Dr. Nicola Patron (Earlham Institute, UK). It contained the Cas9 expression cassette and was suitable for plant transformation. The PCR reaction was prepared as described above, except *BpiI* was used instead of *BsaI*. Positive clones were selected as described before and the final pICSL002208-AtU6p:A2sgRNA and pICSL002208-AtU6p:A7sgRNA plasmids were transformed into *Agrobacterium tumefaciens*.

Table 1. Plasmids and sgRNAs used for generation of CRISPR/Cas9 KO lines of HsfA2 and HsfA7.

Mutant	Gene name	sgRNA (5' to 3')	PAM (5' to 3')	Vector	Final plasmid construct
CR-a2	*Sl*HsfA2 (Solyc08g062960)	TCCGACGGCCGTGCTGCCTA	TGG	pICSL002208	pICSL002208-AtU6p::A2sgRNA
CR-a7	*Sl*HsfA7 (Solyc09g065660)	GCGACACCACAACCAATGGA	AGG	pICSL002208	pICSL002208-AtU6p::A7sgRNA

5.12 TA cloning

For sequencing of splicing isoforms TA cloning was used. PCR products were amplified by Taq polymerase and bands of interest were purified by gel extraction using E.Z.N.A Gel Extraction Kit (OMEGA Bio-Tek Inc., Doraville, GA, USA) according to the manufacturer's protocol. The TA cloning reactions were prepared as described for the TOPO TA Cloning kit (Invitrogen) and

transformed into DH5α competent cells. Blue-white selection was used to pick colonies, grow them in liquid cultures and extract plasmid DNA by mini-prep. Sequencing was performed with the following primer pair for HsfA7: Fw 5' GACGGCGAAGAGGAAGATGTAG 3', Rv 5' CCATAAACTTGATCAGGATCTGC 3'.

5.13 Plasmid DNA extraction

5.13.1 Mini-prep

In order to extract plasmid DNA and screen for positive clones, plasmid mini-prep was used. Colonies were inoculated into 3 ml of LB medium and the cultures were incubated overnight at 37°C in a rotary shaker (120 rpm). On the next day cells were harvested at 5000 rpm for 5 min and the pellet was air-dried and resuspended in 150 µl P1 (50 mM Tris/HCl pH 8.0; 10 mM EDTA; 100 $\mu g ml^{-1}$ RNase A). Further, 200 µl P2 (0.2 M NaOH; 1% SDS), 200 µl of P3 solution (3 M potassium acetate; 11.5% (v/v) glacial acetic acid) and 40 µl of chloroform were added. Samples were mixed by inverting, kept on ice for 5 min and centrifuged for 15 min at 14,000 rpm and 4°C. The supernatant (500 µl) was transferred to a new tube, mixed with 700 µl isopropanol and precipitated at -20°C for at least 1 hour. Plasmid DNA was pelleted (14,000 rpm at 4°C for 15 min) and washed with 70% ethanol (14,000 rpm at 4°C for 5 min). In the end, the DNA pellet was dried at 42°C for 10 min and resuspendend in 30 µl ddH_2O.

5.13.2 Midi-prep

Plasmid midi-prep was used for plasmid DNA extraction for protoplast transformation. First, plasmid DNA was transformed in *E.coli* DH5α and incubated overnight at 37°C and 120 rpm in 100 ml LB medium. The grown bacterial culture was centrifuged (20 min at 5,000 rpm) and the pellet was resuspended in 3 ml lysis buffer (50 mM Tris/HCl pH 8.0; 50 mM EDTA pH 8.0; 15% [w/v] sucrose). Afterwards, 7 ml of freshly prepared P2 solution (0.2 M NaOH; 1% SDS) was added, carefully mixed and incubated at room temperature for 10 minutes. Then, 3.5 ml of P3 solution (3 M potassium acetate; 11.5% (v/v) glacial acetic acid) was added followed by shaking and incubation on ice for 20min. After centrifugation at 5,000 rpm, 4°C for 20 min the clear supernatant was filtered through a funnel with cotton and 7 ml isopropanol was added for precipitation at -20°C for 1 hour or more. In the next step centrifugation for 20 min at 11,000 rpm and 4°C was performed and the pellet was dissolved in 1ml TE buffer (10 mM Tris/HCl pH 7.6; 1 mM EDTA pH 8.0). After addition of an equal volume of 5 M LiCl/50 mM MOPS buffer and vigorous vortexing the samples were left on ice for 30 min to 1 hour. Subsequently samples were centrifuged (for 10 minutes at 8,000 rpm and 4°C) and the supernatant was transferred to a new tube and precipitated with 0.1 V of 3 M sodium acetate (pH 5.2) and 2.5 V 96% EtOH at -20°C for at least 1 hour. DNA was pelleted at 11,000 rpm and 4°C for 20 min and the pellet was dissolved in 300 µl TE buffer supplemented with 10µl of RNase A (500 units/ml in 5 mM Tris/HCl pH 8.0, Roth) and RNase T1 (500 units/ml in 5 mM Tris/HCl pH 8.0, ThermoFisher). Incubation at 37°C was performed for 30 min and then 30 µl of 10x Proteinase K (1000 $\mu g ml^{-1}$; 150 mM NaCl; 15 mM sodium citrate, 1% SDS; 9 mM EDTA pH 8.0, Applichem) was added and the reaction was

incubated for another 15 min at 37°C. An equal volume (350 µl) of phenol/chloroform/isoamylalcohol (25:24:1) was added, samples were vigorously vortexed and centrifuged at 14,000 rpm and room temperature for 2 min. The upper phase was transferred to a new tube and mixed with an equal volume (300 µl) of chloroform, followed by vortexing and centrifugation. The upper phase was transferred to a new tube and precipitated with sodium acetate and ethanol. After centrifugation at 14,000 rpm and 4°C for 15 min the pellet was washed with 70% ethanol, dried at 42°C for 10 min and resuspended in TE buffer. Concentration was adjusted to 1 µg μl^{-1} using NanoDrop™ 1000 (PEQLAB, Erlangen, Germany).

5.14 DNA sequencing

Sequencing reactions were prepared using 80-100 ng plasmid DNA or 20-80 ng PCR product and 5 µl of 5 µM primer in a 10 µl reaction, as recommended by GATC Biotech (Konstanz, Germany). Sequence alignments of .ab1 files were done in CloneManager.

5.15 Protoplast isolation and transformation

Tomato mesophyll protoplasts were isolated and transformed as described by Mishra et al. (2002). In short, wild-type (*Solanum lycopersicum* cv. Moneymaker) or CR-*a7-2* plants were grown in sterile conditions as described above. At 6-7 week-old stage leaves were lightly cut with a scalpel in a petri dish containing 10 ml enzyme solution (K3M-S solution containing: 0.4 M mannitol; 24.7 mM KNO_3; 1.01 mM $MgSO_4x7H_2O$; 1.09 mM $NaH_2PO_4xH_2O$; 1.01 mM $(NH_4)_2SO_4$; 6.12 mM $CaCl_2x2H_2O$; 0.56 mM m-inosid; 3 mM NH_4NO_3; 5ml/L of 2.3 g/250ml $FeSO_4$EDTA; 1x Trace elements (500 ml 100x stock: 37.5 mg KJ; 500 mg $MnSO_4xH_2O$; 100 mg $ZnSO_4xH_2O$; 150 mg H_3BO_3; 12.5mg $Na_2MoO_4x2H_2O$; 1.25 mg $CoCl_2x6H_2O$; 1.25 mg $CuSO_4$), 5.57 mM NES; 0.89 mM BA; 29.65 mM vitamin B1; 4.86 mM vitamin B6; 8.12 mM nicotinamide; 5mM MES; pH 5.7-5.8) containing 0.25% Cellulase and 0.1% Macerozyme (Duchefa). Leaves were incubated overnight in dark at room temperature. On the next, day leaf debris were separated from the protoplasts by gentle shaking and passing through a sieve. The protoplast solution was further cleared from debris by centrifuging for 7 min at 460 rpm in K3-2S (K3M-S with 6% (w/v) sucrose). The upper 2/3 of the supernatant containing intact protoplasts was washed twice in W5 (125 mM $CaCl_2$, 154 mM NaCl, 0.54 mM KCl, 0.56 mM glucose, 0.5 mM MES, pH 5.6-5.8) at 670 rpm for 10 min. In the end, protoplasts were resuspended in K3M solution (K3M-S with 3% (w/v) sucrose) to a final concentration of 10^6 cells per ml.

Depending on the experiment, for one sample 100 or 50 µl (100,000 or 50,000 cells) protoplast solution was mixed with 20 or 10 µg plasmid DNA and an equal volume of PEG solution (25% PEG 6000, 0.45 M mannitol, 0.1 M $Ca(NO_3)_2{\times}4H_2O$, pH 6.0 (KOH)) and incubated at room temperature for 25 min. For all experiments total plasmid amount was adjusted with pRT-Neo construct encoding for the neomycin phosphotransferase II (nptII) gene which served as mock plasmid. The reaction was stopped by adding K3M to a final volume of 1 or 0.5 ml. The samples were incubated at 25°C in the presence of light to allow expression for 6-8 hours, or for another duration based on the individual experiments. Harvesting of protoplasts included centrifugation

at 14,000 rpm and 4°C for 5 min, followed by removal of the supernatant by aspiration. Samples were frozen in liquid nitrogen and kept at -80°C until further processing.

5.16 Protein turnover assays in protoplasts

In order to determine protein turnover in protoplasts by a chase experiment plasmid DNA coding for the protein of interest was transformed into protoplasts in as many replicates as time points as described by Röth et al. (2017). After 4 hours of expression, cycloheximide (CHX) was added to a final concentration of 20 µg μl^{-1}. Samples were harvested at indicated time points and protein extraction was performed as described for protoplasts. Protein extracts were separated using SDS-PAGE and protein signals were quantified following immunoblotting and immunodetection. For every biological replicate at least 3 exposure times were used for quantification. Using ImageJ, first the background was subtracted, followed by quantification of the immunoblot signals. For each immunoblot the mean for each time point and ratio to the mean of T0 were calculated. The curves represent the least square fit analysis with an exponential equation. Graphs were generated in SigmaPlot.

5.17 β-glucuronidase (GUS) reporter assay

A GUS reporter assay was used to assess the activity of Hsfs on a promoter of interest (activator assay). For each experiment 50,000 protoplasts were co-transformed with 1 µg of HSE-containing GUS reporter plasmid and 0.5 µg of one or more Hsf plasmid constructs In the GUS activator assay the TATA box is placed between HS inducible promoter and GUS coding sequence. After expression (6-8 hours) protoplasts were harvested, 50 µl of GUS buffer (50 mM $NaPO_4$, pH7.0; 10 mM $EDTA(Na)_2$ pH 8.0; 0.1% N-Laurylsarcosine-Na-salt (v/v), 0.1% Triton X-100 (v/v); 1:1,000 of 14.3 mM β-mercaptoethanol) was added followed by vortexing and freezing of the samples in liquid nitrogen. A freeze-thaw-vortex cycle was repeated three more times. Afterwards, samples were centrifuged for 5 min at 14,000 rpm and 4°C to pellet cell debris. 25 µl of the supernatant was transferred to a 96-well plate with transparent bottom on ice and then 25 µl of the GUS substrate 4-methylumbelliferyl β-glucuronide (MUG, 0.44 mg ml^{-1} in GUS buffer) was added. The plate was incubated at 37°C in dark and GUS activity was measured as cleavage of the MUG substrate by GUS enzyme to 4-methylumbelliferone (MU) (Jefferson et al., 1987; Gallagher, 1992). MU fluorescence was measured at different time points in a Spark™ 10M Multimode Microplate Reader (Tecan Trading AG) using an excitation wavelength of 365 nm and an emission wavelength of 460 nm. After subtraction of the background fluorescence the GUS activity of the samples was calculated as mean of the triplicates (activator assay) or as the mean of triplicates relative to the “neo” samples transformed only with the GUS reporter construct and pRT-Neo. In case of the GUS activator assay increased enzymatic activity in terms of fluorescence means enhanced binding of the Hsfs to the HS inducible promoter The remaining triplicates (25 µl) were pooled and supplemented with 4xSDS buffer (160 mM Tris/HCl, pH 6.8; 6.4% SDS; 0.32 g ml^{-1} glycerol; 400 mM dithiothreitol (DTT); bromophenolblue) for immunoblot analysis.

5.18 Protein extraction

For protein extraction from young leaves and seedlings 50-100 mg of frozen tissue was ground two times for 30 sec at 30 s^{-1} using a TissueLyser MM300 (Qiagen/Retsch). Sample mass was determined followed by resuspension in the same amount (1:1) of high salt buffer (20 mM Tris/HCl, pH 7.8; 500 mM NaCl; 25 mM KCl; 5 mM $MgCl_2$; 30 mM EDTA; 0.5% Nonidet-P40; 0.2% sarcosyl; 5% sucrose; 5% glycerol; 14.3 mM β-mercaptoethanol; proteinase inhibitor cocktail: 10 µg ml^{-1} Pefabloc (in 10mM Hepes, pH7.5); 1µg ml^{-1} Pepstatin A (in ethanol or isopropanol); 2 µg ml^{-1}Leupeptin; 2 µg ml^{-1} Aprotinin; 50 µg ml^{-1} TLCK (in 0.1 N HCl); 20 µg ml^{-1} TPCK (in ethanol); 150 µg ml^{-1} Benzamidine. The samples were thoroughly vortexed and sonicated using a Sonopuls HD70 (Bandelin) sonicator at an amplitude of 30% and duty cycle 20. Afterwards, the samples were centrifuged at 14,000 rpm and 4°C for 5 min and the supernatant was transferred to a new tube. Protein amount was estimated using Bradford protein assay (BioRad) according to manufacturer's instructions. All samples were diluted with HSB to have the same concentration and supplemented with 4x SDS loading buffer, vortexed and boiled at 95°C for 5 min.

Protein extraction from protoplasts was achieved by adding 60 µl HSB to the frozen protoplast pellet and vigorous vortexing. Freeze-thaw-vortex steps were repeated 3 times. Samples were subsequently centrifuged for 5 min at 14,000 rpm and 4°C, and 50 µl of the supernatant was transferred to a new tube. Afterwards, 4x SDS was added and samples were boiled at 95°C for 5 min. 10-15 µl were used for loading on the SDS-PAGE.

5.19 SDS-PAGE and immunoblot analysis

Protein samples were separated based on molecular weight using sodium dodecyl sulfate polyacrylamide gel electrophoresis (SDS-PAGE) (Laemmli, 1970). Percentage of the mini gels used was 10 or 12% and based on the size of analysed proteins. 20-40 µg of total protein extract was loaded on the SDS-PAGE together with Unstained Protein Molecular Weight Marker (ThermoFisher). Gels were run for 1 hour at 0.5 mA cm^{-2} with 1x SDS-running buffer (50 mM Tris; 200 mM Glycine; 0.1% SDS). After gel electrophoresis, immunoblotting was performed using the semi-dry method (40 mM Tris; 39 mM glycine; 0.037% SDS; 20% methanol; 1 mA cm^{-2} of transferred area for 75 minutes) to an Amersham Protran 0.45 µm nitrocellulose blotting membrane. Subsequently, the membrane was stained with Ponceau S (0.4% (w/v) Ponceau S; 3% (v/v) trichloroacetic acid (TCA); 1% (v/v) acetic acid). Staining of the Rubisco large subunit was used to represent equal loading for the different samples. For blocking, membranes were incubated in 5% (w/v) non-fat milk in phosphate-buffered saline (PBS, 140 mM NaCl; 2.6 mM KCl; 10 mM NaH_2PO_4; 1.8 mM KH_2PO_4) shaking for 1 hour at room temperature. Afterwards, membranes were incubated with the primary antibody diluted with blocking milk solution at room temperature for 1.5 hours or overnight at 4°C. Primary antibodies and dilutions used are listed in Supplemental table 1. For detection of the primary antibody a secondary antibody conjugated to horseradish peroxidase (SigmaAldrich) was used. In the end, protein signals were visualised using the enhanced chemiluminiscence method (ECL kit, Perkin-Elmer Life Sciences).

5.20 RNA extraction

Different plant tissues (50-100 mg) were frozen in liquid nitrogen and homogenized using a TissueLyser MM300 (Qiagen/Retsch) 2 times for 30 sec at 30 s^{-1}. Total RNA was extracted using the E.Z.N.A. Plant RNA kit (Omega Bio-Tek) from leaves, seedlings and protoplasts according to the manufacturer's protocol. Genomic DNA was removed by DNase I treatment on the membrane according to the manufacturer's instructions. For protoplasts, RNA concentration was measured and 1µg RNA was treated with DNase I (Applichem) for 30 min at 37°C for additional plasmid DNA digestion. Total RNA was quantified at 260 nm with a NanoDrop™ 1000 (PEQLAB, Erlangen, Germany). The purity of obtained RNA was inspected by the A260/A280 ratio.

5.21 cDNA synthesis

For cDNA synthesis the reverse transcriptase RevertAid (ThermoFisher) was used on 1 µg of total RNA was according to manufacturer's instructions. In short, the RNA sample was supplemented with 1 µM oligo-dTVN oligonucleotide (T24VN) and DEPC-treated water to a final volume of 11 µl. The mixture was incubated for 5 min at 70°C to remove RNA secondary structures and then on ice for another 5 min. Next, 9 µl of the reverse transcription mix (1 µl RevertAid reverse transcriptase (200U), 2 µl dNTP mix (10 µM), 4 µl 5x RevertAid buffer and 2 µl DEPC-treated water) was added to the RNA samples. The cDNA synthesis reaction was incubated at 42°C for 1 hour followed by inactivation of the reverse transcriptase at 70°C for 15 min. Samples were diluted 1:10 with ddH_2O and kept at -20°C. To test for presence of genomic or plasmid DNA contamination of the cDNAs, PCRs were performed on where the RNA samples were used as template. All samples were clean of genomic or plasmid DNA.

5.22 Reverse transcription-polymerase chain reaction (RT-PCR)

cDNA samples generated by reverse transcription of the RNA were used as template for PCR analysis of various genes. For each gene or region of the gene specific primers (Sigma-Aldrich) were used which are listed in Supplemental table 5. Equal loading was confirmed with primers for Elongation factor 1 alpha (EF1α, Solyc06g005060) which served as a housekeeping gene. PCR reactions were performed in a final volume of 20 µl using Taq or Pfu polymerase and 2 µl of the respective buffers (10x Taq buffer – 100 mM Tris-Hcl pH 8.3; 15 mM $MgCl_2$; 500 mM KCl, 10x Pfu buffer – 100mM Tris-HCl pH 8.85; 250 mM KCl; 50 mM $(NH_4)_2SO_4$; 20 mM $MgSO_4$), 0.2 mM dNTP mix and 1 µM forward and reverse primer, respectively. Annealing and elongation temperature were adjusted depending on the primer melting temperature and sequence length. PCR reactions were analysed on 1-2% agarose gels. The gels were incubated in ethidium bromide (0.5 mg ml^{-1}) for 5-10 min and placed on an UV-trans-illuminator (TFX-20M, Vilber Lourmat) for detection.

5.23 Quantitative RT-PCR

Quantitative real-time PCR (qRT-PCR/qPCR) was used to investigate relative transcript levels of different genes in cDNA samples. A qRT-PCR reaction included 2 µl cDNA (approx. 5-10 ng), 5 µl PerfeCTa SYBR® Green Fast Mix (Quanta Biosciencies, Gaithersburg, MD, USA), 1 µl of specific forward and reverse primer (0.33 µM, Sigma-Aldrich; Supplemental table 4) and 1 µl dd H_2O (10 µl total reaction). Reactions were loaded onto a white semi-skirted 96-well plate (Thermo Scientfic) and sealed with optically clear flat 8 cap strips (Thermo Scientific). A Stratagene Mx3000P cycler (Agilent Technologies, Palo Alto, CA, USA) was used to perform a thermal cycling profile consisting of: initial denaturation at 95°C for 3 min, followed by 95°C for 15 s, 60°C for 30 s, and 72° for 30 s during 40 cycles. EF1α (Solyc06g005060) was included in each plate and served as an internal control to normalize the variations in cDNA amounts across different samples. All qRT-PCR reactions were performed in triplicates. Relative transcript levels were calculated with the mean values of technical replicates according to the ΔΔCt method (Livak and Schmittgen, 2001).

5.24 High-resolution RT-PCR

For high-resolution (HR) RT-PCR tissue preparation, RNA extraction and cDNA synthesis was performed as described in the previous sections. A gene-specific primer pair for HsfA7 (Fw 6616 labelled with 6-carboxyfluorescein and Rv 6473, Supplemental table 5) was used for PCR amplification of maximum of 552 bp and different shorter fragments corresponding to splicing events. A thermal cycling profile consisting of: initial denaturation at 95°C for 3 min, followed by 95°C for 30 s, 58°C for 45 s, and 72° for 30 s during 32-35 cycles was utilized. The resulting labelled RT-PCR products representing AS transcripts were detected on an ABI3730 DNA Analyzer along with GeneScan 1200 LIZ size standard (Applied Biosystems). Electropherograms were analysed using GeneMapper software in order to extract mean peak areas and size of transcript variants with expected sizes. A ratio for the AS events was calculated by dividing the value of the spliced product by the sum of the values of all products.

5.25 Microscopy analysis

For evaluation of the intracellular localization, proteins were fused to GFP, YFP or mCherry and plasmid constructs were transformed into tomato mesophyll protoplasts. After expression, samples were analysed under a Leica SP5 confocal laser scanning microscope (CLSM). Excitation wavelength for GFP was 488 nm, for YFP 514 nm and for mCherry 561 nm. Fluorescence emission was measured at 490-548 nm for GFP, at 520-550 nm for YFP and 570-656 nm for mCherry. Chlorophyll autofluorescence was measured at 665-738 nm. Sequential excitation was used in order to exclude crosstalk between different channels.

5.26 Antibody generation

A specific antibody against HsfA7 was generated by rabbit immunization with a mixture of two synthetic peptides listed in Table 2 (Pineda Antikörper-Service, Berlin).

Table 2. Peptides used for HsfA7 antibody generation.

Gene name	Synthetic peptide	Sequence
*Sl*HsfA7 (Solyc09g065660)	1 (17 aa)	NH2-CLEMQGYGRARKDQQEE-CONH2
	2 (20 aa)	NH2-CSIQRRMKKAAIWIDQLLVG-COOH

5.27 Hsf domain prediction

The domains in Hsf protein sequences were annotated with help of the Heatster database (*http://www.cibiv.at/services/hsf/*) (Scharf et al., 2012).

5.28 Statistical analysis

The statistical analysis in this thesis included ANOVA and Duncan's Multiple Range Test and was performed using the SigmaPlot software.

5.29 Gene numbers

Gene accession numbers of tomato genes used in this study are listed in Table 3. The sequences of these genes were taken from the Sol Genomics Network (SGN) database (*https://solgenomics.net/*). Sequences of the *Arabidopsis thaliana* genes (ENP1 – At1g31660 and OEP7 - At3g52420) can be found on the The Arabidopsis Information Resource (TAIR) website (*https://www.arabidopsis.org/*).

Table 3. Accession numbers of *S. lycopersicum* genes used in this study.

Gene name	Accession number
HsfA1a	Solyc08g005170
HsfA2	Solyc08g062960
HsfA3	Solyc09g009100
HsfA7	Solyc09g065660
HsfB1	Solyc02g090820
Hsp101	Solyc03g115230
Hsp17.7A-CI	Solyc06g076520
Hsp17.4-CII	Solyc08g062340
APX3	Solyc09g007270
Hsa32	Solyc02g079930
Hsp21.5-ER	Solyc11g020330
Actin	Solyc03g078400
EF1α	Solyc06g009970
mutS	Solyc07g018340

6 Results

6.1 HsfA7 transcript and protein abundance in response to temperature changes

6.1.1 Basal thermotolerance regime

A series of experiments were performed in order to determine the temperature regimes that cause alterations on the transcript and protein abundance of HsfA7. First, four-week old *S. lycopersicum* cv. Moneymaker plants were exposed to temperatures ranging from 25-45°C for 1 hour, followed by direct sampling of young leaves (H). In addition, plants were left to recover from the stress for additional 1.5 hours at 25°C which is referred to as the recovery (R) phase. During this time control (C) plants were kept at 25°C. Relative transcript levels of *HsfA7* were determined using qRT-PCR with gene-specific primers that anneal to the second exon in the HsfA7 gene. In parallel, the transcript levels of *HsfA2*, as the Hsf with the highest sequence homology and prominently induced Hsf, as well as of two HS-inducible genes, *Hsp17.7A-CI* and *Hsp101* were examined (Fig. 3A, upper panel). *HsfA7* has an approximately 64-fold induction in plants exposed to 30 or 35°C and an even stronger increase (approximately 2000-fold) in plants kept at 40°C (Fig. 3A). Instead, a higher temperature than 40°C resulted in the weaker accumulation of *HsfA7*. Interestingly, after 1.5 hours of recovery from 30 or 35°C *HsfA7* abundance is diminished almost to the levels of the control sample (Fig. 3A). In comparison, *HsfA2* is 16-fold induced already at 30°C, the induction is the highest at 40°C and remains high at 45°C. Hsp17.7A-CI and Hsp101 show a similar HS-induction profile (Fig. 3A).

The protein levels of these genes were examined by immunoblotting of protein extracts from the same samples (Fig. 3A, lower panel). For immunoblot analysis a specific antibody against HsfA7 was generated (Table 2, Materials and Methods). HsfA7 is present at 35°C, further induced at 40°C but is then reduced in plants exposed to a higher temperature (Fig. 3A). In contrast to the mRNA levels, the protein further accumulates in the recovery compared to the HS samples which points out differences in mRNA and protein stability during the attenuation phase from stress. In comparison, HsfA2 protein is not detectable at 35°C but becomes very abundant at 40°C and is present at lower levels in 45°C-treated leaves (Fig. 3A). These results suggest that HsfA2 and HsfA7 might both function in a redundant manner at temperatures around 40°C, however HsfA7 might specifically act at 35°C. Similar to HsfA7, Hsp101 and Hsp17-CI accumulate already at 35°C and their protein abundance peaks at 40°C. Similar to HsfA2, Hsp101 is present in leaves exposed to 45°C (Fig. 3A).

The temperature-dependent expression profile of HsfA2 and HsfA7 prompted us to examine whether differences in transcript and protein levels occur in response to HS, in a time-dependent manner as well. Young leaves were exposed for a period of 5 min to 4 hours to 40°C. Both, HsfA2 and HsfA7, follow the same expression profile showing a rapid induction within 5 min of stress treatment (Fig. 3B, upper panel). They both reach maximum levels after 60 min and then decrease by approximately 50% after 4 hours of HS. At the protein level, HsfA2 is already present after 15 min of HS, while HsfA7 shows a delay, being present only after 30 min of stress (Fig. 3B, lower panel). As shown before, Hsp17-CI protein levels followed the profile of

HsfA7, while Hsp101 which is already detectable in non-treated sample, shows enhanced abundance within 5 min of HS.

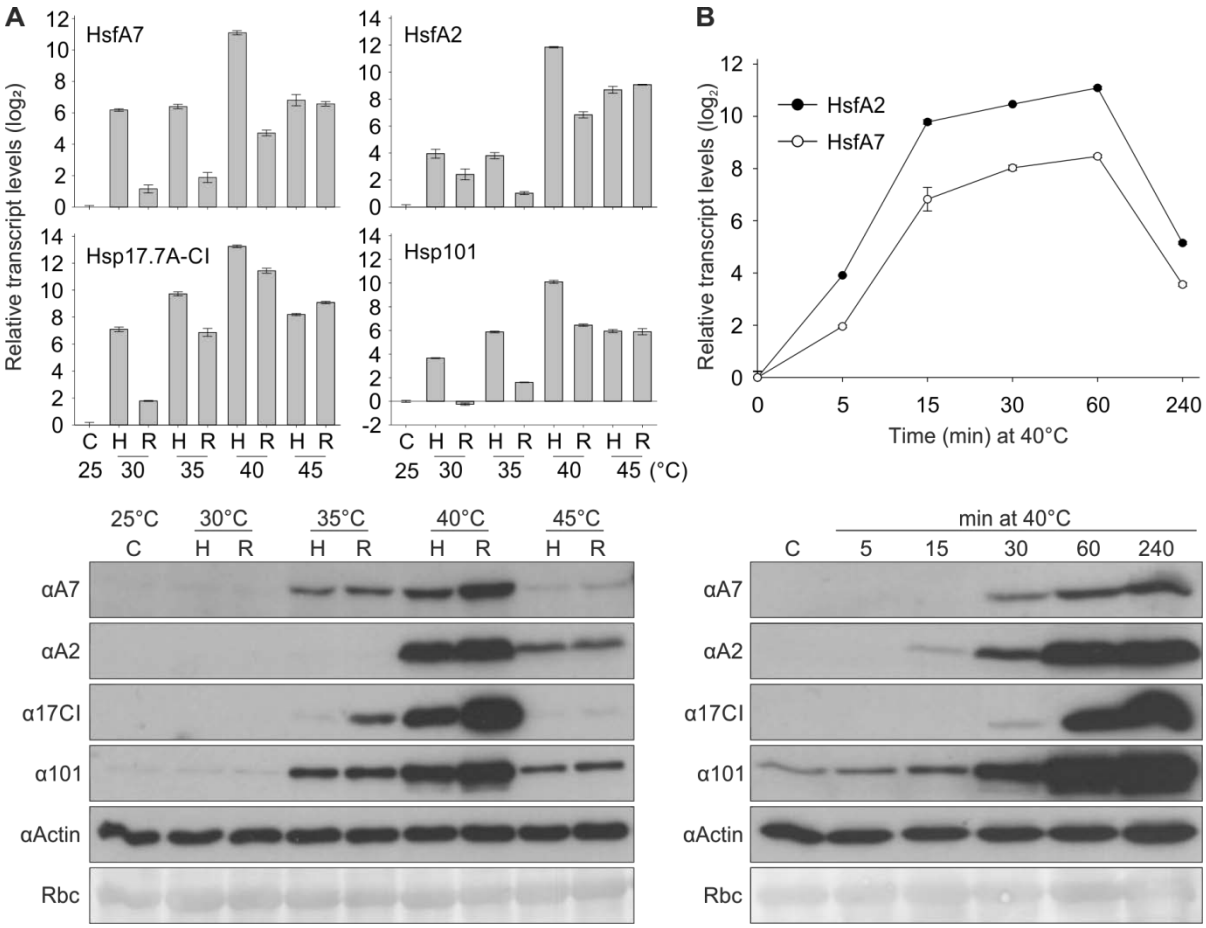

Figure 3. Transcript and protein levels of Hsfs and Hsps in response to elevated temperatures.

(A) Temperature dependent induction of HsfA7, HsfA2, Hsp17.7A-CI and Hsp101. Relative transcript abundance ($2^{-\Delta\Delta Ct}$) of HsfA7, HsfA2, Hsp17.7A-CI and Hsp101 in young wild-type tomato leaves under control conditions (25°C, sample C), exposed to HS (30-45°C) for 1 hour (sample H) or subsequently let to recover for 1.5 hours (sample R) at 25°C. The Ct value of each gene was normalized to the Ct value of EF1α housekeeping gene and to the control. Vertical bars represent the average ± SD of three replicates. Young leaves of wild-type plants were treated in the same way for immunoblotting. Total protein extract in equal amounts (40 µg) was used for SDS-PAGE and immunoblot detection of HsfA7, HsfA2, Hsp17CI, Hsp101 and Actin (loading control) using specific antibodies. Rbc, Ponceau staining of Rubisco large subunit. **(B)** Time dependent induction of HsfA7 and HsfA2. Relative transcript levels ($2^{-\Delta\Delta Ct}$) of HsfA7 and HsfA2 in young wild-type tomato leaves after exposure to 40°C for different time periods ranging from 5 min to 4 hours. The Ct value of each gene was normalized to Ct value of EF1α and to control sample (time 0h). Data points represent the average ± SD of three replicates. Young leaves were treated in the same way and immunoblotting was performed as described in A.

6.1.2 Acquired thermotolerance regime

The expression profile of HsfA7 in response to a stress regime resembling an ATT treatment was examined (Fig. 4A). Young plants were exposed to 37.5°C for 30 min as a pre-treatment, allowed to recover for 3 hours at 25°C, and then exposed to 45°C for 1 hour as a challenging stress. Subsequently, the plants were allowed to recover at 25°C for 24 hours. Samples were taken directly before and after the stress treatments and at different time points during the 24 hour recovery period. HsfA7 transcripts strongly accumulate during the pre-treatment and return to control levels after the three hours of recovery (Fig. 4B). A similar trend was observed for *HsfA2*, *Hsp101* and *Hsp17.7A-CI*, but in contrast to *HsfA7* these three genes retain increased transcript levels compared to the untreated leaves during the recovery from the pre-treatment (Fig. 4B). The transcripts of all four genes were strongly induced by the 45°C treatment and then gradually declined during the course of 24 hours of recovery. Interestingly, after 24 hours, *HsfA2* and *Hsp17.7A-CI* retained increased levels compared to the non-treated plants, *Hsp101* similar to the control plants, while *HsfA7* was further reduced after 3 hours of recovery and onwards compared to the control sample (Fig. 4B).

At the protein level, HsfA7 showed a strong accumulation directly after the pre-treatment and remained at steady protein levels during the 3 hours of recovery (Fig. 4C). The challenging stress led to a further accumulation of HsfA7 and the protein levels were gradually reduced during the recovery from the challenging stress, which correlates with the observed transcript levels (Fig. 4B, C). However, the protein was still detectable after 24 hours of recovery (Fig. 4C). HsfA2 does not show such a strong accumulation after the pre-treatment, but it was very abundant after the challenging stress and followed a gradual decrease during recovery, as shown for HsfA7 (Fig. 4C). In contrast to the two Hsfs, Hsp101 and Hsp17CI sustained very high levels during the recovery from stress and show a slight reduction only after 24 hours (Fig. 4C). Collectively, these results suggest that HsfA7 is a long-lived protein during the recovery from HS, suggesting its involvement in response to repeated cycles of HS and acquired thermotolerance.

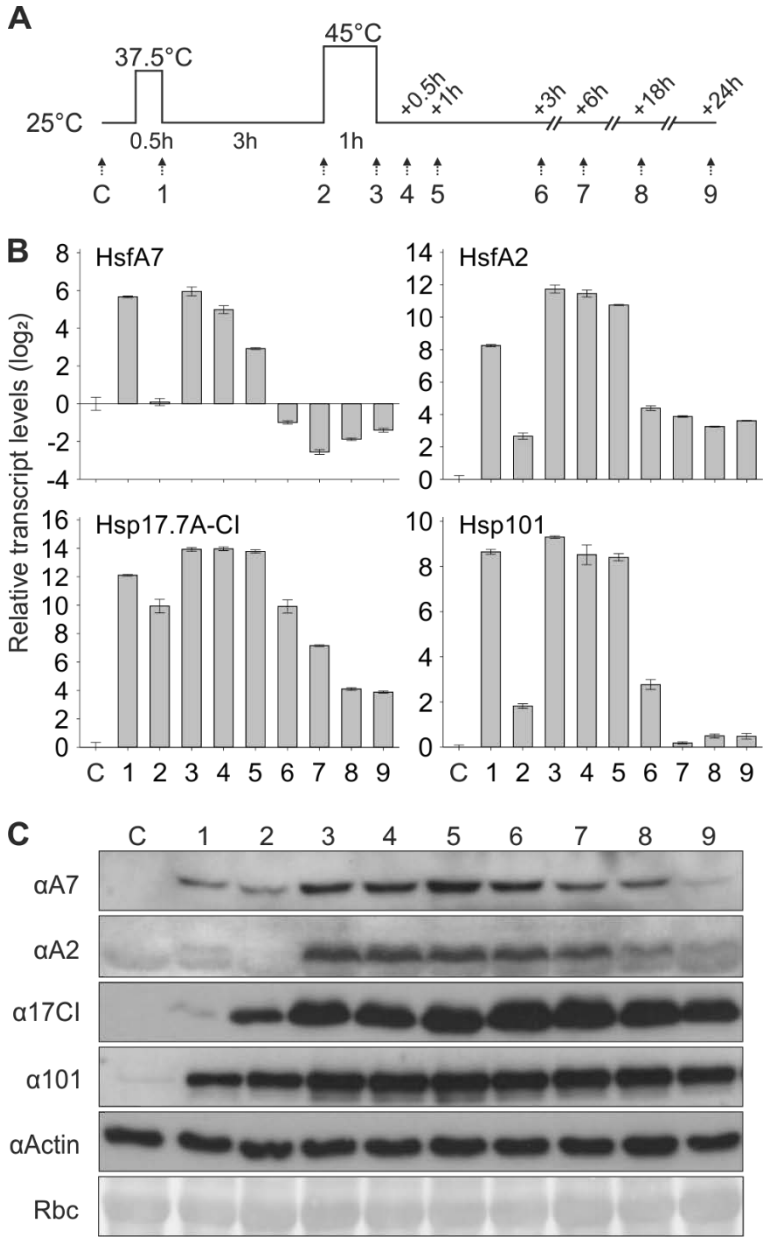

Figure 4. Transcript and protein levels of Hsfs and Hsps in response to an acquired thermotolerance regime. **(A)** The pictogram shows the HS treatment applied to young wild-type plants. Numbered arrows indicate time points of sample harvesting (C, control sample). **(B)** Relative transcript abundance ($2^{-\Delta\Delta Ct}$) of *HsfA7*, *HsfA2*, *Hsp17.7A-CI* and *Hsp101* in young tomato leaves harvested according to A. The Ct value of each gene was normalized to Ct value of EF1α housekeeping gene and to the control sample. Vertical bars represent the average ± SD of three replicates. **(C)** Immunoblot analysis of young leaves of wild-type plants treated as shown in A. Total protein extract in equal amounts (40 µg) were loaded on an SDS-PAGE followed by detection of HsfA7, HsfA2, Hsp17CI, Hsp101 and Actin (loading control) using protein specific antibodies. Rbc, Ponceau staining of Rubisco large subunit.

6.2 HsfA7 pre-mRNA is alternatively spliced

All eukaryotic Hsfs possess an intron spanning the DBD-coding region (Scharf et al., 2012). Tomato HsfA2 has been annotated with a second intron in the carboxyl-terminal coding region (Hu, PhD thesis). Among the tomato Hsfs, HsfA7 shows a remarkably more complex gene structure having 3 introns in the 3'-end in addition to the intron in the DBD-coding region (Fig. 5B, top). Previous results indicated temperature-dependent alternative splicing in introns 2 to 4 (Hu, PhD thesis). In order to examine this in more detail an RT-PCR was conducted using primers annealing to the second and last exon (Fig. 5B, red arrows). The cDNA was prepared from RNA isolated from leaves exposed to 40°C for different time points as described previously (Fig. 3B) or seedlings exposed to temperatures ranging from 30 to 45°C for 1 hour. Agarose gel electrophoresis revealed a high number of amplicons (Fig. 5A). In the leaf samples *HsfA7* expression was gradually increasing in time until one hour exposure (Fig. 5A, left). In the 30 min sample the most abundant band corresponded to the full-length C-terminus of HsfA7 (552 bp, same as gDNA), while in the 60 min sample multiple amplicons of distinct size could be detected suggesting enhanced alternative splicing (Fig. 5A, left). Therefore, the onset of *HsfA7* transcription is characterized by intron retention, while a complex pre-mRNA splicing profile occurs as the stress progresses. Interestingly, alternative splicing in *HsfA7* is enhanced already at 30°C, resulting in multiple amplicons of distinct sizes with apparently similar levels (Fig. 5A, right). Instead, seedlings exposed to 45°C show higher intron retention leading to higher levels of amplicons of increased molecular weight (Fig. 5A, right). Therefore, increasing temperatures are associated with lower splicing efficiency of HsfA7 introns 2-4.

DNA sequencing of these fragments revealed that alternative splicing occurs in intron 2, 3 and 4 and includes intron retention, as well as alternative donor and acceptor site selection (Fig. 5B). Full or partial retention of intron 2 leads to formation of a termination codon in the region of the intron. In that case protein isoform I is produced (Fig. 6). There are three transcripts (α, β, γ) encoding for this isoform which are characterized by a variable 3'-UTR. In the case when intron 2 and intron 3 are efficiently spliced a termination codon occurs in the 5'-end of exon 4. However, if alternative acceptor site selection in exon 4 occurs, 5 nucleotides of exon 4 are omitted and an alternative termination codon in exon 4 is utilized. This leads to formation of protein isoform II and III which differ in length by only one amino acid (Fig. 6). While four transcripts with differing 3'-UTRs were sequenced for isoform II, we identified three transcripts encoding for protein isoform III (Fig. 5B).

The occurrence of a high number of HsfA7 transcript variants suggested that agarose gel electrophoresis is not sufficient to discriminate all the transcripts. We used high-resolution RT-PCR (HR RT-PCR) to determine the relative abundance of splice variants (Fig. 5C, D) (Simpson et al., 2007). The HR RT–PCR system is capable of detecting multiple AS transcripts from a single gene, allowing a two to three nucleotide resolution and identifying small but significant changes in the ratios of alternatively spliced variants (Kalyna et al., 2012). The cDNA samples of leaves (different time points) and seedlings (different temperatures) described above were amplified with the same primers which anneal to exon 2 and exon 5 (Fig. 5B, red arrows). The forward primer was labelled with 6-Carboxyfluorescein (6-FAM) and the resulting PCR products were

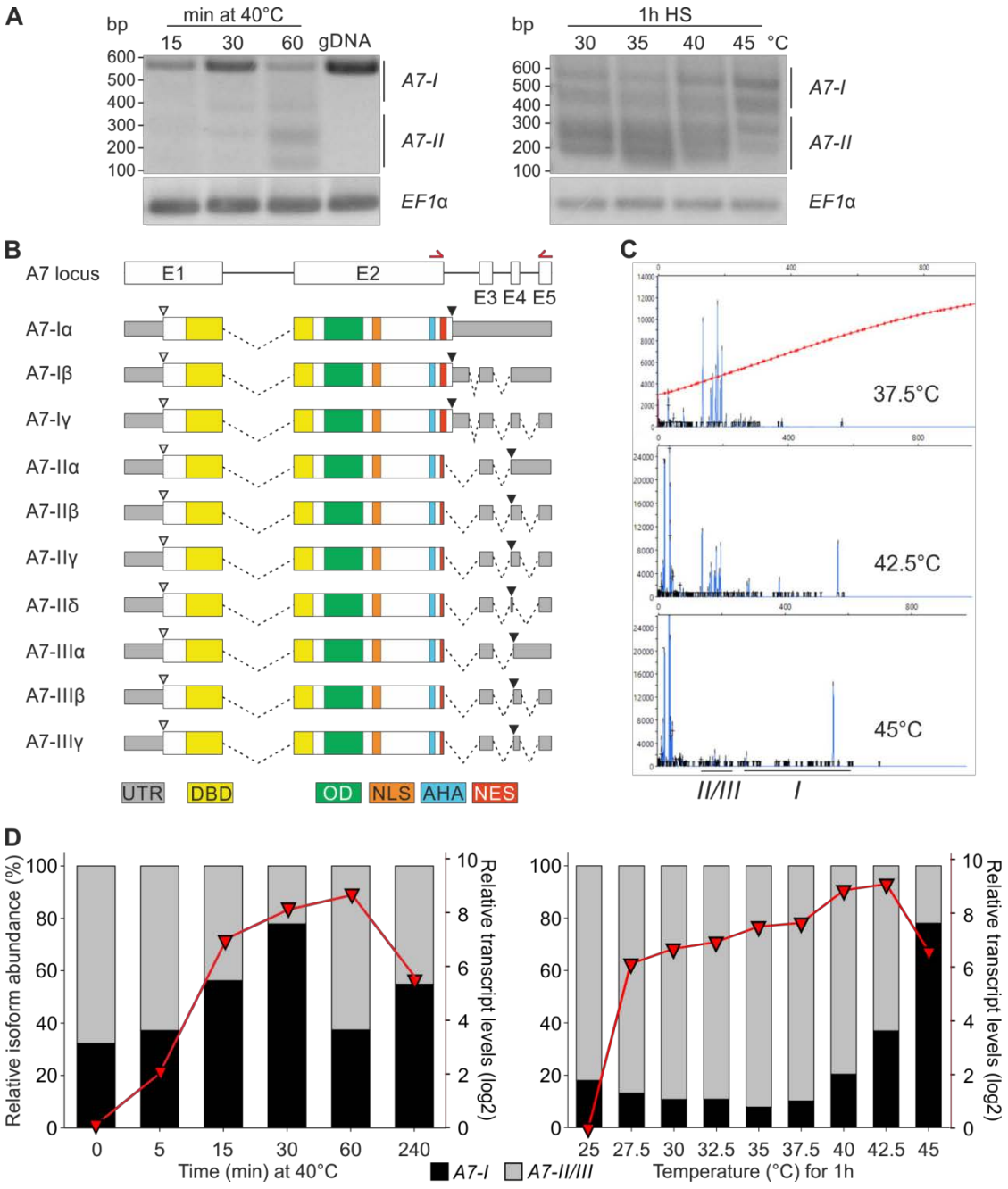

Figure 5. Alternative splicing of HsfA7.

(A) Time- and temperature-dependent alternative splicing of HsfA7. Tomato leaf tissue was exposed to 40°C and harvested at the indicated time points (5-240 min) and seedlings were exposed to different temperatures (25-45°C) for 1 hour. RT-PCR was performed with primers annealing to exon 2 and exon 5 (as indicated by arrows in B). Representative samples are shown. EF1α was used as an indicator of equal loading. **(B)** Splice variants of HsfA7 obtained by Sanger sequencing of the fragments from leaf samples in (A). *Sl*HsfA7 (Solyc09g065660) gene organization with exons depicted as rectangles, and introns as intervening horizontal lines are shown on top and below the transcript structures of ten HsfA7 pre-mRNA isoforms with corresponding domain compositions. White arrowheads indicate positions of the start codon, while black arrowheads indicate stop codons. White boxes highlight coding sequences and grey boxes 5'- and 3'-UTRs. Dotted, black lines depict the spliced regions. DBD: DNA binding domain, OD: oligomerization domain, NLS and NES: nuclear localization and export signal, AHA: activator motif. **(C)** Examples of the electrophoresis profiles of high-resolution RT-PCR (HR RT-PCR) products obtained from seedling tissues exposed to different

temperatures generated by GeneMapper is shown. The scale on the x axis represents the size (bp); the scale on the y axis indicates the relative fluorescence of the PCR products, reflecting transcript abundance. Peaks are representing different isoforms. Red line shows the ladder. **(D)** Relative abundance of HsfA7 transcript variants obtained by HR RT-PCR of the same samples as in (A), amplified with the same set of primers. Integrated peak areas of RT-PCR products from each isoform were used as the relative expression levels. The percentage of the isoforms was calculated by dividing by the sum of all transcripts. The red line represents total HsfA7 transcript levels obtained by qRT-PCR of the same samples. Data points for leaf samples exposed for different time-points to 40°C (left) are the same as in Figure 3B.

analysed for size (length) and relative abundance on an ABI3730 and by the GeneMapper software (see Materials and Methods). Using this method each transcript represents a peak (Fig. 5C) and relative transcript abundance of splice variants corresponding to protein isoform I and splice variants corresponding to protein isoforms II and III are represented as a percentage of the total transcripts (Fig. 5D). Transcripts encoding for protein isoforms II and III were grouped together as they are expected to encode for protein isoforms with only one amino acid residue difference. Upon HS exposure for 5-30 min the induction of *HsfA7* transcripts can mostly be attributed to production of the full-length transcript of *HsfA7* (*HsfA7-Iα*) which corresponded to ~80% of total transcripts at 30 min (Fig. 5D). After 60 min the transcripts encoding for HsfA7-I are represented with less 37% of total transcripts and the remaining 63% are alternatively spliced variants encoding for protein isoforms II and III, which is in agreement with the RT-PCR results (Fig. 5A, D).

Total *HsfA7* transcripts in seedlings are induced after a 1 hour treatment of different temperatures ranging from 27.5-45°C (Fig. 5D, red line). Splicing was more efficient in seedlings exposed to temperatures up to 37.5°C with 90% of transcripts resulting in the A7-II/III group (Fig. 5D). Exposure to temperatures of 40°C and higher led to a gradual increase in the percentage of A7-I transcripts reaching almost 80% at 45°C. These results are in agreement with the RT-PCR results (Fig. 5A).

The immunoblot analysis of heat stressed tissues (Fig. 3, Fig. 4) did not reveal additional HS-inducible signals in addition to the ~55 kDa band corresponding to the full length HsfA7-I. Analysis of the AS pattern of HsfA7 revealed the existence of three putative protein isoforms (Fig. 6). HsfA7-I, which is generated by full or partial retention of intron 2 has all annotated domains including a full C-terminal NES, and a length of 359 aa residues. This protein has been annotated as the HsfA7 protein in a plant Hsf database (HEATSTER), as well as in the current tomato genome annotation (ITAG version 3.2). HsfA7-II is a 373 aa protein generated as a consequence of intron 2 and intron 3 splicing. Due to the frame-shift, HsfA7-II protein contains a truncated NES sequence and a C-terminal extension in comparison to HsfA7-I (Fig. 6). HsfA7-III is produced as a result of alternative acceptor site selection in exon 4 and has the same aa sequence as HsfA7-II with the exception of the C-terminus where instead of Gly in isoform II, an Asp-Ser dipeptide is found in isoform III (Fig. 6).

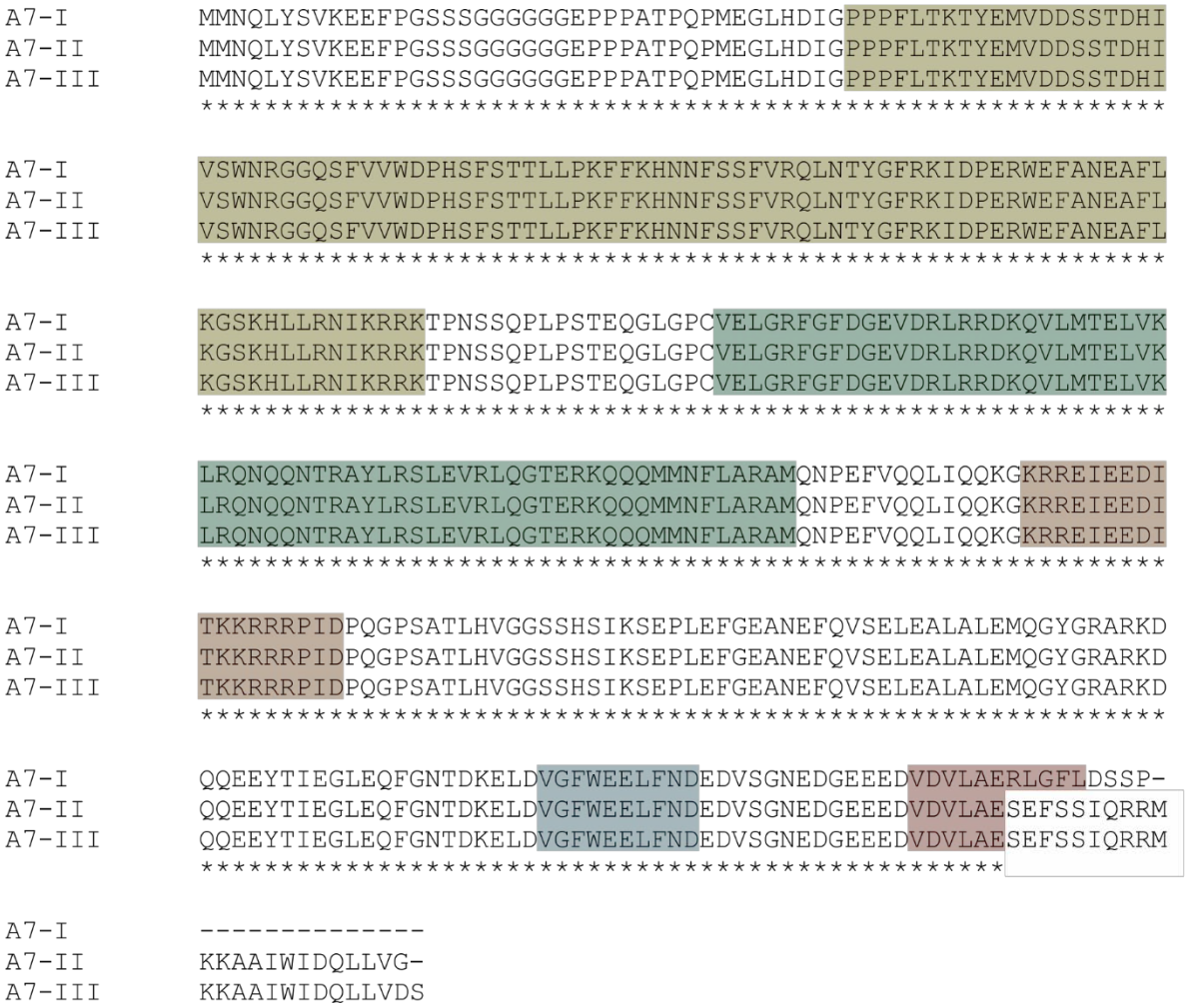

Figure 6. Amino acid sequence alignment of HsfA7-I (359 aa), HsfA7-II (373 aa) and HsfA7-III (374 aa). Functional domains are labelled with colours: DNA binding domain (yellow), oligomerization domain (green), nuclear localization signal (orange), AHA activation motif (blue), nuclear export signal sequence (red).

6.3 Properties of HsfA7 protein isoforms

6.3.1 Intracellular localization of HsfA7 isoforms

Alternative splicing of HsfA7 results in generation of putative protein isoforms which contain a functional NES or lack the C-terminal portion of it (Fig. 5, Fig. 6). The presence of the NES is important for the nucleocytoplasmic shuttling of Hsfs and can have an important functional relevance as shown for HsfA2 (Scharf 1998; Hu PhD thesis). In order to examine the intracellular distribution of HsfA7 proteins, the coding regions of the three HsfA7 isoforms were fused to the C-terminus of GFP, cloned into an expression vector and transformed into tomato mesophyll protoplasts. The intracellular localization of HsfA7-I showed a nucleocytoplasmic distribution (Fig. 7A). In the presence of the nuclear export inhibitor leptomycin B (LMB), HsfA7-I was retained in the nucleus (Fig. 7B), suggesting that the protein is dynamically shuttling between the two cellular compartments, as previously shown for other Hsfs (Scharf et al., 1998, Heerklotz 2001). HsfA7-II and HsfA7-III instead show a strong nuclear retention, as a consequence of the NES truncation (Fig. 7A). Due to the minor difference in the amino acid sequence between HsfA7-II and HsfA7-III (Fig. 6) subsequent transient assay experiments are performed only for HsfA7-I and HsfA7-II, as preliminary activity and stability tests showed that HsfA7-III seems to have similar properties like HsfA7-II.

As mentioned previously, HsfA2 is recruited into HSGs which allows a temporary storage of HsfA2 and keeps it in an inactive state (Nover et al., 1983; Nover et al., 1989; Scharf et al., 1998). Interaction with cytosolic class CI and CII sHsps mediates the recruitment and release of HsfA2 from HSGs (Scharf et al., 1998; Mishra et al., 2002; Port et al., 2004). We examined this possibility for HsfA7 by co-expressing HsfA7-I and HsfA7-II isoforms with Hsp17.4-CII-mCherry in protoplasts for 6 hours under normal conditions and then exposing them to a 39°C stress for 1 hour. Hsp17.4-CII served as a marker protein for HSGs and microscopy analysis revealed that Hsp17.4-CII-mCherry accumulates in cytosolic foci resembling HSGs (Fig. 7C). HsfA7-I, at large, did not co-localize with Hsp17.4-CII and HsfA7-II was completely retained in the nucleus (Fig 7C). Therefore, it is possible that HsfA7-I at most does not underlie repression by cytosolic CII sHsps, and HsfA7-II completely escapes the recruitment to HSGs due to its efficient nuclear retention. These findings point to possible differences in the regulation of activity and intracellular distribution of HsfA7 and HsfA2 under HS.

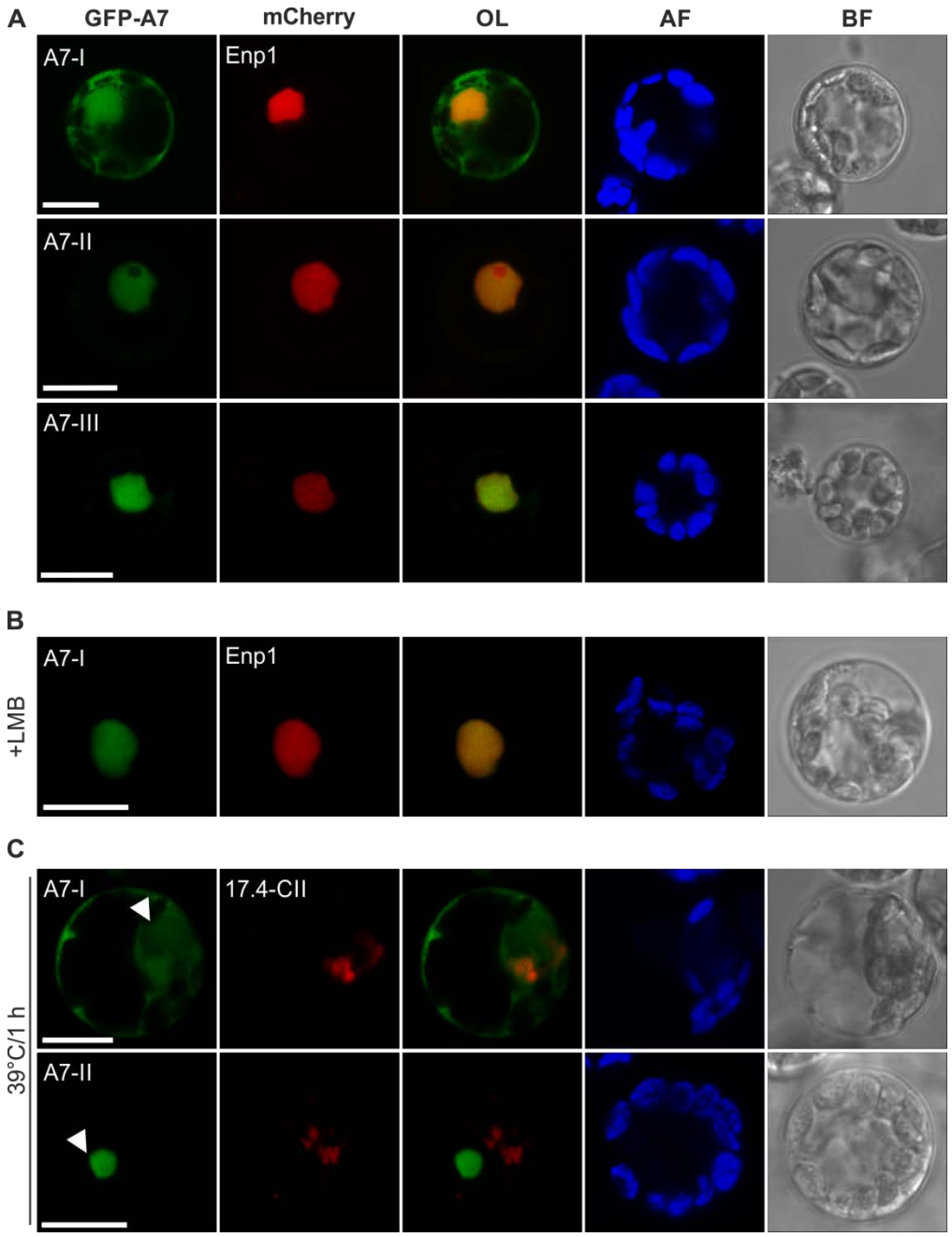

Figure 7. Intracellular localization of HsfA7 isoforms and recruitment to Hsp17.4-CII-containing HSGs.
(A) Intracellular distribution of HsfA7 isoforms in tomato mesophyll protoplasts. Plasmids containing GFP fused to the N-terminus of HsfA7 isoform I or II were transformed into protoplasts together with an ENP1-mCherry construct which served as a nuclear marker protein. GFP and mCherry fluorescence was analysed with CLSM after 6-8 hours of expression. **(B)** Protoplasts were transformed with a GFP-HsfA7-I construct and an equal amount of ENP1-mCherry. After 4 hours of expression the medium was supplemented with 22 ng μl^{-1} of the nuclear export inhibitor leptomycin B (LMB). GFP and mCherry fluorescence was analysed with CLSM after additional 3 hours of expression. **(C)** GFP-HsfA7-I or GFP-HsfA7-II constructs were co-expressed with an equal amount of Hsp17.4-CII-mCherry which served as a marker for the formation of heat stress granules (HSGs). After 6 hours of expression protoplasts were exposed to a HS of 39°C for 1 hour, immediately followed by CLSM detection of GFP and mCherry fluorescence. White arrowheads indicate the position of the nucleus. OL, overlay; AF, autofluorescence; BF, bright field. Scale bar = 10 µm.

6.3.2 Activity and cooperation with other Hsfs

As a class A Hsf, HsfA7 can be considered to function as a transcriptional activator which has already been confirmed for a plethora of class A Hsfs in tomato (Mishra et al., 2002; Chan-Schaminet et al., 2009; Fragkostefanakis et al., 2016). Therefore, we were interested in the transcriptional activation activity of the HsfA7 isoforms. For this purpose a β-glucuronidase (GUS) reporter assay (see Materials and methods) was first performed using the PGmhsp17.3B-CI:GUS reporter construct also named PHsp17*:GUS (Treuter et al., 1993; Bharti, 2004). This reporter plasmid consisted of a promoter fragment derived from the soybean (*Glycine max*) Hsp17.3B-CI gene containing two Hsf binding sites, typically present in promoters of tomato sHsps as well.

Protoplasts were transformed with HsfA7 encoding plasmids alone or in combination with different tomato class A Hsfs namely HsfA1a, HsfA2 and HsfA3 (Fig. 8A). HsfA7 isoforms expressed alone had only weak transactivation activity on this promoter which is similar to the findings for other Hsfs (Fig. 8A) (Bharti, 2004; Chan-Schaminet et al., 2009). However, co-expression of the HsfA7 isoforms with HsfA1a leads to a very strong transcriptional activation ("superactivation") of the GUS reporter indicating a hetero-oligomerization of the two Hsfs (Fig. 8A). The synergism of the two Hsfs can be concluded by comparing their activity when co-expressed to the additive activity of the two individual Hsfs (indicated by white diamonds). Considering this promoter, the synergistic activity of the HsfA1a-HsfA7 complex is even stronger than the one observed for the HsfA1a-HsfA2 complex. Remarkably, co-expression of HsfA3 with either HsfA7 isoform also leads to a very strong activity, similar to that of HsfA1a-HsfA7, while such an effect is not apparent in protoplasts co-expressing HsfA7 and HsfA2 (Fig. 8A). The strong activity of the HsfA7-HsfA3 complex was additionally confirmed by analysing the protein levels of the endogenous Hsp101 (Fig. 8B).

To expand the understanding of Hsf interplay to other promoters an 1 kb fragment of the *Sl*Hsp21.5ER (Solyc11g020330) promoter and an 1.7 kb fragment of the *Sl*HsfA2 (Solyc08g062960) promoter were cloned in front of the GUS coding region in the pRT vector. The promoters of these two tomato genes were chosen as representative of sHsp (high number of HSEs) and Hsf (low number of HSEs) promoters. Both, the combination of HsfA7 with HsfA1a, as well as with HsfA3 showed a strong cooperation capacity on the Hsp21.5-ER promoter (P*Sl*Hsp21.5-ER:GUS) (Fig. 8B). On the other hand, the transcriptional activation activity of HsfA1a-HsfA7 was much stronger compared to HsfA3-HsfA7 on the HsfA2 promoter (P*Sl*HsfA2:GUS). Regardless of the promoter used, HsfA7 and HsfA2 co-expression did not lead to an increase in activity compared to the additive activity of the single Hsfs (Fig 8A, 8B). These findings suggest that there is a preference for hetero-oligomerization among the class A Hsfs and that the transcriptional activity of the putative Hsf hetero-oligomeric complexes is promoter specific. Nevertheless, the HsfA1a-HsfA7 complex showed a rather strong activity on all tested reporter constructs (Fig. 8A, B). Altogether, these results indicate that HsfA7 has synergistic activity with HsfA1a and HsfA3 thereby regulating the transcription of downstream target genes including other Hsfs and Hsps.

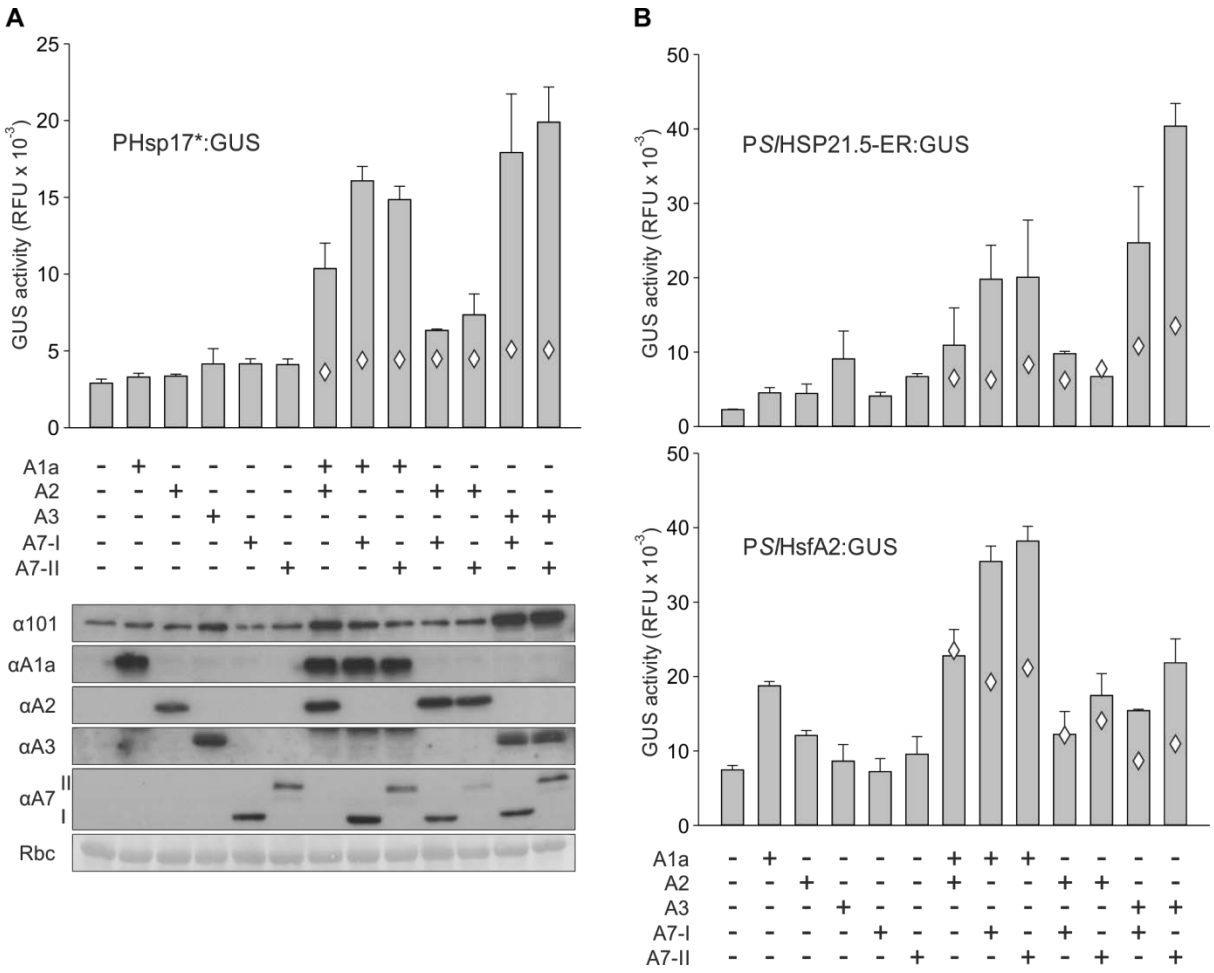

Figure 8. Transciptional activity and co-activator function of HsfA7-I and HsfA7-II.

(A) The Hsf transcriptional activity was monitored by co-expression of Hsf plasmid constructs with the HSE-containing GUS reporter construct PHsp17*:GUS (Bharti et al., 2004) in tomato mesophyll protoplasts. Samples were harvested after 7 hours of expression. Bars represent the average GUS activity of the indicated Hsfs alone or Hsf combinations and error bars the SD of three replicates. Diamonds indicate the calculated additive activity of two single Hsfs transformed alone (Chan-Schaminet et al., 2009). After the GUS fluorescence measurements, samples were subjected to immunodetection of the respective Hsfs and Hsp101 as an additional endogenous Hsf-dependent reporter using specific antibodies against HsfA1a, A2, A3, A7 and Hsp101. Rbc, Ponceau staining of the large subunit of Rubisco. **(B)** The Hsf transcriptional activity was determined as in (A) with the only difference that GUS expression was driven by the *Sl*Hsp21.5-ER and *Sl*HsfA2 promoter, respectively.

6.3.3 Interaction of HsfA7 with HsfA1a and HsfA3

As shown before, HsfA1a and HsfA2 can form hetero-oligomeric complexes which are highly active in transcriptional activation of HS-genes (Chan-Schaminet et al., 2009). This complex formation between tomato HsfA1a and HsfA2 is established through interactions of the linker and HR-B regions in the oligomerization domains of the two Hsfs (Chan-Schaminet et al., 2009). The activity tests indicated that such hetero-oligomers are formed between HsfA7 and HsfA1a, as well as HsfA7 and HsfA3. Localization of GFP-HsfA1a is mainly nuclear with very low cytosolic background (Lyck et al., 1997). GFP-HsfA3 was more evenly distributed between the nuclear and cytosolic compartments in non-stressed cells as shown by immuno-gold labelling (Bharti et al., 2000). In addition, exposure of the cells to HS resulted in a prevalent nuclear staining of HsfA3 (Bharti et al., 2000).

In order to examine whether the proteins physically interact with HsfA7 *in vivo*, bimolecular fluorescence complementation (BiFC) was utilized. The method enables visualization of protein interactions in living cells and is based on the fact that two non-fluorescent fragments of YFP can form a fluorescent complex if they are fused to two proteins that interact with each other (Kerppola, 2008). The C-EYFP tag was fused to the N-terminus of HsfA1a and HsfA3 (C-EYFP-A1a, C-EYFP-A3), while the N-EYFP tag was placed at the N-terminal end of the HsfA7 isoforms I and II (N-EYFP-A7-I, N-EYFP-A7-II). Plasmid constructs were ectopically expressed in tomato protoplasts and following 6-8 hours expression fluorescence was analysed by CLSM. Both HsfA7 protein isoforms interacted with HsfA1a resulting in detection of YFP fluorescence mainly in the nucleus of the cell (Fig. 9A, state 1). In a very few cells perinuclear spots of YFP fluorescence were detected as well (Fig. 9A, state 2). Interaction of HsfA7 isoforms with HsfA3 could also be observed mainly in the nucleus, however in this case, in addition to the diffuse nuclear signal, additional speckle-like structures could be detected in all cells (Fig. 9B).

In the BiFC system, the two YFP fragments have an ability to associate with each other independently of an interaction of the proteins they were fused to (Kerppola, 2008). This can result in weak background fluorescence (Hu et al., 2002; Kerppola, 2008). To test this, as a negative control experiment, the N-EYFP-HsfA7 constructs were co-expressed with plasmid constructs encoding for C-EYFP alone (Fig. 9C). In the majority of cells no YFP signal was detectable and only in very few cases weak fluorescence could be observed in the cytosol or nucleus (Fig. 9C).

Altogether, these results show that HsfA7-I and HsfA7-II can interact with both, HsfA1a and HsfA3.

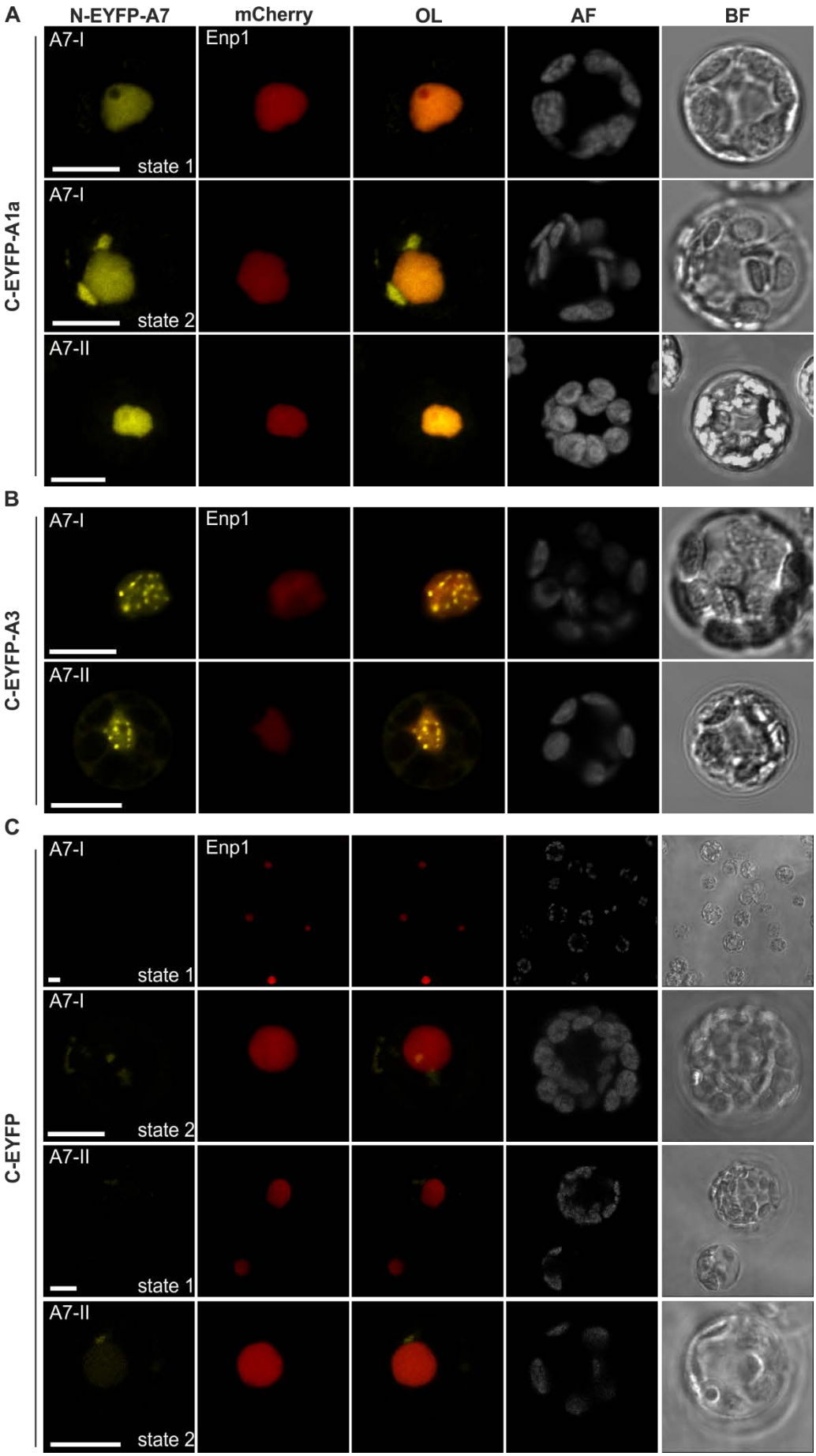
A
N-EYFP-A7
mCherry
OL
AF
BF
C-EYFP-A1a
A7-I
Enp1
state 1
A7-I
state 2
A7-II
B
C-EYFP-A3
A7-I
Enp1
A7-II
C
C-EYFP
A7-I
Enp1
state 1
A7-I
state 2
A7-II
state 1
A7-II
state 2

Figure 9. Interaction of HsfA7 isoforms with HsfA1a and HsfA3.
(A-B) Interaction of HsfA7 protein isoforms with HsfA1a (A) and HsfA3 (B). Protoplasts were transformed with equal amounts of plasmid DNA constructs encoding for the indicated EYFP-fusion proteins of HsfA7, HsfA1a, and HsfA3 and Enp1-mCherry (nuclear marker protein). **(C)** Control experiment to assess background fluorescence. Protoplasts were transformed with equal amounts of plasmid DNA constructs encoding for the indicated N-EYFP-fusion proteins of HsfA7 and the C-EYFP fragment. YFP and mCherry fluorescence was analysed after 6-8 hours of expression using CLSM. OL, overlay; AF, autofluorescence; BF, bright field. Scale bar = 10 µm.

6.3.4 Protein stability of HsfA7 isoforms

Although HsfA7 was found to be alternatively spliced resulting in several protein isoforms, the expression analysis in all cases showed one prominent HS-inducible signal corresponding to HsfA7-I (Fig. 3, Fig. 4). Furthermore, the expression of HsfA7 isoforms I and II in protoplasts revealed differences in their protein abundance in the activity tests, although both variants were expressed under the control of the constitutive CaMV 35S promoter and embedded into the same plasmid backbone (Fig. 8A). This suggested that there might be a difference regarding the regulation of protein turnover between these two protein isoforms.

To compare the rate of degradation of HsfA7 isoforms, protoplasts were transformed with plasmids encoding for N-terminally HA-tagged HsfA7-I or HsfA7-II under control of the CaMV 35S promoter. The isoforms were expressed for 4 hours and subsequently translation was arrested by the addition of cycloheximide (CHX). Protein levels were monitored in protoplasts for 6 hours following CHX treatment at 25°C or at 39°C (Fig. 10A). Under control conditions, HsfA7-II had a fast turnover, with a half-life of approximately 1.5 hours, while HsfA7-I was more stable and showed only a 20% reduction in protein levels after 6 hours following the translation inhibition (Fig. 10A). Exposure of protoplasts to HS resulted in a significant reduction of the stability of both isoforms. HsfA7-II was reduced by 50% within approximately 20 min and HsfA7-I after 6 hours of stress (Fig. 10A). The rapid degradation of HsfA7-II can explain the absence of a signal corresponding to this isoform in the immunoblot analyses of vegetative tissues exposed to different temperature regimes (Fig. 3, Fig. 4).

The stability of transcription factors is dependent on several factors including the activator function and DNA binding, but also interaction with other proteins (Molinari et al., 1999; Sundqvist and Ericsson, 2003; Röth et al., 2017). In order to investigate whether co-activators/interaction partners of HsfA7 affect its stability constant amounts of HsfA7 isoforms driven by the CaMV 35S promoter were co-expressed with increasing amounts of plasmids encoding for HsfA1a or HsfA3 in tomato protoplasts. Both isoforms had increased protein levels when titrated with either HsfA1a or HsfA3, with the effect being much more prominent for HsfA7-II (Fig. 10B). A similar experiment was performed using a 35S-GFP construct instead of HsfA7. In this case, there was no effect of co-expression of increasing amounts of HsfA1a or HsfA3 on the protein levels of GFP suggesting that the stabilizing effect is specific for the interaction with an Hsf partner (Fig. 10C).

RT-PCR was performed in order to examine whether the difference in protein levels of HsfA7-I and HsfA7-II are related to RNA stability or were induced on the protein level by HS and

interaction with the co-activators (Fig. 10D). Protoplasts were either transformed with the expression constructs for HsfA7 isoforms alone under non-stress conditions and treated with HS, or together with HsfA1a or HsfA3 followed by harvesting of the samples at one time-point (Fig. 10D). As shown by RT-PCR, no difference in RNA levels between the isoforms and treatments could be observed that could be correlated to the changes on the level of protein (Fig. 10D). Thus, we can conclude that differences in protein abundance determined by immunoblotting are most likely related to differences in protein turnover.

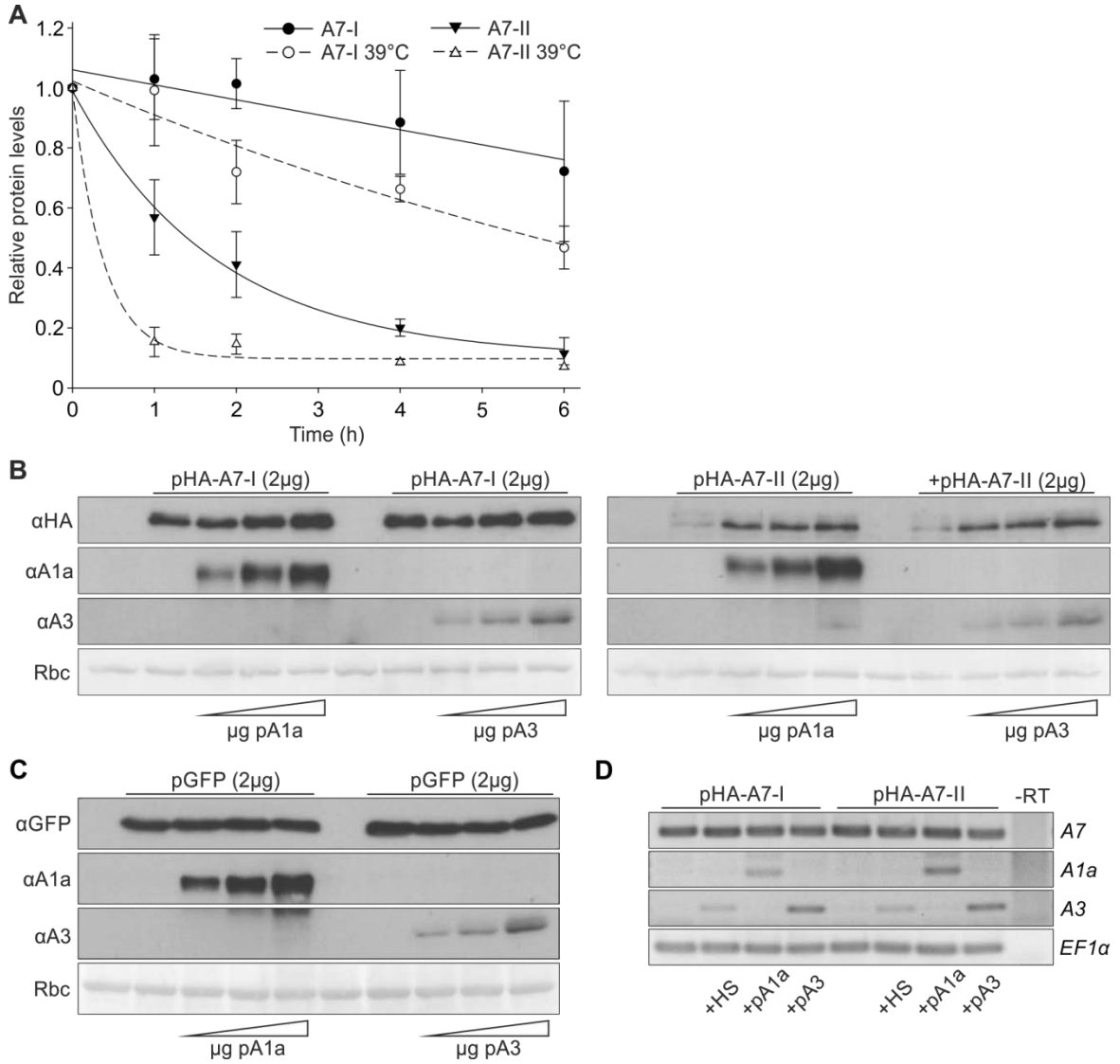

Figure 10. Protein turnover properties of HsfA7 isoforms.

(A) Protein turnover of HsfA7-I and HsfA7-II under control and HS conditions. Tomato mesophyll protoplasts were transformed with the plasmid constructs encoding for HA-A7-I or HA-A7-II and allowed to express the proteins for 4 hours after which the translation inhibitor cycloheximide was added at a final concentration of 20 µg ml^{-1}. Samples were further incubated at 25 or 39°C and harvested at different time points. Protein extracts were subjected to SDS-PAGE and immunoblotting, followed by detection with an HA specific antibody and quantification of protein signals using ImageJ. Data points represent averages of at least three independent experiments and error bars are SE. Lines represent the least square fit analysis with an exponential equation. **(B, C)** Effect of HsfA1a or HsfA3 co-expression on the protein levels of HsfA7 isoforms

and GFP. Protoplasts were transformed with a constant amount (2 µg) of the plasmid indicated on top of the panel and increasing amounts (2, 4 and 8 µg) of plasmid indicated at the bottom of the panel. After 7 hours of expression protoplast samples were harvested and subjected to SDS-PAGE and immunoblotting using specific antibodies for GFP, HsfA1a and HsfA3 and the HA antibody for the detection of HsfA7 proteins. Rbc, Ponceau staining of Rubisco large subunit shown as loading control. **(D)** Effect of HS, HsfA1a or HsfA3 co-expression on the RNA levels of HsfA7 isoforms. Equal amounts of plasmid encoding for HA-HsfA7-I or HA-HsfA7-II were transformed alone or together with HsfA1a or HsfA3 encoding plasmid into tomato protoplasts. pRT-Neo served as mock plasmid DNA. Expression time was 7 hours (in the +HS samples the HS was applied after 6 hours and harvesting was performed after an additional hour). PCR on cDNA was performed using a forward and reverse primer binding to HA and HsfA7, respectively to amplify HsfA7 transcript. HsfA1a and HsfA3 were amplified using gene specific primers. EF1α was used as a housekeeping gene.

6.4 Regulation of HsfA7 protein turnover

6.4.1 Protein turnover is dependent on the localization

In order to get more insights into the distinctive protein turnover profile between the two HsfA7 isoforms the first question was whether this discrepancy was related to the nucleocytoplasmic balance. For this purpose plasmid constructs encoding for the GFP-tagged protein isoforms I and II harbouring a mutation in the NLS were cloned as described in Materials and methods. NLS mutants (mNLS) were generated by mutating the lysine and arginine (K/R2) residues of the second part of the bipartite NLS into alanine residues (Fig. 11A), as previously described for tomato HsfA2 (Lyck et al., 1997). Additionally, an NES mutant (mNES) of isoform I was generated by replacement of hydrophobic and aromatic residues with alanines (Fig. 11A). To confirm that the mutation had the desired effects on protein localization, the corresponding plasmids were transformed into tomato mesophyll protoplasts and the intracellular localization of the proteins was analysed by CLSM (Fig 11B). The mNLS constructs showed an exclusive cytosolic localization suggesting that due to defective NLS the protein could not be imported into the nucleus. On the other hand, HsfA7-I-mNES showed a very dominant nuclear retention in contrast to the wild-type protein, however, in some cells residual cytosolic fluorescence signal could be observed (Fig. 11B).

To test the effect of the mutations on the protein levels of HsfA7, wild-type and mutant encoding plasmid constructs were transformed into protoplasts and protein levels were determined by immunoblot analysis after seven hours of expression (Fig. 11C). Mutation of the NLS leads to a significant increase in protein levels of both isoforms compared to the wild type (Fig. 11C). On the contrary, HsfA7-I-mNES showed reduced abundance when compared to wild-type HsfA7-I (Fig. 11C). In order to quantify this observation, protoplasts were transformed and treated with CHX, followed by harvesting of the cells at different time points as described previously (Fig. 10A). Remarkably, both mNLS proteins retained steady state levels during the 6 hours following CHX treatment (Fig. 11D). From these results it can be concluded that HsfA7 protein degradation occurs in the nucleus.

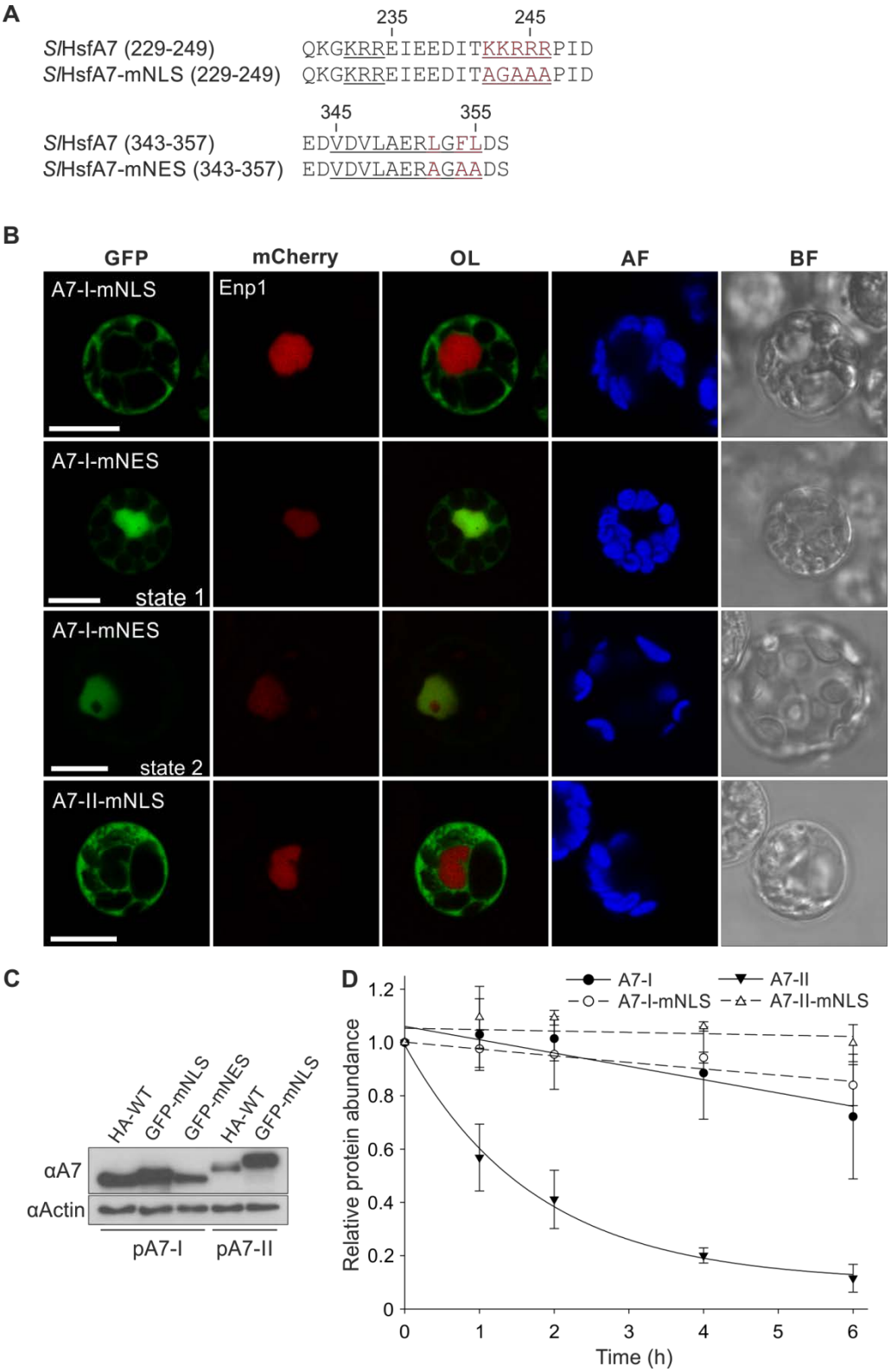

Figure 11. Effect of intracellular localization on the protein turnover of HsfA7.

(A) Amino acid replacements introduced in order to generate NLS (mNLS) and NES mutant (mNES) isoforms of HsfA7. The NLS and NES is underlined and changes are depicted in red. **(B)** Intracellular localization of NLS and NES mutant isoforms of HsfA7. Protoplasts were transformed with plasmid constructs encoding for the indicated mutant isoforms and an equal amount of ENP1-mCherry (nuclear marker protein). GFP and mCherry fluorescence was analysed with CLSM after additional 7 hours of expression. OL, overlay; AF, autofluorescence;

BF, bright field. Scale bar = 10 µm. **(C)** Tomato protoplasts were transformed with equal amounts of the plasmid constructs for WT, mNLS and mNES isoforms of HsfA7 as indicated on the top of the panel. After 7 hours of expression samples were harvested and immunoblotting was performed. HsfA7 protein variants were detected using a specific antibody. Actin served as a loading control. **(D)** Protein turnover of mNLS isoforms of HsfA7. The experiment was performed like described in Figure 10A and only control conditions (25°C) were applied. Data points shown for WT HsfA7 isoforms are the same as in Figure 10A and are shown here for comparison.

6.4.2 Proteasome-dependent protein degradation

Many transcription factors undergo degradation in the nucleus which is mediated by the ubiquitin-proteasome pathway (Kodadek et al., 2006). Over the years it became clear that in some systems activator turnover is tied to the ability of the factor to drive transcription. Furthermore, it has been shown that the VP16 activation domain activity is dependent on ubiquitination (Salghetti, 2001). Tomato HsfB1 abundance is regulated by the ubiquitin-proteasome system (Hahn et al., 2011; Röth et al., 2017). However, so far, this has not been shown for class A Hsfs. For this purpose tomato protoplasts were transformed with the plasmid construct encoding for HsfA7-II, which is the rapidly degraded HsfA7 isoform. Following 4 hours of expression, the cells were treated with CHX and MG132, where the latter has been shown to be an efficient proteasome inhibitor (Lee and Goldberg, 1998). Samples were taken one and two hours following the treatment. Immunoblotting revealed a significant decrease in protein levels of HsfA7 after 2 hours in the DMSO-treated control samples (Fig. 12A). In contrast, when MG132 was added to the cells, there was almost no decline in protein abundance. The protein levels after 2 hours (T_2) were comparable to the sample taken immediately following the treatment (T_0) (Fig 12A).

In a similar experiment, a tomato cell suspension culture was used to test whether the endogenous proteins also undergo proteasomal degradation similar to the findings in protoplasts. The cell culture was either treated with MG132 or DMSO as control, followed by direct exposure to either 30, 35 or 40°C for 1 hour, while control samples were kept at 25°C. Cells were harvested directly after the stress exposure. Remarkably, in this cell type in addition to the ~55 kDa HsfA7-I protein another HS inducible band at ~60 kDa could be detected by immunoblotting (Fig. 12B). This protein band runs at the same size as HsfA7-II and III and the abundance was comparable to isoform I at 30°C and lower than isoform I at 35°C (Fig. 12B). At 40°C both isoforms had low abundance (Fig. 12B). Therefore, we conclude that HsfA7-II, HsfA7-III or both HsfA7 protein isoforms which are generated as a consequence of alternative splicing can be produced endogenously at a sufficient amount to be detected in tomato cell suspension culture. Furthermore, the intensity of both HsfA7 protein signals was greatly enhanced in MG132-treated cells compared to untreated cells (Fig. 12B). HsfA2-I protein was induced at 35 and 40°C and accumulated at even higher levels following proteasome inhibition (Fig. 12B). Interestingly, although HsfA2 is not detectable at 30°C the protein accumulates at low levels in the MG132-treated cells (Fig. 12B). Another remarkable observation is that not only HsfA2 and HsfA7 but also HsfA1a showed a dramatic increase in MG132-treated cells (Fig. 12B). In addition, HsfA1a accumulated in DMSO-treated cells exposed to 40°C, suggesting temperature-dependent regulation of the master regulator at the post-transcriptional level, considering that

several studies have shown that at transcript level HsfA1a is a constitutively expressed gene under various conditions (Mishra et al., 2002; Hahn et al., 2011).

Taken together, these results highlight the impact of proteasomal degradation on the stress-induced HsfA2 and HsfA7 but also on the master regulator of HSR HsfA1a.

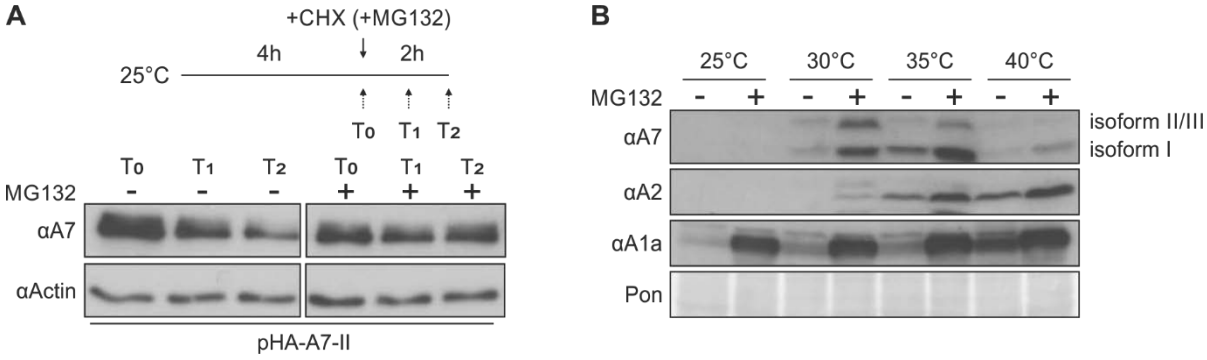

Figure 12. Inhibition of HsfA7 degradation by MG132.
(A) Protoplasts were transformed with an expression plasmid carrying the HA-HsfA7-II cassette and treated like indicated in the scheme on top. After 4 hours of expression CHX was added to a final concentration of 20 µg ml^{-1} together with 1 µl DMSO (-) or 50 µM MG132 (+). Samples were harvested immediately (T0), after 1 (T1) and 2 (T2) hours. HsfA7 protein was detected using a specific antibody after immunoblotting. Actin is shown as an equal loading control. **(B)** Tomato cell culture was treated with 50 µM MG132 (+) or the corresponding volume of DMSO (-) and immediately exposed to 30, 35, or 40°C for 1 hour or kept at 25°C for the same time. Following the HS treatment samples were harvested and subjected to SDS-PAGE and immunoblotting. A specific antibody against HsfA7, HsfA2 and HsfA1a was used to detect the Hsfs. Ponceau staining of the immunoblot is shown as an indication of equal loading.

6.4.3 The AHA motif is not essential for degradation

Different studies reported a link between degradation rate and the activation domain potency of transcriptional activator proteins. The transcriptional activity targets these proteins for degradation by the ubiquitin-proteasome system (Molinari et al., 1999; Thuerauf et al., 2002; Sundqvist and Ericsson, 2003). In this direction, mutations that abolish the activator function have been shown to make the protein more resistant to proteasomal degradation and therefore increase their half-life (Molinari et al., 1999; Sundqvist and Ericsson, 2003). As recently shown, proteasomal degradation of HsfB1 is dependent on DNA binding and the repressor function as demonstrated by mutations of the R/KLFGV motif (Röth et al., 2017). Whether the degradation of class A Hsfs is triggered by the AHA motifs has not been investigated so far.

Short peptide motifs enriched in aromatic and large hydrophobic amino acid residues embedded in an acidic surrounding are essential for transcriptional activity of the majority of class A Hsfs (Döring et al., 2000; Nover et al., 2001; Kotak et al., 2004). An FWxxF/L,F/I/L has been described as a conserved prototype of the AHA motif present in the CTADs of many class A Hsfs (Kotak et al., 2004) as well as in HsfA7 (Fig. 13A). Mutation analysis showed that aromatic and large hydrophobic aa residues have an important role in AHA motif function (Döring et al., 2000). However, alanine substitutions of the central tryptophan residues could significantly

reduce the transcriptional activity of HsfA2, but did not completely abolish the transcriptional activity of HsfA1a which has been related to the presence of acidic regions adjacent to the AHA motifs contributing to the activity of the factor (Döring et al., 2000).

Point mutations were introduced to replace the aromatic and large hydrophobic amino acids by alanine. In addition to this, deletion mutants were created by deletion of 9 aa residues of the AHA motif (ΔAHA, Δ324-332) (Fig. 13A). Neither the mutation nor the deletion of the AHA motif completely abolished the activity of the HsfA7 isoforms as tested by a GFP reporter assay (Fig. 13B). The expression vectors of mAHA or ΔAHA variants were co-expressed either with a GFP reporter controlled by the *S*lHsp21.5-ER or *S*lHsfA2 promoter. Regardless of the utilized promoter, HsfA7-I-mAHA and HsfA7-I-ΔAHA had a similar activity which was significantly reduced compared to the WT HsfA7-I, but not completely abolished. On the other hand, HsfA7-II-mAHA had a comparable activity to the WT protein on both promoters while HsfA7-II-ΔAHA had a significantly lower activity on the *S*lHsp21.5-ER promoter (Fig. 13B).

Since deletion of the AHA motif had a slightly stronger impact on the activity we used it to investigate whether a reduction in the transcriptional activity has an influence on the half-life of HsfA7 protein isoforms. The stability assay was performed as described above (Fig. 13C). As a result, HsfA7-I-ΔAHA had a slightly faster protein turnover compared to the full-length HsfA7-I while HsfA7-II-ΔAHA had a half-life of ~2.5 hours compared to the 1.5 hours of the full-length HsfA7-II. However, after 6 hours the protein abundance of WT and ΔAHA HsfA7-II was the same (Fig. 13C). This difference might be related to the fact that the loss of activity was more prominent for HsfA7-II than for HsfA7-I. Nevertheless, it can be concluded that the deletion of the important residues in the AHA motifs of HsfA7-I and HsfA7-II does not significantly alter their protein stability.

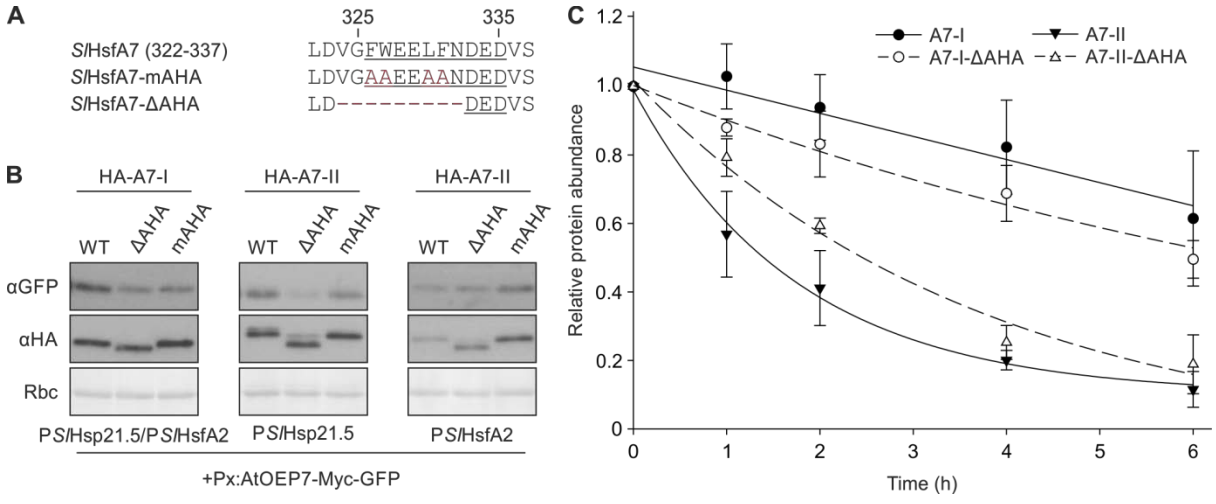

Figure 13. Importance of the AHA domain in HsfA7 activity and protein turnover.
(A) Amino acid replacements and deletion performed in order to generate AHA mutants and deletions of HsfA7-I and HsfA7-II. The AHA motif is underlined and changes/deletion is depicted in red. **(B)** Basal transcriptional activity of mAHA and ΔAHA HsfA7 isoforms. Tomato mesophyll protoplasts were transformed with equal amounts of the reporter plasmid P*S*lHsp21.5:AtOEP7-Myc-GFP or P*S*lHsfA2:AtOEP7-Myc-GFP and a plasmid encoding for HsfA7 WT, mAHA or ΔAHA with an HA tag as indicated on the top and bottom of the

panels. After 6-8 hours of expression protoplast samples were harvested and subjected to SDS-PAGE and immunoblotting. A specific antibody was used to detect GFP, while HsfA7 variants were detected using an HA antibody. Rbc, Ponceau staining of Rubisco large subunit shown as loading control. **(D)** Protein turnover of WT and ΔAHA isoforms of HsfA7. The experiment was performed like described in Figure 10A and only control conditions (25°C) were applied on two biological replicates. Data points shown for WT HsfA7 isoforms are the same as in Figure 10A and are shown here for comparison.

6.5 Significance of HsfA7 as a transcriptional co-activator

6.5.1 The role of HsfA7 in the oligomeric complex with HsfA1a and HsfA3

Since deletion of the complete AHA motif did not completely abolish the activity of HsfA7 we were interested whether these deletion mutants still had the co-activator function leading to high transcriptional activity when co-expressed with HsfA1a or HsfA3. A GFP-reporter assay was performed in tomato protoplasts in a similar manner as the previously described GUS reporter assay (Fig. 8B). In this case instead of GUS, GFP expression was driven by the *Sl*Hsp21.5-ER promoter. After harvesting, samples were subjected to SDS-PAGE and immunoblotting to compare the protein levels of GFP in different samples as an indication for Hsf-transcriptional activity.

Plasmid constructs encoding for HsfA1a, HsfA7 and HsfA7-ΔAHA were expressed either alone or in combination as indicated on top of the panel (Fig. 14A). We found that the AHA motif deletion in HsfA7 isoforms I and II did not influence the co-activator potential of the factor. The co-expression of either WT HsfA7 or HsfA7-ΔAHA constructs with either HsfA1a or HsfA3 led to a very high transcriptional activation activity as shown by the GFP signal intensities (Fig. 14A). This indicates that the AHA motif of HsfA7 in the HsfA7-HsfA1a or HsfA7-HsfA3 complex does not play a crucial role in the resulting transcriptional activity of the hetero-oligomeric complexes.

In the next step we analysed the role of the NLS domain of HsfA7 in the co-activator complexes. The same experiment as described above was performed, only this time with the HsfA7-mNLS instead of HsfA7-ΔAHA constructs (Fig. 14B). NLS mutants of HsfA7 isoforms I and II did not have any transcriptional activity on the *Sl*Hsp21.5-ER promoter due to their cytosolic retention. When the NLS mutants were co-expressed with HsfA1a the strong transcriptional activity of the co-activator complex was lost (Fig. 14B). The combination of HsfA7-II-mNLS and HsfA3 lead to a similar result. Remarkably, when HsfA3 was co-expressed with HsfA7-I-mNLS this almost completely abolished the activity of HsfA3 alone. This could indicate a cytosolic retention of HsfA3 by the HsfA7-I-mNLS (Fig.14B).

Taken together, these results show that although the AHA motif does not play a significant role in the activity of the HsfA7-HsfA1a or HsfA7-HsfA3 complex, the NLS of HsfA7 enhances the activity of the complex by promoting its nuclear translocation and retention.

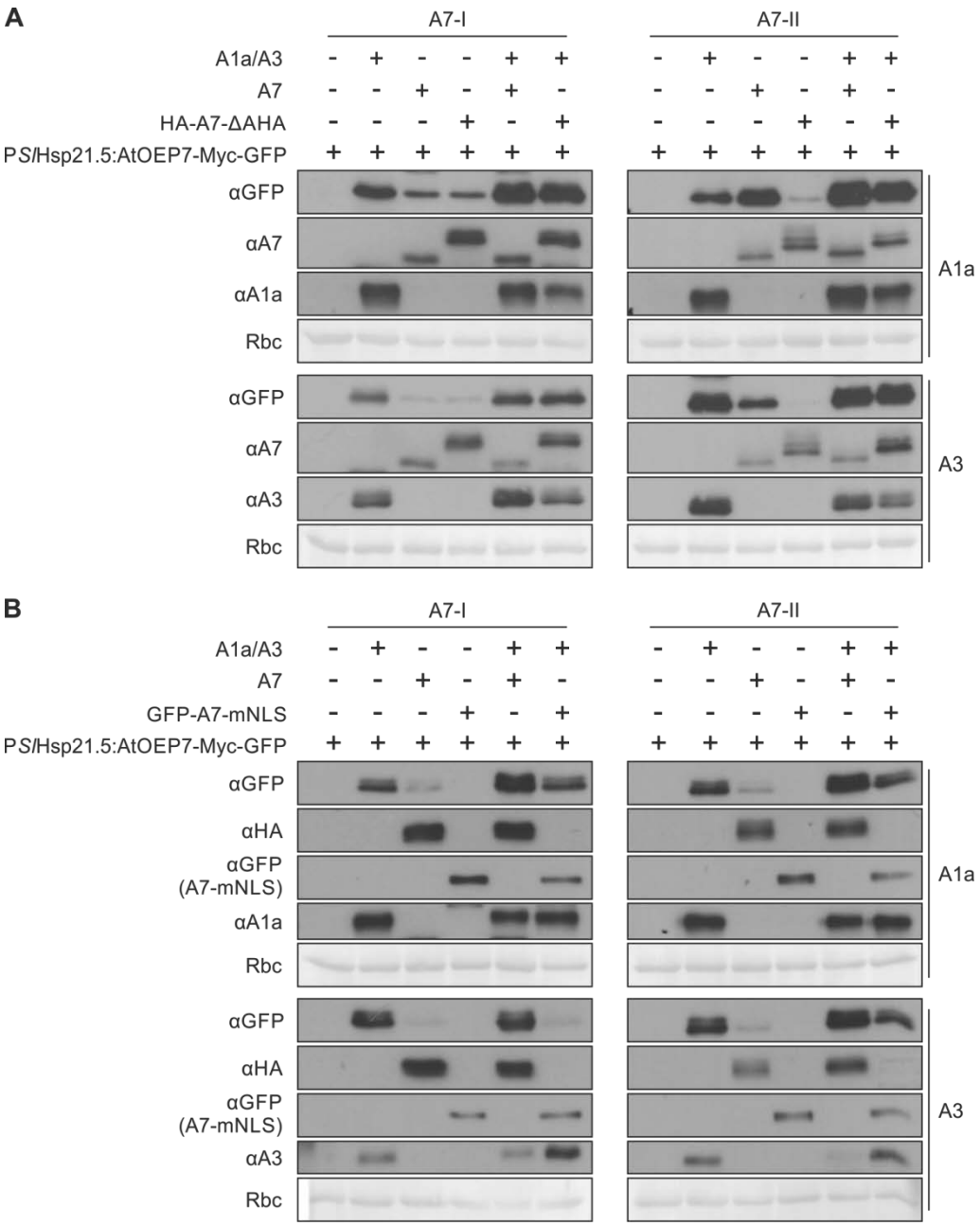

Figure 14. The importance of HsfA7 AHA and NLS domain for its function as a transcriptional co-activator.
(A, B) Tomato mesophyll protoplasts were transformed with equal amounts of the reporter plasmid P*S*Hsp21.5:AtOEP7-Myc-GFP and Hsf-encoding plasmids as indicated on top of the panels. After 6-8 hours expression protoplast samples were harvested and subjected to SDS-PAGE and immunoblotting. In (A) specific antibodies were used to detect GFP, HsfA1a, HsfA3 and HsfA7 WT and ΔAHA proteins. In (B) the WT HsfA7 isoforms were detected using an HA specific antibody, while the mNLS isoforms were detected using a GFP antibody. Rbc, Ponceau staining of Rubisco large subunit shown as loading control.

6.5.2 A functional NLS of HsfA7 is prerequisite for nuclear import of hetero-oligomers

The previous activity results indicated two different modes regarding the interaction of HsfA1a and HsfA3 with the mNLS isoforms of HsfA7 (Fig. 14B). In the first scenario, HsfA7-mNLS does not interact with HsfA1a, therefore, the co-expression leads to a transcriptional activity similar to the one of HsfA1a alone. In the second case, the strong inhibition of HsfA3 activity by HsfA7-I-

mNLS co-expression could be caused by cytosolic retention of a complex containing the two factors.

In order to address this question, a BiFC experiment was performed as described previously (Fig. 9). In here, the N-EYFP was placed at the N-terminus of the HsfA7-mNLS isoforms I and II, whereas C-EYFP was fused to the N-terminus of HsfA1a and HsfA3. The plasmid constructs were co-transformed into tomato mesophyll protoplasts as indicated on the panels and CLSM was performed following a 6-8 hours expression time (Fig. 15A). As a result, fluorescence of the reconstituted YFP was detected only in the cytosol and this was the case for all observed cells. Furthermore, there were two types of fluorescent signal in the cytosolic compartment of the cells. The YFP signal was either homogenously distributed in the cytosol (as shown on the example of HsfA7-I) or patches of YFP fluorescence localized in the periphery of the nucleus could be observed (Fig. 15A). The perinuclear spots could indicate that hetero-oligomers were formed but could not be imported into the nucleus and accumulated in its proximity. One cell for each isoform is shown to describe the effects although for both isoforms both examples could be detected (Fig. 15A). As a negative control, like in the previous YFP experiment (Fig. 9), EYFP-HsfA7-mNLS was co-expressed with the C-EYFP fragment resulting in similar results - in most cases no fluorescence or very weak background fluorescence could be seen (data not shown).

This observation made clear that NLS mutants of HsfA7 can interact with HsfA1a and HsfA3 in the cytosol, however, these hetero-oligomeric complexes cannot be imported into the nucleus. Nevertheless, this type of experimental setup could not show the fraction of HsfA1a and HsfA3 which is not affected by the interaction with NLS mutant of HsfA7. In this direction, GFP-tagged HsfA1a or HsfA3 was co-expressed with the double amount of plasmid carrying the ORF encoding the untagged HsfA7-I-mNLS. By this we could visualize the total HsfA1a and HsfA3 protein in the cell, while HsfA7 presence was confirmed by immunoblotting (Fig. 15B, C). As a control, GFP-HsfA1a and GFP-HsfA3 were expressed alone. While HsfA1a has a dominant nuclear localization with occasional low cytosolic fluorescence, HsfA3, which has no annotated NES, is evenly distributed between the nucleus and cytosol (Fig. 15B). One possibility is that there is an NES which has not been discovered so far or the protein is efficiently co-imported by interacting with some other factors (Hsfs). Nevertheless, by adding HsfA7-I-mNLS, the nucleocytoplasmic balance of HsfA1a localization shifted and a major fraction of the protein was retained in the cytosol while HsfA3 was almost entirely cytosolic (Fig. 15B).

These results explain the observed effects of HsfA7-mNLS co-expression in the activity experiment (Fig 14B) – the NLS mutant of HsfA7-I interacts with and keeps a big portion of HsfA1a in the cytosol, whereas interaction with HsfA3 restricts HsfA3 almost exclusively from entering the nucleus.

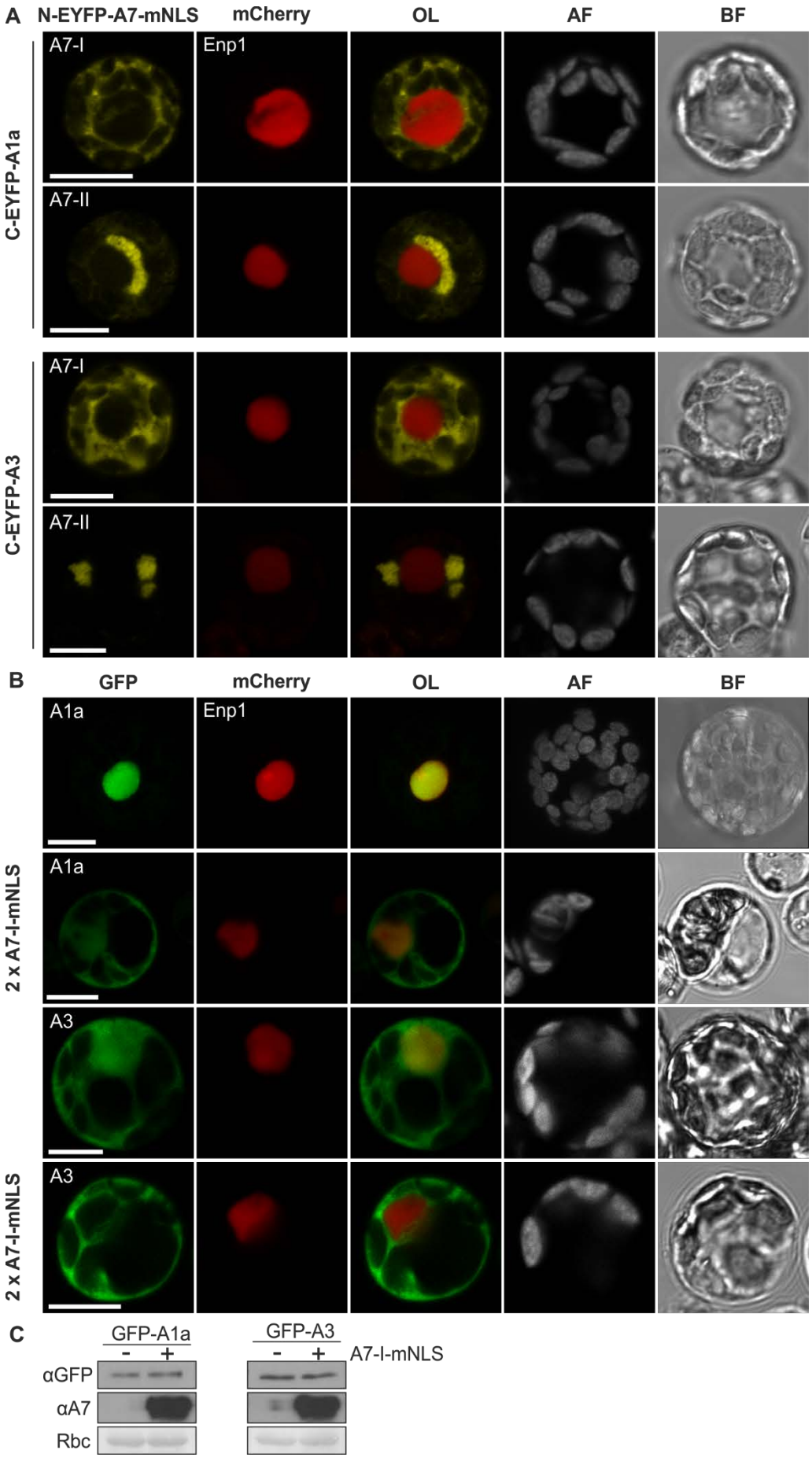
A
N-EYFP-A7-mNLS
mCherry
OL
AF
BF
C-EYFP-A1a
A7-I
Enp1
A7-II
C-EYFP-A3
A7-I
A7-II
B
GFP
mCherry
OL
AF
BF
2 x A7-I-mNLS
A1a
Enp1
A1a
A3
2 x A7-I-mNLS
A3
C
GFP-A1a
- +
GFP-A3
- +
A7-I-mNLS
αGFP
αA7
Rbc

Figure 15. Cytosolic retention of HsfA1a and HsfA3 is enhanced through Interaction with HsfA7-mNLS.
(A) Interaction of HsfA1a/HsfA3 with the HsfA7-mNLS isoforms I and II. Protoplasts were transformed with equal amounts of plasmid DNA constructs encoding for the indicated YFP-fusion proteins of HsfA7-mNLS, HsfA1a and HsfA3, and Enp1-mCherry (nuclear marker protein). YFP and mCherry fluorescence were analysed after 6-8 hours of expression using CLSM. **(B)** Effect of HsfA7-I-mNLS co-expression on the localization of HsfA1a and HsfA3. Protoplasts were transformed with plasmid constructs encoding GFP-tagged HsfA1a or HsfA3 and an equal amount of ENP1-mCherry. An additional sample was transformed with the double amount of the plasmid construct encoding for HsfA7-I-mNLS, as indicated on the side of the panel. GFP and mCherry fluorescence were analysed after 6-8 hours of expression using CLSM. OL, overlay; AF, autofluorescence; BF, bright field. Scale bar = 10 µm. **(C)** Immunoblot of protein extracts of protoplast samples shown in (B). HsfA7-I-mNLS protein was detected using an antibody specific for HsfA7, while HsfA1a and HsfA3 were detected using a GFP specific antibody. Ponceau staining of Rubisco large subunit is shown as a loading control.

6.5.3 HsfA7 enhances the protein turnover of HsfA1a and HsfA3

The observed effects of interaction partner co-expression on the protein levels of HsfA7 (Fig. 10B) made us ask the question about what effect HsfA7 could have on the protein turnover of HsfA1a or HsfA3. Furthermore, the activity assays performed in order to dissect the function of HsfA7 in the hetero-oligomeric complexes (Fig. 14A, B) showed that HsfA1 and HsfA3 protein levels were differentially affected by co-expression of the mutant and wild-type isoforms.

To investigate this phenomenon in more detail, we co-expressed constant amounts of HsfA1a or HsfA3 encoding plasmid in tomato protoplasts with increasing amounts of plasmid encoding for HsfA7-I or HsfA7-II. Interestingly, increasing amounts of HsfA7 coincided with a gradual decrease in protein levels of both, HsfA1a and HsfA3 (Fig. 16A). The effect was more prominent with HsfA7-I than HsfA7-II (Fig. 16A). Increasing amounts of HsfA7-II led to a gradual decrease of HsfA3 levels, however, this had a much weaker effect on the amount of HsfA1a protein as only the highest amount of HsfA7-II had a significant effect on HsfA1a (Fig. 16A). To understand whether a nuclear localization of the HsfA7-HsfA1a complex is needed for the enhanced degradation of HsfA1a we added increasing amounts of HsfA7-I-mNLS plasmid to a constant amount of HsfA1a (Fig. 16A). Remarkably, the levels of HsfA1a remained stable and even slightly increased with the highest amount of HsfA7-I-mNLS, possibly due to partial cytosolic retention of HsfA1a (Fig. 15B) which suggests that the HsfA7-mediated enhancement of HsfA1a degradation requires nuclear import.

The same experiment was performed with increasing amounts of HsfA2 and a constant amount of HsfA1a. Here, already a plasmid DNA ratio of 1:1 caused the accumulation of HsfA1a at higher levels (Fig. 15C, third lane) which remained unchanged when increasing amounts of HsfA2 plasmid were utilized (Fig. 15C). In addition, a control experiment with GFP instead of HsfA1a was performed (Fig 15D). Co-expression of increasing amounts of HsfA7-I or HsfA7-II encoding plasmid did not affect the protein levels of GFP.

The stability of HsfA1a and HsfA3 gradually declined by titrating with plasmid encoding for the HsfA7 isoforms even in the presence of the GFP reporter controlled by the *Sl*Hsp21.5-ER promoter, suggesting that the presence of additional DNA binding sites does not further affect the stability of the factors (Fig. 16E). Interestingly, GFP which indicate the activity of the hetero-

oligomeric complex remained at steady state levels despite the significant reduction of HsfA1a levels (Fig. 16E). In the case of HsfA3, GFP levels declined in accordance to the HsfA3 protein levels (Fig. 16E). The same reporter experiment with constant amounts of HsfA1a and titration of HsfA2 showed again an enhancement of HsfA1a levels (Fig. 16E). The GFP reporter levels were, in this case, slightly increased by co-expression of the two factors, and stayed at a similar level regardless of a further increase of HsfA2 plasmid amount, which is in agreement with the saturation of HsfA1a protein amount (Fig. 16E).

All in all, the interaction of HsfA1a with HsfA2 or HsfA7 has a significant impact on the fate of the factors and thereby the activity of the complex. In addition, HsfA7 co-expression leads to destabilization of HsfA3.

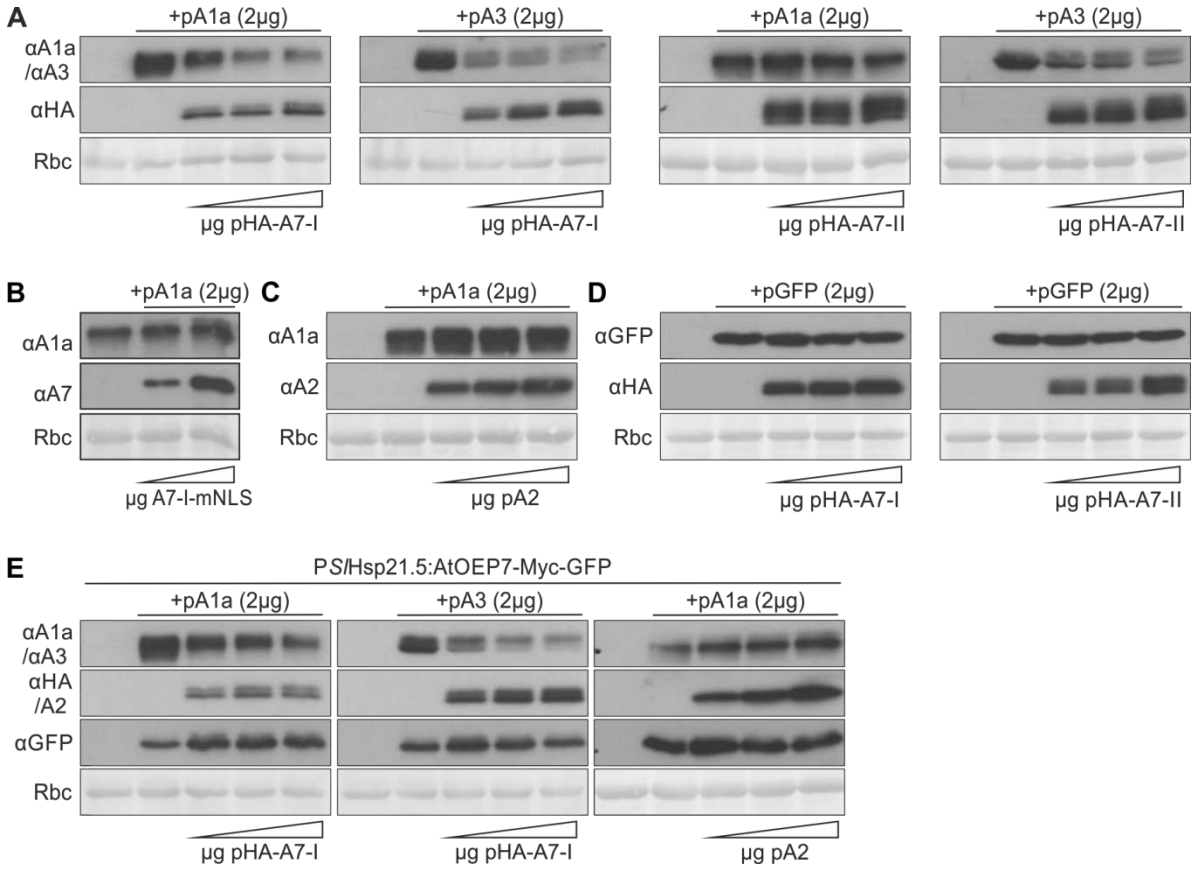

Figure 16. Effect of HsfA7 co-expression on the protein turnover of HsfA1a and HsfA3.
(A, D) Effect of HsfA7-I or HsfA7-II co-expression on the protein levels of HsfA1a, HsfA3 and GFP. Protoplasts were transformed with a constant amount (2 µg) of the plasmid indicated on top of the panel and increasing amounts of plasmid encoding for HsfA7-I or HsfA7-II (2, 4 and 8 µg) as indicated at the bottom of the panel. **(B, C)** Effect of HsfA7-I-mNLS or HsfA2 co-expression on the protein levels of HsfA1a. The experiment was performed as described in (A, C). **(E)** Effect of HsfA7-I, HsfA7-II or HsfA2 co-expression on the protein levels of HsfA1a or HsfA3 like described in (A, C). Additionally, a P*S*/Hsp21.5:AtOEP7-Myc-GFP construct was co-transformed. In all experiments protoplast samples were harvested and subjected to SDS-PAGE and immunoblotting after 7 hours of expression. The Hsfs and GFP protein were detected using specific antibodies or HA specific antibody when HA-tagged Hsfs were used. Rbc, Ponceau staining of Rubisco large subunit shown as loading control.

6.5.4 HsfA7 and HsfA2 compete for hetero-oligomerization with HsfA1a

The master regulator HsfA1a can interact with HsfA2 (Chan-Schaminet et al., 2009) as well as with HsfA7 (Fig. 8, Fig. 9) which has a differential impact on its fate and thereby activity (Fig. 16A, C). Considering that HsfA2 and HsfA7 co-exist under specific temperature regimes (Fig. 3) we asked whether HsfA1a shows a preferential interaction with any of the two co-factors.

To dissect this situation a "competition assay" was performed based on the activity of Hsfs on a GUS reporter construct (Fig. 17). While both HsfA2 and HsfA7 are co-activators of HsfA1a (Fig. 8), the NLS mutant of HsfA7-I neither had any activity per se, nor did it have a co-activator function when co-expressed with HsfA1a (Fig. 14B). Therefore, protoplasts were transformed with the PHsp17*:GUS reporter construct and HsfA1a, A2, A7-I-mNLS plasmid constructs in amounts indicated at the bottom of the bar charts (Fig. 17A, B). Co-expression of HsfA1a and HsfA2 in equal amounts led to a synergistic activation of GUS expression as described previously (Fig. 17A). Adding an HsfA7-I-mNLS encoding plasmid in the ratio 1:1:0.5 or 1:1:1 (HsfA1a:HsfA2:HsfA7-I-mNLS) had almost no effect on GUS activity. However, 2- or 4- fold higher amount (1 µg or 2 µg) of HsfA7-I-mNLS plasmid compared to the other Hsfs caused a gradual inhibition of the GUS activity conferred by HsfA1a-HsfA2 interaction (Fig. 17A).

In an opposite experimental setup, protoplasts were transformed with constant amounts of HsfA1a (0.5 µg) and HsfA7-I-mNLS (0.5 µg) plasmids and increasing amounts of HsfA2 (0.25-2 µg) (Fig. 17B). Increased HsfA2 levels led to higher GUS activity overcoming the repressor effect of HsfA7-I-mNLS (Fig. 17B). Interestingly, GUS activity was similar in protoplasts transformed with equal amounts of HsfA1a:HsfA2:HsfA7-I-mNLS or with equal amounts of HsfA1a:HsfA2 (Fig. 17B).

All in all, the results of this assay indicate that, when all three factors are present in the cell (HsfA1a, HsfA2 and HsfA7) HsfA2 and HsfA7 can compete for interaction with the master regulator HsfA1a, thereby regulating at the same time the transcription of HS inducible genes as well as the protein turnover of HsfA1a.

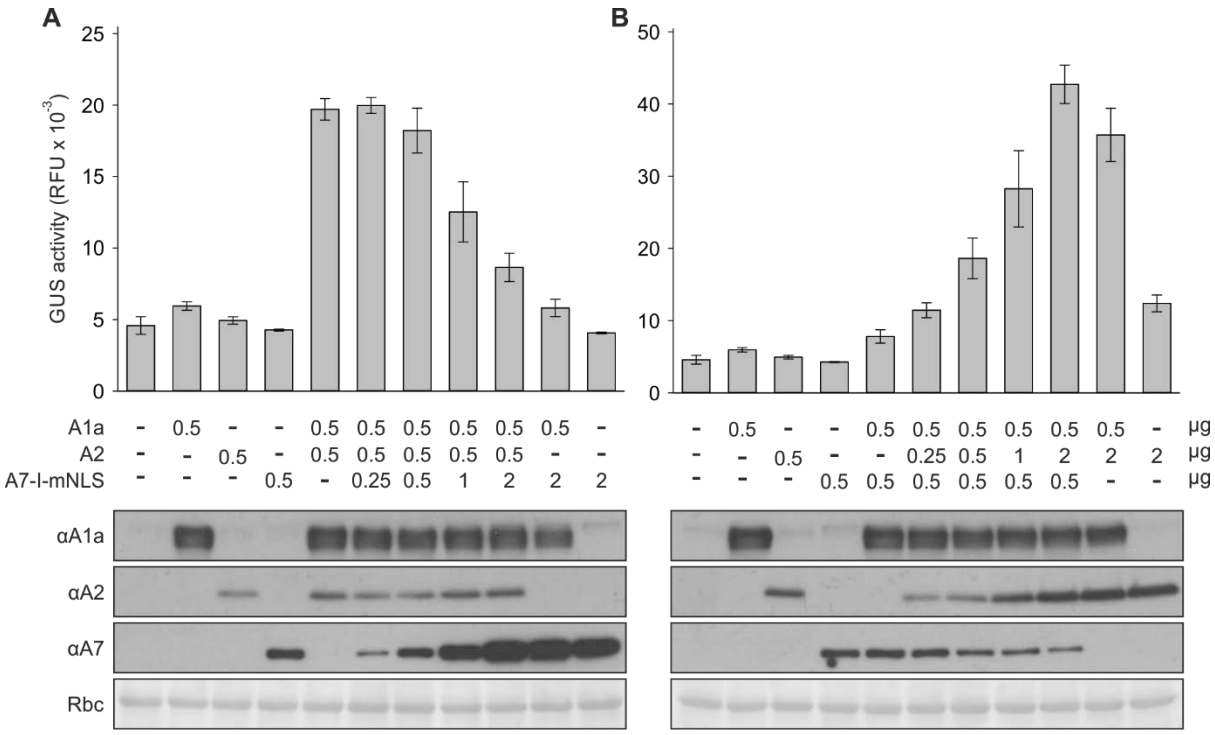

Figure 17. HsfA7 and HsfA2 compete for oligomerization with HsfA1a.
(A, B) The transcriptional activity was monitored by co-expression of the indicated amounts of Hsf plasmid constructs with 1 µg of the HSE-containing GUS reporter construct PHsp17*:GUS (same as in Fig. 8A) in tomato mesophyll protoplasts. Samples were harvested after 7 hours of expression. Bars represent the average GUS activity of the indicated Hsfs alone or Hsf combinations. Error bars are SD of three replicates. After the GUS fluorescence measurements, samples were subjected to SDS-PAGE and immunodetection of the respective Hsfs with specific antibodies. Rbc, Ponceau staining of the large subunit of Rubisco.

6.6 Functional relevance of HsfA7 for the regulation heat stress response and thermotolerance

6.6.1 Generation and identification of CRISPR/Cas9 mediated knockout mutants

To study the function of HsfA7, CRISPR/Cas9 KO mutants were generated in the *S. lycopersicum* cv. Moneymaker background. For direct comparison, HsfA2 KO mutants were produced in parallel.

Genome editing by CRISPR/Cas9 requires two components: the Cas9 nuclease and a sgRNA (consisting of a fusion of a crRNA and a fixed tracrRNA) (Sander and Joung, 2014). In order to achieve a knockout of HsfA7 and HsfA2 target sequences close to the 5´-ends of both genes were selected (Fig. 18A, D). Each of the 20 nt target sequences was fused together with a tracrRNA into an sgRNA under the control of an *At*U6 promoter. The target sites are placed immediately before the canonical 5'-NGG protospacer-adjacent motif (PAM). The plant transformation vector (pICSL02208, see Materials and methods, Table 1) construct contained the sgRNA expression cassette, the cassette containing Cas9 controlled by a CaMV 35S promoter and the nptII (kanamycin resistance) cassette for selection between left and right border (LB and

RB) of the T-DNA. The T-DNA was delivered via Agrobacterium-mediated transformation of cotyledon sections and subsequent plant regeneration.

T_0 plants (42 plants for HsfA2 and 32 for HsfA7) were subjected to genotyping by DNA sequence analysis using specific primers for each gene (Fig. 18A, D). Seeds from T_0 plants with the desired mutations were grown and their progeny was examined for homozygocity by DNA sequencing and confirmation by immunoblotting. Two mutants harbouring indels in each gene were identified and used for further analyses (Fig. 18). For HsfA7, a 4 bp deletion (*CR-a7-1*) and an insertion of a T nucleotide (*CR-a7-2*) were the result of double-strand break induction by Cas9 followed by nonhomologous end-joining (Fig. 18A). Both mutations lead to a frameshift and generation of a premature termination codon. HsfA2 mutants, *CR-a2-1* and *CR-a2-2*, had a 2 and 8-bp deletion 3 bp upstream of the PAM region (Fig. 18D). In all four cases, a putative protein would harbour only part of the DBD lacking the essential structural properties for DNA binding (Fig. C, F). Instead, such mRNAs should be targeted for NMD.

The KO mutation in HsfA2 and HsfA7 was confirmed by immunoblot analysis. Young leaves of WT, *CR-a7* and *CR-a2* plants were exposed to 40°C for 1 hour and a specific antibody against HsfA7 and HsfA2 was used to identify the protein in leaf protein extracts after SDS-PAGE and immunoblotting. Indeed, compared to the WT which produces HsfA7 and HsfA2 at this temperature, *CR-a7* and *CR-a2* plants had no detectable protein signal (Fig. 18B). By this, we confirmed the generation of two independent HsfA7 and HsfA2 gene KO mutants. Subsequent experiments were performed on plants from the T_2 and T_3 generations.

By Agrobacterium-mediated plant transformation it is possible to introduce multiple copies of a T-DNA at multiple sites in the genome. These insertions could be integrated into intergenic regions, but also disrupt other, possibly important genes. Except for the *CR-a7-2* line, the three other mutant lines had still one or more T-DNA cassettes integrated into their genome which was confirmed by PCR amplification of Cas9 on gDNA extracted from the T_1 plants (Fig. 18G). The *CR-a7-2* line lost the T-DNA already in the T1 generation by segregation while the mutation in the HsfA7 coding sequence was stably transmitted to the next generations.

Interestingly, in order to cleave, Cas9 requires extensive homology between the guide RNA and target DNA. PAM-distal bases (5'-end of the sgRNA) of the guide sequence are less important for Cas9 specificity, meaning that mismatches at those positions often do not interfere with Cas9 activity and 8–12 bp at the 3' end of the target are more important for recognition and cleavage (Hsu et al., 2014; Sander and Joung, 2014). Importantly, off-target sites followed by PAM can also lead to off-target cleavage. To examine the possibility of Cas9 off-target activity in the *CR-a7* mutant plants we used an off-target finder tool of the CRISPR-P 1.0 website. Among sequences belonging to intergenic regions, the only coding sequence with a high off-target score for the HsfA7 sgRNA guide was a DNA mismatch repair protein mutS (Solyc07g018340). Primers were designed to sequence the putative target site and sequencing of the fragments amplified from genomic DNA of the T_2 generation of both *CR-a7* lines. There was no indel in the putative Cas9 off-target site and, therefore, no frameshift in the ORF of the DNA mismatch repair protein

mutS. A similar putative off-target screening was performed for the *CR-a2* plants and the results were also negative for off-target activity of Cas9 (Sibel Söker, unpublished results, 2017).

The HsfA7 and HsfA2 KO lines generated by CRISPR/Cas9 genome editing had no phenotypic growth alterations compared to WT plants when grown under normal greenhouse conditions. This is in agreement with the behaviour of HsfA2 knock-down plants (Fragkostefanakis et al., 2016) and related to the fact that HsfA7 and HsfA2 expression is HS inducible in vegetative tissues.

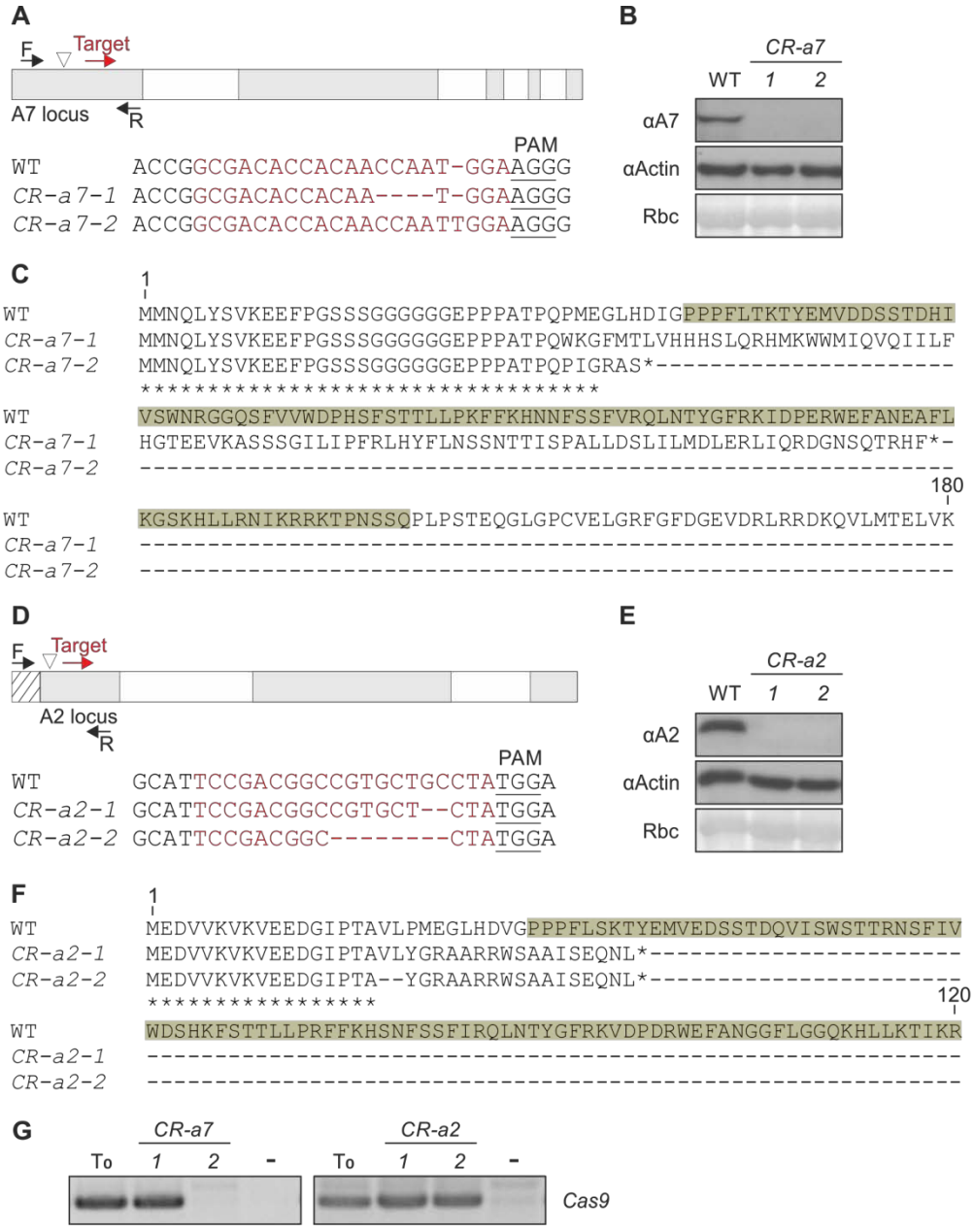

Figure 18. CRISPR/Cas9-engineered mutations in HsfA7 and HsfA2.

(A, D) The first exon of HsfA7 or HsfA2 was targeted by Cas9 using a single-guide RNA (sgRNA; Target (red arrow). Black arrows indicate forward (F) and reverse (R) primers used for genotyping and sequencing. Grey boxes indicate exon and white boxes introns of the genomic *Sl*HsfA7 or *Sl*HsfA2 sequence. Dashed box indicates the promoter region. White arrowheads indicate the position of the start codon. Nucleotide

sequences of two mutants identified from the second generation (T_1) of *CR-a7* and *CR-a2* transgenic plants are shown. sgRNA sequence is highlighted in red while the deletions are indicated by red dashes. The protospacer-adjacent motif (PAM) sequence is underlined. **(B, E)** Immunoblot analysis of wild-type and transgenic plants. Young leaves of wild-type, *CR-a7* and *CR-a2* plants were exposed to 40°C for 1 hour. Total protein extract in equal amounts (40 µg) was used for immunoblot detection of HsfA7, HsfA2 and Actin (loading control) using specific antibodies. Rbc, Ponceau staining of Rubisco large subunit. **(C, F)** Amino acid sequence alignment of wild-type HsfA7 and HsfA2 with the truncated proteins putatively generated in the *CR-a7* and *CR-a2* mutant plants. DBD is highlighted in yellow. **(G)** PCR on gDNA from *CR-a7* and *CR-a2* mutants using primers binding to Cas9. A gDNA sample of the T_0 generation served as a positive control while ddH_20 was used as negative control (-) for the PCR reaction.

6.6.2 Effect of HsfA7 and HsfA2 knockout on HS-gene expression

To dissect the effect of HsfA7 and HsfA2 loss of function on the overall HSR in vegetative (leaf) tissues, we performed an expression analysis with focus on specific stress induced Hsfs and Hsps.

Four-week-old WT, *CR-a7-1* and *CR-a2-1* plants were exposed to 35°C or 40°C for 1 hour. The protein levels of HsfA1a, HsfA2, HsfA7 and HsfB1 as well as Hsp101, Hsp70, Hsp90 and Hsp17-CI were analyzed by immunoblotting (Fig. 19). HsfA1a showed higher levels in *CR-a7-1* plants at 35 and 40°C compared to the WT and *CR-a2-1* plants (Fig. 19). Similar to HsfA1a, HsfA2 is also increased in treated *CR-a7-1* plants when compared to WT (Fig. 19). In contrast, HsfA2 KO did not affect the levels of HsfA7. Interestingly, HsfB1 levels were significantly reduced in both HsfA2 and HsfA7 mutants at 40°C compared to WT (Fig. 19).

In terms of Hsp abundance, Hsp101 and Hsp17-CI were differentially expressed (Fig. 19). At 35°C, the levels of both proteins were enhanced in the HsfA7 KO background, while Hsp101 levels were slightly lower in the HsfA2 KO at 40°C. Hsp17-CI protein was very abundant at 40°C where the protein levels were similar in all genotypes (Fig. 19). At 35°C a faint Hsp17-CI signal was detected which was more prominent in the *CR-a7-1* sample. Hsp90 was moderately induced at 35 and strongly at 40°C, while Hsp70 accumulated at higher levels only at 40°C. However, neither Hsp90 nor Hsp70 were affected by knockout of HsfA7 or HsfA2.

All in all, the expression analysis confirmed that HsfA7 negatively affects the protein abundance of the master regulator HsfA1a. Moreover, the regulation of HsfA2 as well as HsfB1 protein abundance seems to be affected by knockout of HsfA7. Hsp70 and Hsp90 did not show a significant change in abundance while HS inducible Hsp101 and Hsp17-CI seem to be differentially regulated by HsfA7 or HsfA2 in response to different temperatures.

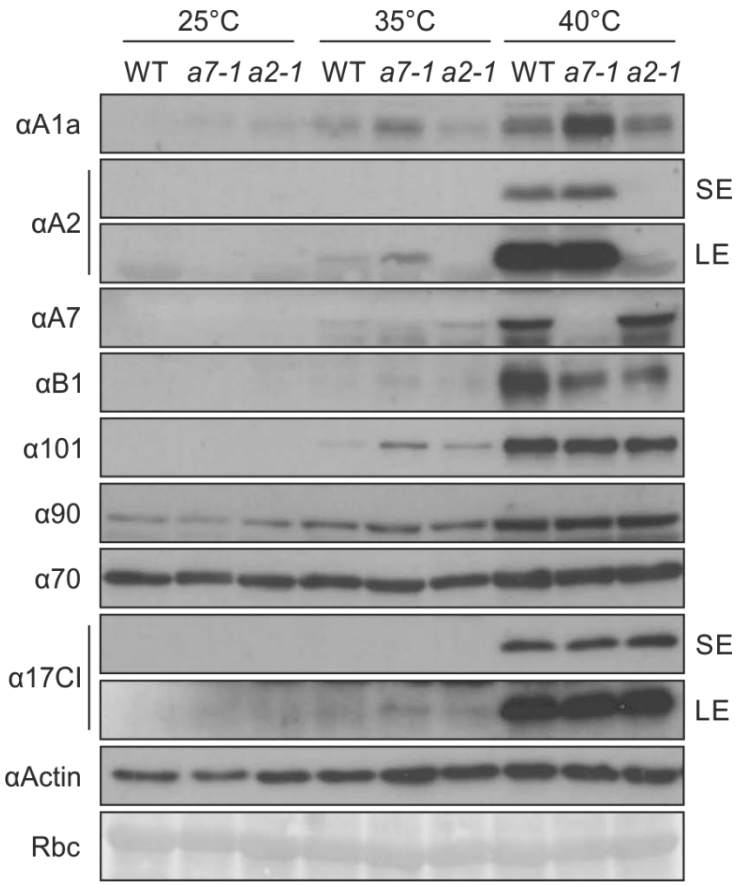

Figure 19. Expression analysis of Hsfs and Hsps in leaves of WT, HsfA7 KO and HsfA2 KO plants.
Temperature dependent induction of HsfA1a, HsfA2, HsfA7, HsfB1, Hsp101, Hsp90, Hsp70 and Hsp17-CI. Four-week old wild-type, *CR-a7-1* and *CR-a2-1* tomato plants were exposed to a single HS of 35 or 40°C for 1 hour or kept under control conditions (25°C) for the same period of time. Leaf samples were harvested immediately following the treatment. Total protein extract in equal amounts (40 µg) was used for SDS-PAGE and immunoblot detection of HsfA1a, HsfA2, HsfA7, HsfB1, Hsp101, Hsp90, Hsp70, Hsp17-CI and actin (loading control) using specific antibodies. Rbc, Ponceau staining of Rubisco large subunit.

The transcript levels of four HS-induced genes in WT, two HsfA7 and one HsfA2 KO were examined by qPCR. The samples were treated in the same way as for the protein expression analysis (Fig. 19). All genes were expressed at similar levels to WT in the mutants under non-stress conditions. *APX3* and *Hsa32* showed a stronger induction in both HsfA7 KO lines at 35°C and *APX3* a weaker induction in *CR-a2-1* at 35°C compared to WT (Fig. 20). Similarly, *Hsp101* and *Hsp17.7A-CI* were expressed at higher levels in *CR-a7* lines at 35°C, in agreement with immunoblot findings for the two proteins (Fig. 19), and lower levels in the *CR-a2* line at 35°C compared to WT (Fig. 20).

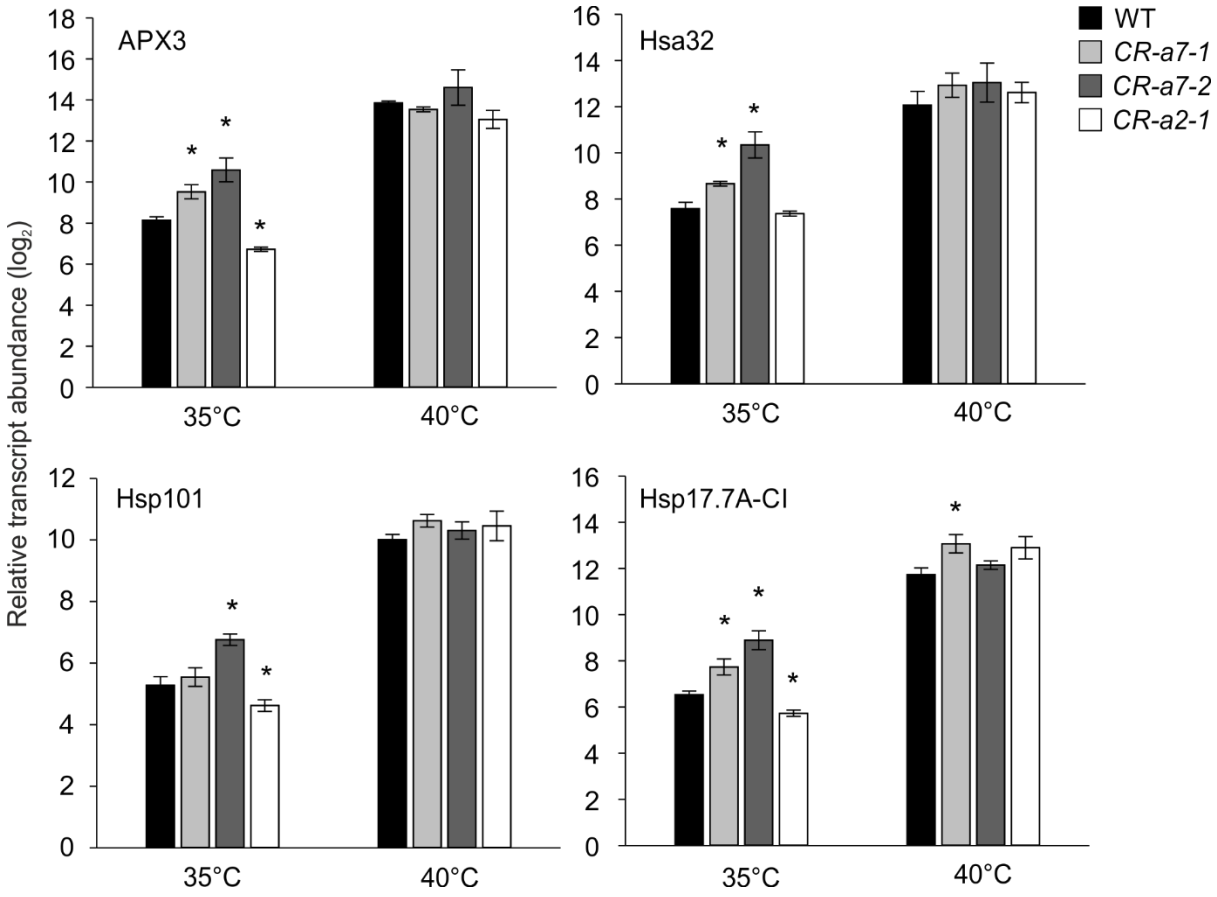

Figure 20. Expression analysis of putative HS-inducible target genes in leaves of WT, HsfA7 KO and HsfA2 KO plants.

Temperature dependent induction of *APX3*, *Hsa32*, *Hsp101* and *Hsp17.7A-CI*. Four-week old wild-type, *CR-a7-1*, *CR-a7-2* and *CR-a2-1* tomato plants were exposed to a single HS of 35 or 40°C for 1 hour or kept under control conditions (25°C) for the same period of time. Leaf samples were harvested immediately following the treatment. Following RNA extraction and cDNA synthesis, relative transcript abundance ($2^{-\Delta\Delta Ct}$) of APX3, Hsa32, Hsp101 and Hsp17.7A-CI was determined using gene specific primers. The Ct value of each gene was normalized to the Ct value of EF1α housekeeping gene and to the control sample. Vertical bars represent the average ± SD of three replicates. Asterisks depict statistical significance (p<0.05) based on one–way ANOVA followed by Duncan's Multiple Range Test.

To confirm that the KO of HsfA7 is the cause for the increased accumulation of HS-inducible transcripts in the *CR-a7* background, we performed a transient complementation of HsfA7 KO using mesophyll protoplasts. In brief, protoplasts from *CR-a7-2* plants were transformed with either the pRT-Neo mock plasmid or a construct containing the coding sequence for HsfA7-I or HsfA7-II under the control of the endogenous *Sl*HsfA7 promoter (1.2 kb promoter fragment). For comparison, WT protoplasts were transformed only with the mock plasmid. Following an incubation of 6 hours the cells were exposed to 35 or 40°C for 1 hour. qPCR analysis confirmed the higher accumulation of *APX3* and *Hsa32* in *CR-a7* protoplasts compared to WT at 35°C and for APX3 at 40°C as well (Fig 21), thereby by large matching the expression data obtained for leaves described above (Fig. 20). *APX3* and *Hsa32* transcripts accumulated at lower levels in *CR-a7* protoplasts expressing HsfA7 isoforms compared to the mock control, and similar to WT at

35°C (Fig. 21). The weaker gene induction in complemented *CR-a7* protoplasts was confirmed for *APX3* at 40°C as well (Fig. 21). These results clearly demonstrate that the accumulation of HsfA7 results in weaker induction of HS-induced genes.

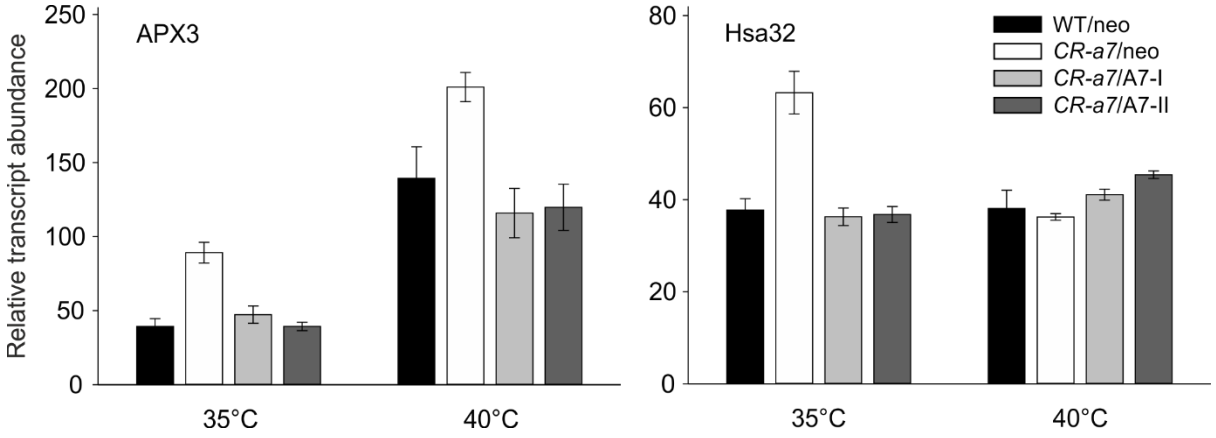

Figure 21. Expression analysis of *APX3* and *Hsa32* in WT and HsfA7 KO protoplasts.
Temperature-dependent induction of *APX3* and *Hsa32*. Tomato mesophyll protoplasts having a WT (cv. Moneymaker) background were transformed with the mock plasmid pRT-Neo while HsfA7 KO (*CR-a7*) protoplasts were transformed either with pRT-Neo or with plasmid constructs harbouring HsfA7-I or HsfA7-II under the control of the endogenous HsfA7 promoter (1.2 kb fragment). Protoplasts were incubated at 25°C for 6 hours to allow expression, exposed to HS at 35 or 40°C for 1 hour and harvested immediately following the stress treatment. After RNA extraction and cDNA synthesis, relative transcript abundance ($2^{-\Delta\Delta Ct}$) of *APX3* and *Hsa32* was determined using gene specific primers. Vertical bars represent the average ± SD of three replicates.

6.6.3 Seedling thermotolerance

To get a better understanding of the consequences of HsfA7 knockout on physiological responses to increased temperatures, a seedling thermotolerance assay was conducted. For this, four-day-old, dark grown seedlings were either kept at 25°C as control or exposed to a prolonged temperature treatment of 35°C for 6 or 24 hours. Hypocotyl length was measured after the treatment and allowed to determine the hypocotyl elongation rate for each genotype and treatment. Thermotolerance for each genotype individually was calculated as relative hypocotyl elongation rate of stressed seedlings compared to control. It is worth noticing that at early stages after germination seedlings of the *CR-a7* and *CR-a2* mutants had a growth rate similar to the wild type (data not shown). The mild stress treatment of 35°C was chosen since it is a moderately increased temperature specific for induction of HsfA7 but not HsfA2 (Fig. 3A). The relative elongation rate was significantly higher for both HsfA7 KO mutants than for the wild type (Fig. 22). Furthermore, this effect was present after both treatments (6 and 24 hours). On the other hand, HsfA2 KO seedlings elongated at a similar rate as the wild type during the mild stress treatment (Fig. 22).

The higher thermotolerance of *CR-a7* seedlings, as indicated by the increased hypocotyl elongation rate during a mild stress is in agreement with the higher accumulation of transcripts and proteins of stress induced genes.

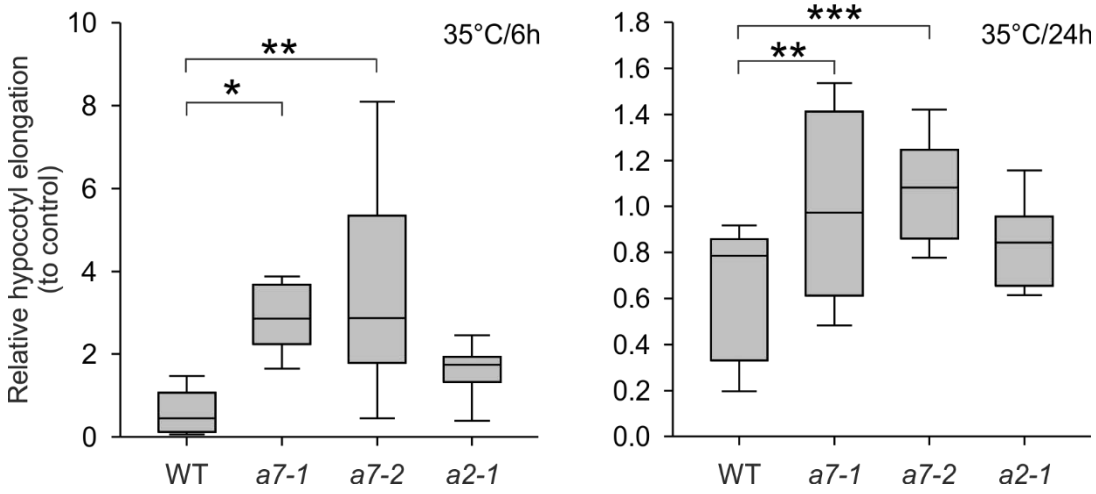

Figure 22. Seedling thermotolerance of WT, HsfA7 KO and HsfA2 KO plants.

Etiolated, four-day-old tomato wild-type, *CR-a7-1*, *CR-a7-2* and *CR-a2-1* seedlings were exposed to 35°C for 6 or 24 hours or kept at control conditions (25°C). Hypocotyl length was measured after the temperature treatment. Relative hypocotyl elongation in percentage of seedlings after the stress is shown as relative to the elongation at 25°C for each genotype. At least 10 seedlings were used per genotype and treatment. Asterisks denote significant difference: * $p<0.05$, ** $p<0.01$, *** $p<0.001$ as shown by one-way ANOVA and Duncan's Multiple Range Test.

7 Discussion

Understanding the molecular events underlying the impact of elevated temperatures on plants can lead to development of new strategies to increase stress tolerance and yield. The currently available data on tomato HSR (Fig. 2) were gained by focusing on three factors (HsfA1a, A2, B1) out of 27. Furthermore, the current models (Fig. 2) are based on observations under temperatures which are optimal for induction of a strong HSR, meaning 38-40°C. Therefore the knowledge has to be expanded from one side to new factors which might contribute with specific functions and undergo other regulatory pathways, and on the other side to alternate temperature regimes. The latter is particularly important as Hsfs have been recently shown to control cellular responses to warm aberrant temperatures in *A. thaliana* (Cortijo et al., 2017). The warming transcriptome was shown to be dependent on HsfA1s that are rapidly recruited to promoters of responsive genes, and activate their transcription. As shown by the same study, HsfA7a was in the gene cluster described as “rapidly temperature responsive” showing maximal expression. Moreover, HsfA1a was essential for H2A.Z eviction occurring in response to warm temperature at the target genes (Cortijo et al., 2017).

Studying the involvement of other class A Hsfs in HSR regulation is crucial for understanding how plants cope with stress and lead us closer to answering how we can improve crop thermotolerance. This study focuses on the functional characterization of HsfA7, a previously uncharacterized tomato Hsf, showing its, up to now, unique role in controlling cellular responses at suboptimal temperature conditions.

7.1 HsfA7 is induced by elevated temperatures and undergoes alternative splicing

Studies on *Arabidopsis thaliana* and rice mention HsfA7 as a HS-inducible class A Hsf (Liu et al., 2009; Sugio et al., 2009). We were able to confirm that HsfA7 transcription and protein synthesis are induced by a range of temperature regimes (Fig. 3 and 4). The transcriptional regulation of HsfA7 is mediated by the activity of the master regulator HsfA1a as HsfA7 is not induced in HsfA1a co-suppression (*A1CS*) plants (unpublished results, AK Schleiff).

In contrast to HsfA2 which follows a gradual temperature induction (Fig. 3A; Hu, PhD thesis), HsfA7 is induced in a stronger manner in response to small temperature changes (Fig. 3A and 5D). This difference might be related to a distinct promoter architecture including HSE structure and nucleosome positioning.

A transcriptome analysis in leaves and anthers of HS-exposed (39°C) WT and HsfA2 knock-down (antisense, *A2AS*) tomato plants showed on the one hand that *HsfA7* is induced independently of HsfA2 in tomato vegetative tissues (leaves). On the other hand, in male gametophyte tissues (anthers), *HsfA7* transcripts are induced more strongly in three independent *A2AS* lines (Fragkostefanakis et al., 2016). Although the regulation remains unclear, the effect was proposed as a feedback mechanism that balances HsfA2 and HsfA7 levels (Fragkostefanakis et al., 2016). In addition, the effect could attribute to the difficulties in assessing Hsf function due

to non-existing or weak phenotypes. It is possible that a visible phenotype can only be observed at specific conditions where loss of a specialized Hsf might not become compensated by the function or enhanced expression of other Hsfs.

Except transcriptional control mechanisms, processing of the RNA including pre-mRNA splicing is important for gene expression. A recent study involving transcriptome assembly of heat stressed tomato pollen of two cultivars showed that AS occurs more frequently than expected as one cultivar had 76% more genes expressed with IR and ES after HS exposure in comparison to control conditions (Keller et al., 2016). Most of the alternatively spliced transcripts in the two cultivars were related to genes involved in protein folding, gene expression and heat response related processes. Plant Hsfs have been reported to be alternatively spliced in different plant species, such as *A. thaliana*, *Medicago sativa*, *Oryza sativa* and *Solanum lycopersicum* (He et al., 2007; Liu et al., 2013b; Cheng et al., 2015; Hu, PhD thesis).

In the closely phylogenetically related HsfA2/A6/A7 group (Scharf et al., 2012), *Solanum lycopersicum* HsfA7 has the most complex gene structure. While HsfA2 and HsfA6b contain two introns each and HsfA6a only one intron, the HsfA7 gene is composed of five exons and four introns (Fig. 5B). Sequencing of HsfA7 3'-end amplicons (exon 2 to exon 5, Fig. 5B) revealed the existence of at least 10 transcript variants generated in a temperature-dependent manner. Alternative splicing which includes full or partial retention of intron 2, and alternative donor and acceptor site selection in exon 4 results in ORFs of three putative HsfA7 protein isoforms (Fig. 5B and 6). Multiple transcripts encoding for a single protein are characterized by a variable 3'-UTR which could be involved in regulation of mRNA stability, nuclear export or translation efficiency (Moore, 2005). Interestingly, while retention of intron 2 (and generation of HsfA7-I) is favoured upon the onset of HS and exposure to an acute HS (45°C), intron 2 splicing (and generation of HsfA7-II/III) is more prominent upon 1 hour of exposure to 40°C and moderately increased temperatures as shown by RT-PCR and HR RT-PCR (Fig. 5A, D). Increasing temperatures are mainly associated with intron retention and inhibition of pre-mRNA splicing particularly for 3'-terminal introns as shown for both, HsfA7 and HsfA2 (Hu, PhD thesis). This is in agreement with the high rate of intron retention observed in stress-related genome wide studies (Filichkin et al., 2015; Keller et al., 2016).

HsfA7 and HsfA2 are the only two tomato Hsfs in which AS of the pre-mRNA leads to the production of more than one functional protein isoform (Fig. 5; Hu, PhD thesis). Splicing of HsfA2 intron 2 leads to the generation of a shorter HsfA2 protein lacking the NES domain and five out of nine amino acids comprising AHA2 (Hu, PhD thesis). HsfA2-I has been described by previous studies as the only functional HsfA2 protein (Lyck et al., 1997; Scharf et al., 1998). However, it has been recently shown that HsfA2-I is important for ATT, while HsfA2-II is most likely involved in regulation of the direct HSR (Hu, PhD thesis).

The main difference between HsfA7 protein isoforms created by AS events is that in comparison to HsfA7-I, HsfA7-II and -III have a truncated NES and a C-terminal extension. This NES truncation resulted in a loss of NES function since intracellular localization of isoforms II and III was almost nuclear, while isoform I showed a nucleocytoplasmic shuttling (Fig. 7A). Whether the

C-terminal extensions in isoforms II and III (Fig. 6) have additional functions remains unclear. The CTAD accommodates AHA motifs embedded in an acidic surrounding which help to recruit components of the transcriptional machinery (Yuan and Gurley, 2000; Kotak et al., 2004). Possible functions of these extensions could be related to interactions with other factors like components of the basic transcriptional machinery or to conformational changes including intramolecular interactions. HsfA7-II and –III have only a minor difference in amino acid sequence (Fig. 6) and initial analyses in protoplast-based assays did not reveal significant differences between these two proteins in terms of activity. Thereby we assume that they are functionally redundant.

Alternative splicing in intron 1 of tomato and *A. thaliana* HsfA2 can lead to inclusion of a mini-exon resulting in transcript variants possessing PTCs and long 3'-UTRs which are degraded by the NMD pathway (Sugio et al., 2009; Hu, PhD thesis). The conserved intron 1 spanning the DBD of HsfA7 is constitutively spliced as shown by RT-PCR analysis in tomato seedlings exposed to different temperatures (Hu, PhD thesis). It is well known that transcripts subjected to NMD are barely detectable and difficult to identify due to efficient removal (Houseley and Tollervey, 2009). However under high temperatures, NMD might be less efficient, particularly considering that NMD target recognition requires translation which might be impaired in response to high temperatures (McCormick and Penman, 1969). It would be interesting to investigate whether AS of HsfA7 varies upon exposure of different tissues to increased temperatures or to different HS regimes and whether under specific circumstances PTC-containing transcripts can accumulate. Some predicted PTC-containing NMD target mRNAs have been shown to escape this mechanism and play an important role in development (Reddy et al., 2013). For example, in microspores of the fern *Marsilea vestia*, IR is a functional mechanism used for stalling of translation (Boothby et al., 2013). Intron-containing transcripts are probably stored in nuclear ribonucleoprotein particles until spermatogenesis, which leads to temporally regulated splicing and translation initiation.

Upon exposure of vegetative tissues to different temperatures HsfA7 transcript and protein synthesis are induced, although not in a similar manner (Fig. 3A). There is a gradual transcript and protein induction peaking at 40°C. Further increase in temperature, leads to weaker transcript and protein accumulation probably due to the severe stress imposed on the transcriptional machinery and other cellular processes. Even though the relative transcript abundance of HsfA7 is similar at 30 and 35 as well as at 45°C the protein levels in all three samples differ suggesting the importance of post-transcriptional regulation in gene expression at different temperatures (Fig. 3A). Furthermore, it was interesting to observe that the transcripts in recovery samples are rapidly reduced to basal levels, which is likely related to HsfA1a repression by molecular chaperones upon attenuation of the stress cue. In contrast, the protein accumulates during recovery indicating a functional relevance of HsfA7 during the attenuation phase (Fig. 3A).

Although HsfA2 transcripts are induced at temperatures lower than 40°C the protein is not detectable (Fig. 3A). However, it cannot be excluded that HsfA2-I or HsfA2-II are produced at these temperatures at very low levels and/or are rapidly degraded. Supporting this notion,

inhibition of proteasome-dependent degradation by MG132 in tomato cell suspension culture exposed to 30°C leads to the accumulation of HsfA2 (Fig. 12B). Hence, low protein levels of HsfA2 at mildly elevated temperatures are degraded via the 26S proteasome which consequently leads to very low or even non-detectable levels in tissues under mild temperature conditions.

Nevertheless, in vegetative tissues, HsfA7 protein accumulates at 35°C, while HsfA2 accumulation requires higher temperatures (Fig. 3A). Instead, Hsps like Hsp17-CI and Hsp101 show also a strong accumulation at 35°C suggesting an HsfA7-dependent regulation. This supports the importance of HsfA7 for the cellular HSR at moderately increased temperatures while HsfA2 becomes very abundant at temperatures around 40°C. Furthermore, since leaves and cell culture show both a temperature-dependent shift in expression of the two Hsfs we can conclude that this regulation is not cell-type specific (Fig. 3A, 12B). Although a high sequence homology is shared between HsfA7 and HsfA2, a temperature-specific regulation allows a differential involvement of these Hsfs in the regulation of the HSR.

The functional diversification of Hsfs is to some extent related to the factor-specific interactions with members of different chaperone families, such as Hsp90, Hsp70 and sHsps (Port et al., 2004; Hahn et al., 2011). Interestingly, despite the high sequence similarity with HsfA2, HsfA7 is not regulated by cytosolic Hsp17.4C-II as it can escape the recruitment to HSGs (Fig. 7C). For HsfA7-II this is related to a strong nuclear retention as shown for HsfA2-II (Hu, PhD thesis). In case of HsfA7-I, possible structural or amino acid differences between HsfA2-I and HsfA7-I are responsible for the selective co-repressor activity of the sHsp on the former. Such differences are probably due to variations in the C-terminal domains as this is the interaction site of HsfA2 with Hsp17.4-CII (Port et al., 2004). However this does not rule out the possibility that there might be other Hsps responsible for specific repression of HsfA7 activity.

The overall importance of HsfA2 for the HSR and its involvement in ATT have been related to the fact that it is a highly stable protein over several hours following stress exposure, both in tomato and *Arabidopsis thaliana* (Charng et al., 2006; Schramm et al., 2006; Fragkostefanakis et al., 2016). Previous studies on *A. thaliana* indicated, HsfA7a/A7b might play a role in heat acclimation and CPR (Charng et al., 2006; Larkindale and Vierling, 2007; Sugio et al., 2009). As shown by the ATT treatment, HsfA7-I is a stable protein for several hours following a pre-induction stress and up to 24 hours following the stronger stress treatment (Fig. 4). This indicated that HsfA7 could be involved in heat acclimation under repeated cycles of HS and recovery. Preliminary results showed that there was no significant difference in hypocotyl elongation of *CR-a7* compared to WT seedlings in response to an ATT treatment (35°C pre-treatment following 3 hours recovery at 25°C and exposure to a challenging stress of 47.5°C, data not shown). Whether HsfA7 is involved in ATT after longer recovery periods like it is the case for *A. thaliana* Hsa32 is not clear. Since HsfA7 is involved in regulation of *Hsa32* transcript abundance in tomato (Fig. 20) it would be interesting to investigate this further.

7.2 Regulation of HsfA7 fate by proteasomal degradation

Transcripts of HsfA7 (and HsfA2) are rapidly degraded following stress attenuation while the proteins further accumulate over a certain period of time and then undergo a gradual degradation (Fig. 3, Fig. 4). In tomato, only the protein turnover of HsfB1 has been extensively studied (Röth et al., 2017). DNA-bound HsfB1 is efficiently targeted for degradation by the nuclear ubiquitin-proteasome pathway when active as a transcriptional repressor and in the presence of nuclear localized Hsp90. This observation points out that a strict control of Hsf protein abundance is needed for a tight regulation of their function upon attenuation of the stress cue.

Although the antibody against HsfA7 was produced to recognize all HsfA7 isoforms, only HsfA7-I protein was identified in leaves in response to a 1 hour treatment at different temperatures or a treatment resembling an ATT regime (Fig. 3 and 4). HsfA7-II and HsfA7-III proteins gained by splicing of intron 2 were not detectable by immunoblotting of heat stressed leaf tissue. However, exposure of tomato cell culture to 30 and 35°C revealed a temperature-inducible (~60 kDa) signal in addition to the HsfA7-I (~55 kDa) signal (Fig. 12B). By comparing the separation behaviour of antiHsfA7 specific signals on immunoblots of cell culture extracts as well as tomato protoplast extracts after ectopic expression of HsfA7-II/III, we could confirm that the signal corresponds exactly to the apparent molecular size of the two proteins after SDS-PAGE separation. Therefore, it is possible that these isoforms are detectable in other tissues or specific cell-types (e.g. root, meristem, flower, pollen) and/or that these are produced in response to specific HS regimes, e.g. prolonged HS, gradual temperature increase, which might promote the stabilization of these isoforms.

A protoplast-based assay performed to test the protein stability of HsfA7-I and HsfA7-II revealed that there is a remarkable difference in protein turnover between the two proteins (Fig. 10A). HsfA7-I was a relatively stable protein, while HsfA7-II had a significantly faster turnover. This shows that the HsfA7-II/III protein is likely produced but rapidly degraded resulting in protein amounts below the detection limit in vegetative tissues. The degradation rates of the HsfA7 isoforms are similar to those of HsfA2-I and HsfA2-II (Hu, PhD thesis). Only here, HsfA2-II could be detected in heat stressed vegetative tissues, although at much a lower amount than HsfA2-I.

The difference in protein stability between HsfA7-I and HsfA7-II is related to their localization. Both NLS mutant isoforms had steady state protein levels persisting over 6 hours after adding CHX showing that degradation takes place in the nucleus (Fig. 11). Therefore, HsfA7-I could escape degradation by nucleocytoplasmic shuttling while the nuclear HsfA7-II was rapidly removed. This result also indicates that there is no co-import of the NLS mutants in the nucleus by interaction with endogenous Hsfs as shown for an NLS mutant of HsfB1 (Röth et al., 2017). HsfB1-mNLS was degraded at a slow rate during 6 hours after translation inhibition which was discussed to be related to interaction with endogenous Hsfs facilitating its nuclear import.

Furthermore, degradation of HsfA7 is mediated by the ubiquitin-proteasome system as shown by stabilization of HsfA7-II in protoplasts treated with MG132 and for both HsfA7 isoforms in tomato cell culture after treatment with the same inhibitor (Fig. 12A, B). HsfA2 also showed an

accumulation in the presence of MG132 which was less prominent compared to HsfA7, while the most significant turnover rate was observed for HsfA1a. Hence, the proteasome plays an important role in the regulation of Hsf abundance.

Protein turnover of both, HsfA7-I and HsfA7-II was enhanced when exposed to HS conditions compared to the stability of the proteins at room temperature (Fig. 10A). The same HS of 39°C inhibited the degradation of HsfB1 while co-expression of plasmids harbouring an HSE9-GUS construct restored the decay of *Sl*HsfB1 almost to control levels (Röth et al., 2017). The proposed explanation for this phenomenon was that its co-activator function with HsfA1a (mediated by formation of the ternary HAC1 complex with both Hsfs) shields HsfB1 from degradation. HsfA7 isoforms are also stabilized by co-expression of increasing amounts of HsfA1a as well as HsfA3. This effect was more prominent on HsfA7-II, possibly due to a very high basal protein turnover rate of this isoform compared to HsfA7-I (Fig. 10A, B). By this, the enhanced HsfA7 degradation under HS cannot be explained by taking into account the interaction with HsfA1a or HsfA3. There are many alternative explanations, including a difference in promoter accessibility, expression of other factors, post-translational modifications or activity enhancement which could affect the stability of HsfA7 and are distinctive in control compared to increased temperature conditions. Because nuclear localization is prerequisite of HsfA7 degradation (Fig. 11), it would be also interesting to investigate whether DNA binding affects the turnover of HsfA7 as it was shown for HsfB1 and other transcription factors (Sundqvist and Ericsson, 2003; Röth et al., 2017). Co-transformation of plasmids containing HSE elements providing additional Hsf-binding sites did not significantly affect HsfA7 stability (data not shown) which is in agreement with the results obtained for several other class A Hsfs including HsfA1a, HsfA2, HsfA3, HsfA4a and HsfA9 (Röth, PhD thesis). Hence, even if DNA binding is crucial for degradation it is not the limiting factor.

Transcriptional activity and the phenomenon of “unstable when active” has been proposed as a mechanism to control the duration of transcriptional responses so that the activation of genes is linked to the ongoing synthesis of the transcriptional activator (Muratani and Tansey, 2003). How transcriptional activation is coupled to degradation is still not exactly known. Some evidence was drawn from the observation that in many unstable transcription factors an sequential overlap was found between transcriptional activation and degradation motifs, the so-called degrons (Muratani and Tansey, 2003). For example, the same C-terminal region of the transcriptional activator WRKY45, involved salicylic acid defense signalling in rice, was essential for both transcriptional activity and ubiquitin proteasome-dependent degradation (Matsushita et al., 2013). Additionally, the transcriptional activity of WRKY45 after salicylic acid treatment was impaired by proteasome inhibition. It would be interesting to investigate whether the ubiquitin-proteasome system regulates Hsf activity in a similar manner.

To determine whether the transcriptional activator potential of HsfA7 affects its stability we aimed to generate AHA domain mutants. However, the result was not as expected since deletion or mutation of important amino acid residues did not give rise to an entirely inactive mutant (Fig. 13A, B). In contrast to this, mutating the AHAs of HsfA1a or HsfA2 in the same way resulted in completely inactive Hsfs (Chan-Schaminet et al., 2009). In the future, introducing of

proline or positively charged residues in or adjacent to the AHA motifs could help to further reduce or abolish HsfA7 activity as proposed by Döring et al. (2000). Nevertheless, deletion of a large portion of the predicted AHA motif in the HsfA7 isoforms, which partially abolished their activity, did not significantly alter their protein stability (Fig. 13C). This is in agreement with the results of Döring et al. (2000) and Kotak et al. (2004), which showed that the transactivation activity of Hsfs does not always negatively correlate with the protein abundance.

Although HsfB1 also undergoes ubiquitin-proteasome degradation in the nucleus, regulation of HsfA7 protein turnover seems to be different to the regulation of HsfB1 turnover in many aspects including temperature dependency, DNA binding and transcriptional activity. Such a distinct mode of abundance control in the same protein family further demonstrates the complexity of the regulation of Hsf activity.

7.3 Interplay of HsfA7 with other members of the Hsf network

Despite the difference in protein stability HsfA7-I and HsfA7-II have both a low basal activity as shown by GUS reporter assays on different HS-inducible promoters (Fig. 8A). To induce the transcription of target genes HsfA7 requires interaction with other Hsfs like HsfA1a and HsfA3. This is in contrast to HsfA2-II, which shows a higher activity than HsfA2-I due to its nuclear retention (Hu, PhD thesis).

The synergistic activity, previously described as an HsfA1a-HsfA2-specific effect (Chan-Schaminet et al., 2009) was even stronger for HsfA1a-HsfA7 and HsfA3-HsfA7 complexes (Fig. 8). The capacity of Hsf combinations to activate transcription, however, varied depending on the tested promoter (Fig. 8). This could be related to differences in HSE structure resulting in differential binding abilities as well as to the composition of the AHA motifs in the hetero-oligomeric complex. Differential interaction of individual AHA motifs with components of the transcriptional machinery could contribute to functional diversity among the Hsf complexes. While the activation domain of HsfA7 is a classical AHA motif as described previously for HsfA1a and HsfA2 (Fig. 13A) (Döring et al., 2000), the transcriptional activation activity of HsfA3 depends on four short AHA-like motifs (Fig. 1) with central tryptophan residues but lacking the second hydrophobic dipeptide motif (Bharti et al., 2000).

In addition, both isoforms showed a similar co-activator activity when co-expressed with HsfA1a. In contrast, co-activator complexes composed of HsfA7-II-HsfA3 had a slightly higher activity compared to HsfA7-I-HsfA3 (Fig. 8). This might indicate a specific function of the C-terminal extension in HsfA7-II when hetero-oligomers with HsfA3 are assembled. Nevertheless, deletion of the HsfA7 AHA motif did not abolish the co-activator potential of HsfA7 isoforms when co-expressed with HsfA1a or HsfA3 (Fig. 14A). This could be related to the fact that the acidic surrounding of the AHA motif contributes to the activity of HsfA7 (Fig. 3). In contrast, in the HsfA1a-HsfA2 complex AHA motifs of both interaction partners contributed to the resulting transcriptional activity of the complex (Chan-Schaminet et al., 2009).

Combination of the CTADs from both partners in the HsfA1a-HsfA2 co-complex is mediated or reinforced by interaction of the two heterologous ODs which was essential for the synergistic function of HsfA1a-HsfA2 (Chan-Schaminet et al., 2009). Although highly conserved in sequence and domain organization (Scharf et al., 2012), there is still a remarkable specificity among the class A Hsfs for hetero-oligomerization capacity since ectopically overexpressed HsfA7 and HsfA2 showed no cooperation on any of the tested promoters (Fig. 8). In this way, by formation of specific hetero-oligomers the already complex Hsf network gains further flexibility for targeted gene regulation. The OD is composed of a heptad repeat pattern of hydrophobic amino acid residues (HR-A/B region), which is predicted to form a trimeric, α-helical coiled-coil structure of the leucine zipper-type (Chan-Schaminet et al., 2009; Scharf et al., 2012). Furthermore, it has been proposed that newly synthesized Hsf molecules are assembled in homotrimeric subcomplexes, which is mediated by interaction between their HR-A regions. On the example of HsfA1a-HsfA2 a subsequent formation of hexameric hetero-oligomers through the linker and the adjacent HR-B region has been demonstrated (Chan-Schaminet et al., 2009). It is very likely that the same mechanism is responsible for the interaction of HsfA7 with HsfA1a or HsfA3 (Fig. 9A, B). As demonstrated by localization analysis, all the putative hetero-oligomeric complexes have a prevalent nuclear localization although a significant portion of HsfA7-I and HsfA3 is localized in the cytosol when they are expressed alone (Fig. 7, 9 and 15).

Both, HsfA1a and HsfA3 interact with the NLS mutant of HsfA7-I exclusively in the cytosol and these complexes cannot be imported in the nucleus as shown by BiFC (Fig. 15A). When total GFP-tagged HsfA1a and HsfA3 were detected the NLS mutant of HsfA7 could significantly shift the equilibrium of HsfA1a towards the cytosol while HsfA3 showed an almost exclusive cytosolic retention (Fig. 15B). A stronger interaction of the HsfA3-HsfA7 ODs, the stronger NLS responsible for import of HsfA1a, or simply differences in stoichiometry of the proteinaceous factors might be the source for the observed differences. Therefore, co-transformation of the HsfA7 NLS mutant with HsfA1a diminished the co-activator function of HsfA7 and the transcriptional activity corresponded to the activity of HsfA1a alone (Fig. 14B). A similar scenario was observed for HsfA3 when co-expressed with HsfA7-II-mNLS, but interaction with HsfA7-I-mNLS almost completely abolished even the activity observed for HsfA3 alone (Fig. 14B). The fact that a mutated NLS of HsfA7 can have such a strong effect on localization and activity of either HsfA1a or HsfA3 leads to the conclusion that there is formation of stable hetero-oligomeric complexes already in the cytosol and the NLS of HsfA7 is important for their nuclear import. In the combination of an HsfA2 NLS mutant with HsfA1, part of HsfA1 was also retained in the cytoplasm (Scharf et al., 1998). Therefore, it is possible that all subunits of an oligomeric Hsf complex need a functional NLS for an efficient import. However, Röth et al. (2017) showed that an HsfB1-mNLS could be co-imported into the nucleus when a WT HsfB1 was co-expressed, most likely by formation of homo-dimers (Nover et al., 2001). It is not clear whether there are different modes of import regulation for Hsf trimers or hexamers. In conclusion, we show that HsfA7 acts as a co-activator of HsfA1a/HsfA3 by formation of hetero-oligomeric complexes and cooperation in nuclear targeting. However, the annotated AHA motif of HsfA7 as such seems to play a minor role in the hetero-oligomeric complex and is not essential for interaction with the basal transcriptional machinery and transcriptional activation.

Even though GFP-HsfA3 and GFP-HsfA7, when expressed alone, have a diffuse nucleo-cytoplasmic distribution (Fig. 7 and 15), co-expression of cEYFP-HsfA3 with either nEYFP-HsfA7-I or nEYFP-HsfA7-II resulted in formation of a characteristic speckle-like nuclear YFP signal (Fig. 9B). To the best of our knowledge, the existence of such Hsf-containing speckles has not been described previously in plants. In stressed human cells, HSF1 and HSF2 have been found to form a physically interacting complex which accumulates in so-called nuclear stress bodies (NSBs) (Jolly et al., 1999; Alastalo et al., 2003). These NSBs localize to specific chromosomal loci where HSFs bind to and actively transcribe satellite III repeats. Furthermore, several splicing factors of the SR family were found to be recruited to NSBs while components of the splicing machinery were found closely associated (Metz, 2004). The role of NSBs in HSR has not been elucidated – they have been proposed to play a role in control of transcription and splicing activities, regeneration of heterochromatin structure or even transcriptional de-repression of genes located in the vicinity of NSBs (Biamonti and Vourc'h, 2010). In plants, the only similar structures which have been characterized so far are called nuclear speckles. These are often located near active transcription sites and serve as a storage place for splicing factors (Reddy et al., 2012). The understanding of different speckle types in plants, their biogenesis and functions is still poorly explored (Reddy et al., 2012).

Tomato HsfA3 is a constitutively expressed and HS-inducible Hsf. Under physiological conditions it is mainly cytosolic and its balance is shifted to the nucleus upon HS exposure (Bharti et al., 2000). Although the functional relevance of HsfA3 in *Solanum lycopersicum* is not known the specific AHA composition, interaction and cooperation with HsfA7 on different promoters, as well as localization in speckle-like structures in the nucleus points out that it has specific roles in the Hsf-network. *A. thaliana* HsfA3 has been shown to be induced during HS by DREB2A, and regulate the expression of Hsp-encoding genes (Schramm et al., 2008). Ectopic overexpression of tomato HsfA3 in *A. thaliana* lead to increased thermotolerance but also salt hypersensitivity during germination (Li et al., 2013). Considering that overexpression of *Os*HsfA7 in rice resulted in enhanced salt and drought tolerance (Liu et al., 2013a), we can assume that an HsfA3-HsfA7 interaction might by relevant for other abiotic stresses beyond temperature stress.

7.4 Regulation of the HSR by HsfA7 and HsfA2

Chan-Schaminet et al. reported in 2009 stabilization of both HsfA1a and HsfA2 in their hetero-oligomeric complexes. We were able to confirm the positive effect of HsfA2 on protein stability of HsfA1a (Fig. 16C). A similar effect was observed for the stabilization of the HsfA4b-HsfA5 pair in tomato as well as for heterotrimers formed between mammalian HSF1 and HSF2 (Baniwal et al., 2007; Sandqvist et al., 2009) .

To our surprise, HsfA7 had an opposite effect on both HsfA1a and HsfA3 (Fig. 16A, E). The effect was somewhat weaker when HsfA7-II was co-expressed which can be related to lower protein levels of this isoform in general compared to isoform I. It is unclear why increasing amounts of HsfA1a or HsfA3 stabilize HsfA7 while increasing amounts of HsfA7 lead to a destabilization of the two factors (Fig. 10A, 16A, E). One possible explanation might be that the transcriptional

activity of the complex determines the degradation rate of the interaction partners as shown on the mammalian SREBP family of transcription factors involved in cholesterol and lipid metabolism (Sundqvist and Ericsson, 2003). Co-expressing HSE as binding sites did not further affect the protein levels of HsfA1a thereby indicating that this effect is not dependent on DNA binding (Fig. 16E). Furthermore, HsfA7 needs to be nuclear since HsfA7 with an inactive NLS did not enhance the turnover of HsfA1a. The NLS mutant can enhance the cytosolic retention of HsfA1a (Fig. 15B) which is a strong indicator that WT HsfA7 and HsfA1a are co-imported into the nucleus and a nucleus-localized HsfA7 is crucial for promoting the proteasomal degradation of HsfA1a. However, we do not know whether specific temperature conditions could reverse this effect and stabilize HsfA1a or HsfA3 because they are targeted to specific chromatin environments to perform their function.

According to previous studies HsfA1a was considered as a relatively stable protein as shown by proteasome inhibitor I (PSI) and N-acetyl-Lleucinyl-L-leucinylmethional (LLM) treatment (Hahn et al. 2011). Protein levels of HsfA1a were only slightly enhanced by treatment with increasing amounts of these two chemicals. In contrast, our results show that HsfA1a has an efficient protein turnover at control and HS conditions (Fig. 12B). Differences in the experimental setups could explain the two distinct conclusions. First of all, we used MG132 while Hahn et al. used LLM and PSI as proteasomal inhibitors. In addition, the treatment time was 14 hours in the experiments performed by Hahn et al. (2011), while only 1 hour was applied in this study. Nevertheless, there is a clear and remarkable effect of proteasome inhibition on the protein levels of HsfA1a which shows that even the master regulator is subjected to constant protein clearance irrespective of the temperature conditions. In general, increasing temperatures lead to a moderate increase in HsfA1a protein abundance in different cell types (Fig. 19) (Bharti et al., 2000; Fragkostefanakis et al., 2016) while the transcript abundance of HsfA1a is not affected by temperature changes (Hu, PhD thesis). This leads to the conclusion that the protein which is under a constant turnover is stabilized through a mechanism that has yet to be discovered. Slightly enhanced levels of HsfA1a protein at 40°C in cell culture (Fig. 12B) might be related to the presence of specific interaction partners. At this temperature HsfA7 expression declines while HsfA2 is still synthesized and might lead to HsfA1a stabilization by HsfA1a-HsfA2 complex formation.

Transcription factors are well known to be regulated by an array of post-translational modifications orchestrating its DNA binding, activity, protein-protein interactions and protein stability (Filtz et al., 2014). In addition, interaction of two factors can also stimulate post-translational modifications or degradation. For example, mammalian transcription factor Smad7 interacts with the transcriptional co-activator p300 resulting in acetylation of Smad7 at two lysine residues (Grönroos et al., 2002). This acetylation prevents ubiquitination of the same residues, stabilizes Smad7 and protects it against degradation. Furthermore, p300 binding enhances p53 stability while the p300 bound MDM2 is an ubiquitin protein ligase (E3) and acts as a p53 destabilizer (Grossman et al., 1998; Fang et al., 2000). Specific interactions between these three factors are involved in control of p53 abundance (Grossman et al., 1998). In hematopoietic cells SCL-LMO2 interaction is required for endogenous erythroid gene activation while at the same time interaction with SCL prevents LMO2 from proteasomal degradation.

Therefore, interaction with HsfA2 might stabilize HsfA1a by shielding from or allowing certain post-translational modifications which could lead to stabilization of the complex, while the complex formation with HsfA7 might eventually enforce HsfA1a ubiquitination and degradation.

HsfA7 and HsfA2 can both act as co-activators and their functions might be redundant, however, with respect to HsfA1a regulation they have distinct functions. At specific temperatures (~40°C in leaves and ~35°C in cell culture, Fig. 3A, 12B) HsfA7 and HsfA2 co-exist in the cell simultaneously with HsfA1a. Since both can interact and assemble in hetero-oligomers with HsfA1a, thereby having different effect on its stability, it is important to understand the interplay and affinity of HsfA1a for the two HS-inducible Hsfs. Using the "competition" assay we were able to show that HsfA7 can replace HsfA2 in the HsfA1a-HsfA2 hetero-oligomer if the protein is sufficiently abundant (Fig. 17A). Vice versa, HsfA2 can also successfully compete with HsfA7 for interaction with HsfA1a (Fig. 17B). By this, we propose that different interaction partners mediate the stability of HsfA1a depending on the relative amounts of the co-factors, in this case that of HsfA2 and HsfA7.

Despite its co-activator function, HsfA7 knockout at 35°C enhances protein levels of several HS-induced genes (HsfA2, Hsp101, Hsp17-CI) in leaves which is very likely related to the accumulation of HsfA1a in *CR-a7* plants (Fig. 19). Why the same genes did not follow a similar behaviour at 40°C where HsfA1a levels are also enhanced is unclear and might be related to enhanced expression of other HS-inducible factors and additional levels of regulation. The negative regulation of HSR at mildly elevated temperatures (35°C) was confirmed by qPCR analysis of *APX3* and *Hsa32* (Fig. 20). Furthermore, induction of these two genes in the HsfA7 KO background has been exclusively related to loss of HsfA7 as supported by complementation of HsfA7 in tomato protoplasts (Fig. 21). APX enzymes are important for catalysing the conversion of H_2O_2 into H_2O, using ascorbate as an electron donor. In this way it helps protecting the cells from damages caused by accumulation of ROS (Caverzan et al., 2012). Hsa32 is highly conserved in land plants but absent in most other organisms. In *A. thaliana*, it is important for ATT following a recovery period of more than 24 hours after the pre-treatment and therefore, it was proposed to play an important role in maintenance of ATT (Charng, 2006). Thus, these results show that there is likely a wider gene network affected by the knockout of HsfA7 and a transcriptome analysis would be a valuable tool to understand how far reaching the loss of this factor is.

In contrast, the role of HsfA2 as an essential co-activator was confirmed in *CR-a2* mutants which show reduced accumulation of Hsp 101 as well as slightly lower levels of HsfA1a (Fig. 19). The reduction of Hsp101 levels at 40°C in the HsfA2 KO leaves was similar to the results obtained in HsfA2 knock-down plants (Fragkostefanakis et al., 2016). Furthermore, *APX3* and *Hsa32* transcript abundance was not significantly affected in *CR-a2* leaves (Fig. 20) while results obtained in transgenic plants overexpressing HsfA2 showed an enhanced expression of these genes after exposure to 39°C for 1 hour (Fragkostefanakis et al., 2016).

Interestingly, even though Hsp90 levels were not enhanced in either HsfA7 or HsfA2 KO background, HsfB1 abundance was significantly reduced in both genotypes compared to the WT

(Fig. 19). The reason behind this downregulation of HsfB1 abundance and how this affects target genes remains unclear. It is possible that HsfA7 and HsfA2 have an essential role in the transcriptional induction of HsfB1.

The abundance of endogenous HsfA2 and HsfA7 is regulated in a temperature-dependent manner (Fig. 3A, Fig. 12B) It is therefore likely that upon a gradual temperature increase or mild HS exposure prevalently HsfA7 is synthesized and acts as a co-activator, but at the same time regulates the abundance of HsfA1a (and HsfA3 under relevant conditions) by enhancing its turnover. By this, the cell does not activate a strong HSR and ensures a moderate activity of HsfA1a. If temperatures rise further HsfA2 is produced, which competes for interaction with HsfA1a, stabilizes the master regulator and stimulates a stronger HSR. This hypothesis is supported by thermotolerance assessment of mutant seedlings. Seedlings with an HsfA7 KO background had an increased thermotolerance compared to WT or HsfA2 KO seedlings as shown by hypocotyl growth elongation under a prolonged mild stress treatment (35°C) (Fig. 22). The fact that seedlings that do not produce HsfA7 have an improved performance in contrast to the WT is likely related to stabilization of HsfA1a.

HsfA7 seems to be important for modulation of stress response at moderate temperatures while HsfA2 does not play a crucial role at these conditions because it is not expressed or expressed in very low amounts. Ectopic overexpression of HsfA2 enhanced BTT at 42 and 45°C in transgenic seedlings compared to WT seedlings while at the same time HsfA2 knock-down seedlings did not show impaired growth (Fragkostefanakis et al., 2016). It would be interesting to see whether HsfA2 overexpression could also enhance tolerance to 35°C. Tomato HsfA2 has also been shown to be involved in short-term ATT after a 37.5°C pre-treatment. As mentioned previously, initial attempts were made to understand whether HsfA7 is involved in ATT which did not affect the seedlings in a positive or negative manner. Further experiments with various HS regimes are necessary in order to dissect the involvement of HsfA7 in the response to different temperatures, stress durations, as well as during recurrent stress situations.

In the end, when investigating functions of Hsfs, the contribution of one single factor is represented not only in its own function, but also in the interplay with and influence on other factors in the HS network. In here, we show how two highly homologous Hsfs can act as co-activators and differentially influence the degradation of the master regulator HsfA1a. This mechanism is likely to be important for moderation of the HSR during constantly changing temperatures.

8 Conclusion and outlook

The results of this study allow the generation of a new working hypothesis regarding the regulation of temperature- and Hsf-dependent gene networks (Fig. 23). In response to moderately elevated temperatures (30-35°C) the activation of HsfA1a leads to transcription of HsfA7. HsfA7 pre-mRNA is alternatively spliced and the mature transcripts encode for three protein isoforms (HsfA7-I, HsfA7-II and HsfA7-III) with differential properties regarding localization and stability. HsfA7 can form hetero-oligomeric complexes with the master regulator of HSR, HsfA1a, to activate downstream genes in a stronger manner. Concomitantly, this interaction leads to the increased turnover of HsfA1a, thereby ensuring the moderate transcriptional activation of target genes under mild heat stress conditions. At further increasing temperatures, HsfA2 strongly accumulates and becomes dominant in stressed cells. Its activity is controlled by either interaction with HsfA1a to form transcriptional active and stable "superactivator" complexes leading to even stronger stimulation of transcription of HS-related genes, or with sHsps to be kept inactive and recruited into cytoplasmic HSGs. In contrast to HsfA7, HsfA2 allows the stabilization of HsfA1a probably by prohibiting its ubiquitination. Molecular details of the differential influence of HsfA7 and HsfA2 on the regulation of HsfA1a turnover need to be further examined.

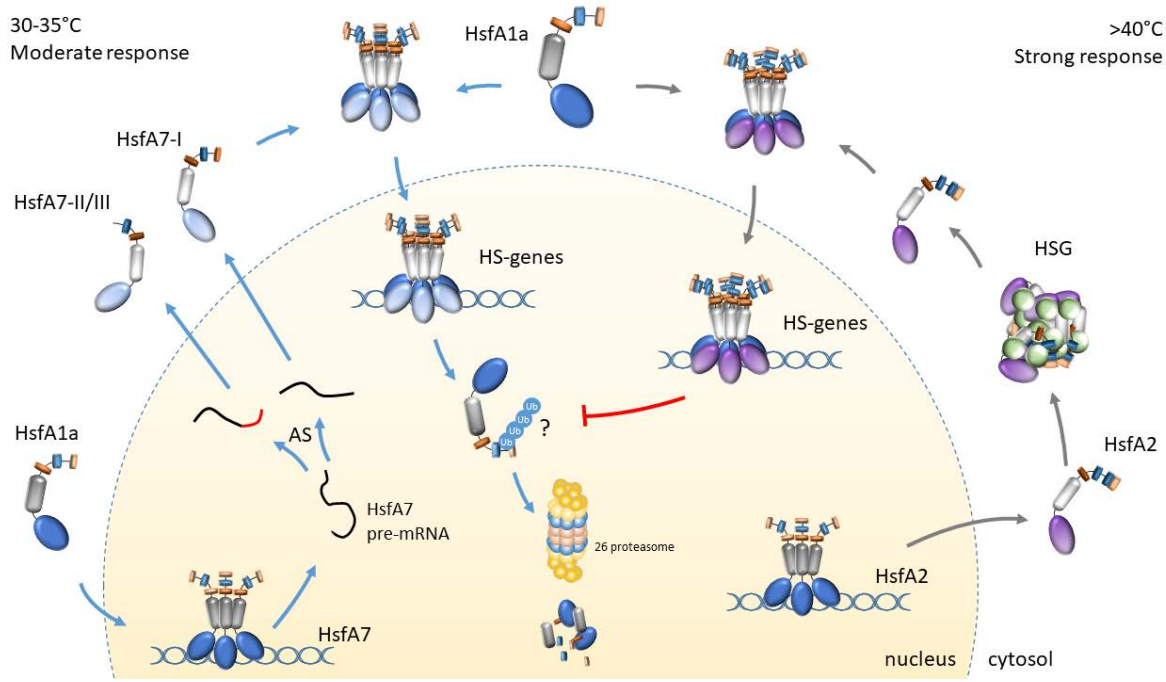

Figure 23. Working hypothesis of the regulation of cellular responses under elevated temperatures.
Under mildly elevated temperatures (30-35°C, left) HsfA7 is induced by the activity of HsfA1a. Alternative splicing leads to the generation of three protein isoforms: HsfA7-I comprising an NES, and HsfA7-II and III not. The HsfA7 isoforms are able to interact with HsfA1a, form putative hetero-oligomeric hexamers that increase the nuclear retention of the complex and transcriptional activation of stress-induced genes. Through a yet to be identified mechanism, the interaction of HsfA7 with HsfA1a enhances the degradation of the latter by the 26S proteasome in the nucleus, thereby weakening the strength of the response. In turn, under temperatures higher than 40°C, HsfA2 becomes more abundant which leads to the preferential formation of HsfA1a-HsfA2 complexes with synergistic activity. In contrast to the HsfA7 effect, interaction of HsfA2 with HsfA1a leads to

the stabilization of the latter leading to stronger induction of HS-genes as required for enhancing thermotolerance.

Genetic engineering based on transcription factors has the potential to improve crop tolerance in the safest way without affecting the yield under non-stress conditions (Century et al., 2008). Although some Hsfs have been extensively studied and details on their molecular mode in stress response have been elucidated, this has been limited only to a few members of the family; thereby the contribution of others in the dynamic nature of the regulation of temperature-responses is still largely elusive. In here, insights into the function of HsfA7 are given and a new mechanism for controlling the activity of Hsf-dependent gene regulatory networks has been unravelled. Whether other Hsfs contribute in a similar or different manner to temperature responses has yet to be studied. In this direction, HsfA6 proteins which also belong to the same phylogenetic clade as HsfA2 and HsfA7 could also be part of this mechanism.

Nevertheless, future experiments should focus on the molecular details of the HsfA7 and HsfA2 interplay with HsfA1a but also with other Hsfs. For example, investigating how HsfA7 triggers degradation of HsfA1a and analysing the timing and regulation of this process is important to understand this type of interaction partner behaviour which could be similar for other Hsfs or transcription factors. Thus, the role of ubiquitination, ubiquitin ligases and other proteasomal components in Hsf-mediated transcription is an important area of future studies.

To fully understand the genes affected by loss of HsfA7 or HsfA2, transcriptome and proteome analyses of the mutant plants would be beneficial. In addition to Hsps, it would be interesting to know which genes related to other cellular processes are directly or indirectly affected in the mutant plants. ChIP-seq experiments will allow the identification of specific targets, for each Hsf and its isoforms in response to elevated temperatures.

Furthermore, since HsfA7 and HsfA2 might be redundant in their co-activator function, crossing the mutant plants and generation of double knock-out mutants will give more insights into their functional interplay. HsfA2 is so far the only known developmentally regulated Hsf in pollen. It is not known whether HsfA7 undergoes a similar regulation and whether it is involved in protection of the male gametophyte as proposed by Fragkostefanakis et al. (2016). If so, the impact of HsfA2 and HsfA7 double KO on male gametophyte development and thermotolerance should be investigated.

In addition, it would be interesting to understand to what extent HsfA7 shares similar properties among different species, e.g. similarities and differences between tomato HsfA7 and *A. thaliana* HsfA7a/b proteins. Interestingly, several species like *A. thaliana* have two or more HsfA7 paralogues. Understanding the evolutionary advantage gained by such an expansion in the context of a large gene family will offer better insights into temperature responses, adaptation and thermotolerance of plants.

This work shows that knockout of HsfA7 leads to enhanced hypocotyl growth. Whether this is beneficial for the plant remains to be examined in the context of various biological processes including reproduction, yield and other traits important for agronomic purposes. If mutating

HsfA7 improves thermotolerance in general, similar approaches adopted here for research purposes could be used for breeding and improvement of thermosensitive germplasm on the basis of the status of the legal framework. Alternatively, in a more conventional manner, identification of HsfA7 haplotypes with reduced activity in tomato germplasm could be useful tools for breeders as exotic genes with distinct properties from wild crop ancestors are a valuable genetic pool for crop improvement.

9 References

Abdul-baki AA (1992) Determination of Pollen Viability in Tomatoes. J Amer Soc Hort Sci **117**: 473–476

Agarwal M, Katiyar-Agarwal S, Sahi C, Gallie DR, Grover A (2001) Arabidopsis thaliana Hsp100 proteins: kith and kin. Cell Stress Chaperones **6**: 219–224

Ahmed FE, Hall AE, DeMason DA (1992) Heat Injury During Floral Development in Cowpea (Vigna unguiculata, Fabaceae). Am J Bot **79**: 784

Akerfelt M, Henriksson E, Laiho A, Vihervaara A, Rautoma K, Kotaja N, Sistonen L (2008) Promoter ChIP-chip analysis in mouse testis reveals Y chromosome occupancy by HSF2. Proc Natl Acad Sci **105**: 11224–11229

Åkerfelt M, Morimoto RI, Sistonen L (2010) Heat shock factors: Integrators of cell stress, development and lifespan. Nat Rev Mol Cell Biol **11**: 545–555

Alastalo T-P, Hellesuo M, Sandqvist A, Hietakangas V, Kallio M, Sistonen L (2003) Formation of nuclear stress granules involves HSF2 and coincides with the nucleolar localization of Hsp70. J Cell Sci **116**: 3557–70

Almoguera C, Prieto-Dapena P, Díaz-Martín J, Espinosa JM, Carranco R, Jordano J (2009) The HaDREB2 transcription factor enhances basal thermotolerance and longevity of seeds through functional interaction with HaHSFA9. BMC Plant Biol **9**: 75

Almoguera C, Rojas A, Díaz-Martín J, Prieto-Dapena P, Carranco R, Jordano J (2002) A Seed-specific Heat-shock Transcription Factor Involved in Developmental Regulation during Embryogenesis in Sunflower. J Biol Chem **277**: 43866–43872

Aviezer-Hagai K, Skovorodnikova J, Galigniana M, Farchi-Pisanty O, Maayan E, Bocovza S, Efrat Y, von Koskull-Döring P, Ohad N, Breiman A (2007) Arabidopsis immunophilins ROF1 (AtFKBP62) and ROF2 (AtFKBP65) exhibit tissue specificity, are heat-stress induced, and bind HSP90. Plant Mol Biol **63**: 237–255

Avramova Z (2015) Transcriptional "memory" of a stress: transient chromatin and memory (epigenetic) marks at stress-response genes. Plant J **83**: 149–159

Baniwal SK, Bharti K, Chan KY, Fauth M, Ganguli A, Kotak S, Mishra SK, Nover L, Port M, Scharf KD, et al (2004) Heat stress response in plants: a complex game with chaperones and more than twenty heat stress transcription factors. J Biosci **29**: 471–87

Baniwal SK, Kwan YC, Scharf KD, Nover L (2007) Role of heat stress transcription factor HsfA5 as specific repressor of HsfA4. J Biol Chem **282**: 3605–3613

Basha E, O'Neill H, Vierling E (2012) Small heat shock proteins and α-crystallins: dynamic proteins with flexible functions. Trends Biochem Sci **37**: 106–117

Bhadula SK, Elthon TE, Habben JE, Helentjaris TG, Jiao S, Ristic Z (2001) Heat-stress induced synthesis of chloroplast protein synthesis elongation factor (EF-Tu) in a heat-tolerant maize line. Planta **212**: 359–366

Bharti K (2004) Tomato Heat Stress Transcription Factor HsfB1 Represents a Novel Type of General Transcription Coactivator with a Histone-Like Motif Interacting with the Plant CREB Binding

Protein Ortholog HAC1. Plant Cell Online **16**: 1521–1535

Bharti K, Schmidt E, Lyck R, Heerkoltz D, Bublak D, Scharf K-D (2000) Isolation and characterization of HsfA3, a new heat stress transcription factor of *Lycopersicon peruvianum*. Plant J **22**: 355–366

Biamonti G, Vourc'h C (2010) Nuclear stress bodies. Cold Spring Harb Perspect Biol **2**: a000695

Bita CE, Gerats T (2013) Plant tolerance to high temperature in a changing environment: scientific fundamentals and production of heat stress-tolerant crops. Front Plant Sci **4**: 1–18

Blanvillain R, Young B, Cai Y, Hecht V, Varoquaux F, Delorme V, Lancelin J-M, Delseny M, Gallois P (2011) The Arabidopsis peptide kiss of death is an inducer of programmed cell death. EMBO J **30**: 1173–1183

Bokszczanin K (2013) Perspectives on deciphering mechanisms underlying plant heat stress response and thermotolerance. Front Plant Sci **4**: 1–20

Boothby TC, Zipper RS, van der Weele CM, Wolniak SM (2013) Removal of Retained Introns Regulates Translation in the Rapidly Developing Gametophyte of Marsilea vestita. Dev Cell **24**: 517–529

Borg M, Brownfield L, Twell D (2009) Male gametophyte development: a molecular perspective. J Exp Bot **60**: 1465–78

Boscheinen O, Lyck R, Queitsch C, Treuter E, Zimarino V, Scharf KD (1997) Heat stress transcription factors from tomato can functionally replace HSF1 in the yeast Saccharomyces cerevisiae. Mol Gen Genet **255**: 322–31

Boyko A, Kovalchuk I (2011) Genome instability and epigenetic modification—heritable responses to environmental stress? Curr Opin Plant Biol **14**: 260–266

Braunschweig U, Gueroussov S, Plocik AM, Graveley BR, Blencowe BJ (2013) Dynamic Integration of Splicing within Gene Regulatory Pathways. Cell **152**: 1252–1269

Brzezinka K, Altmann S, Czesnick H, Nicolas P, Gorka M, Benke E, Kabelitz T, Jähne F, Graf A, Kappel C, et al (2016) Arabidopsis FORGETTER1 mediates stress-induced chromatin memory through nucleosome remodeling. Elife **5**: 1–23

Busch W, Wunderlich M, Schöffl F (2005) Identification of novel heat shock factor-dependent genes and biochemical pathways in Arabidopsis thaliana. Plant J **41**: 1–14

Camejo D, Jiménez A, Alarcón JJ, Torres W, Gómez JM, Sevilla F (2006) Changes in photosynthetic parameters and antioxidant activities following heat-shock treatment in tomato plants. Funct Plant Biol **33**: 177

Carranco R, Espinosa JM, Prieto-Dapena P, Almoguera C, Jordano J (2010) Repression by an auxin/indole acetic acid protein connects auxin signaling with heat shock factor-mediated seed longevity. Proc Natl Acad Sci **107**: 21908–21913

Caverzan A, Passaia G, Rosa SB, Ribeiro CW, Lazzarotto F, Margis-Pinheiro M (2012) Plant responses to stresses: role of ascorbate peroxidase in the antioxidant protection. Genet Mol Biol **35**: 1011–1019

Century K, Reuber TL, Ratcliffe OJ (2008) Regulating the Regulators: The Future Prospects for Transcription-Factor-Based Agricultural Biotechnology Products. Plant Physiol **147**: 20–29

Chan-Schaminet KY, Baniwal SK, Bublak D, Nover L, Scharf KD (2009) Specific interaction between tomato HsfA1 and HsfA2 creates hetero-oligomeric superactivator complexes for synergistic activation of heat stress gene expression. J Biol Chem **284**: 20848–20857

Chang CC, Huang PS, Lin HR, Lu CH (2007) Transactivation of protein expression by rice HSP101 in planta and using Hsp101 as a selection marker for transformation. Plant Cell Physiol **48**: 1098–1107

Charng Y-y. (2006) Arabidopsis Hsa32, a Novel Heat Shock Protein, Is Essential for Acquired Thermotolerance during Long Recovery after Acclimation. Plant Physiol **140**: 1297–1305

Charng Y-y., Liu H-c., Liu N-y., Chi W-t., Wang C-n., Chang S-h., Wang T-t. (2006) A Heat-Inducible Transcription Factor, HsfA2, Is Required for Extension of Acquired Thermotolerance in Arabidopsis. Plant Physiol **143**: 251–262

Chaturvedi P, Ischebeck T, Egelhofer V, Lichtscheidl I, Weckwerth W (2013) Cell-specific Analysis of the Tomato Pollen Proteome from Pollen Mother Cell to Mature Pollen Provides Evidence for Developmental Priming. J Proteome Res **12**: 4892–4903

Che P (2006) Gene Expression Programs during Shoot, Root, and Callus Development in Arabidopsis Tissue Culture. Plant Physiol **141**: 620–637

Che P, Gingerich DJ, Lall S, Howell SH (2002) Global and hormone-induced gene expression changes during shoot development in Arabidopsis. Plant Cell **14**: 2771–85

Chen WR, Zheng JS, Li YQ, Guo WD (2012) Effects of high temperature on photosynthesis, chlorophyll fluorescence, chloroplast ultrastructure, and antioxidant activities in fingered citron. Russ J Plant Physiol **59**: 732–740

Cheng MY, Hartl F-U, Martin J, Pollock RA, Kalousek F, Neuper W, Hallberg EM, Hallberg RL, Horwich AL (1989) Mitochondrial heat-shock protein hsp60 is essential for assembly of proteins imported into yeast mitochondria. Nature **337**: 620–625

Cheng Q, Zhou Y, Liu Z, Zhang L, Song G, Guo Z, Wang W, Qu X, Zhu Y, Yang D (2015) An alternatively spliced heat shock transcription factor, OsHSFA2dI , functions in the heat stress-induced unfolded protein response in rice. Plant Biol **17**: 419–429

Ciechanover A (1998) The ubiquitin-proteasome pathway: on protein death and cell life. EMBO J **17**: 7151–7160

Cohen-Peer R, Schuster S, Meiri D, Breiman A, Avni A (2010) Sumoylation of Arabidopsis heat shock factor A2 (HsfA2) modifies its activity during acquired thermotholerance. Plant Mol Biol **74**: 33–45

Cortijo S, Charoensawan V, Brestovitsky A, Buning R, Ravarani C, Rhodes D, van Noort J, Jaeger KE, Wigge PA (2017) Transcriptional Regulation of the Ambient Temperature Response by H2A.Z Nucleosomes and HSF1 Transcription Factors in Arabidopsis. Mol Plant **10**: 1258–1273

Crisp PA, Ganguly D, Eichten SR, Borevitz JO, Pogson BJ (2016) Reconsidering plant memory: Intersections between stress recovery, RNA turnover, and epigenetics. Sci Adv **2**: e1501340–e1501340

Czarnecka-Verner E, Pan S, Salem T, Gurley WB (2004) Plant class B HSFs inhibit transcription and exhibit affinity for TFIIB and TBP. Plant Mol Biol **56**: 57–75

Dagert M, Ehrlich SD (1979) Prolonged incubation in calcium chloride improves the competence of Escherichia coli cells. Gene **6**: 23–28

Dai S, Li L, Chen T, Chong K, Xue Y, Wang T (2006) Proteomic analyses of Oryza sativa mature pollen reveal novel proteins associated with pollen germination and tube growth. Proteomics **6**: 2504–29

Davletova S (2005) Cytosolic Ascorbate Peroxidase 1 Is a Central Component of the Reactive Oxygen Gene Network of Arabidopsis. Plant Cell Online **17**: 268–281

Diaz-Martin J (2005) Functional Interaction between Two Transcription Factors Involved in the Developmental Regulation of a Small Heat Stress Protein Gene Promoter. Plant Physiol **139**: 1483–1494

Döring P, Treuter E, Kistner C, Lyck R, Chen A, Nover L (2000) The role of AHA motifs in the activator function of tomato heat stress transcription factors HsfA1 and HsfA2. Plant Cell **12**: 265–78

Driedonks N, Xu J, Peters JL, Park S, Rieu I (2015) Multi-Level Interactions Between Heat Shock Factors, Heat Shock Proteins, and the Redox System Regulate Acclimation to Heat. Front Plant Sci **9**: 244-252

Duck NB, Folk WR (1994) Hsp70 heat shock protein cognate is expressed and stored in developing tomato pollen. Plant Mol Biol **26**: 1031–1039

Engler C, Gruetzner R, Kandzia R, Marillonnet S (2009) Golden gate shuffling: A one-pot DNA shuffling method based on type ils restriction enzymes. PLoS One **4**: e5553

Engler C, Youles M, Gruetzner R, Ehnert TM, Werner S, Jones JDG, Patron NJ, Marillonnet S (2014) A Golden Gate modular cloning toolbox for plants. ACS Synth Biol **3**: 839–843

Erkina TY, Tschetter PA, Erkine AM (2008) Different Requirements of the SWI/SNF Complex for Robust Nucleosome Displacement at Promoters of Heat Shock Factor and Msn2- and Msn4-Regulated Heat Shock Genes. Mol Cell Biol **28**: 1207–1217

Evrard A, Kumar M, Lecourieux D, Lucks J, von Koskull-Döring P, Hirt H (2013) Regulation of the heat stress response in *Arabidopsis* by MPK6-targeted phosphorylation of the heat stress factor HsfA2. PeerJ **1**: e59

Eyles SJ, Gierasch LM (2010) Nature's molecular sponges: Small heat shock proteins grow into their chaperone roles. Proc Natl Acad Sci U S A **107**: 2727–2728

Fang S, Jensen JP, Ludwig RL, Vousden KH, Weissman AM (2000) Mdm2 Is a RING Finger-dependent Ubiquitin Protein Ligase for Itself and p53. J Biol Chem **275**: 8945–8951

Feder ME, Cartaño N V, Milos L, Krebs RA, Lindquist SL (1996) Effect of engineering Hsp70 copy number on Hsp70 expression and tolerance of ecologically relevant heat shock in larvae and pupae of Drosophila melanogaster. J Exp Biol **199**: 1837–44

Ferreira S, Hjernø K, Larsen M, Wingsle G, Larsen P, Fey S, Roepstorff P, Salomé Pais M (2006) Proteome profiling of Populus euphratica Oliv. upon heat stress. Ann Bot **98**: 361–77

Filichkin S, Priest HD, Megraw M, Mockler TC (2015) Alternative splicing in plants: directing traffic at the crossroads of adaptation and environmental stress. Curr Opin Plant Biol **24**: 125–135

Filtz TM, Vogel WK, Leid M (2014) Regulation of transcription factor activity by interconnected post-translational modifications. Trends Pharmacol Sci **35**: 76–85

Fragkostefanakis S, Mesihovic A, Simm S, Paupière MJ, Hu Y, Paul P, Mishra SK, Tschiersch B, Theres K, Bovy A, et al (2016) HsfA2 Controls the Activity of Developmentally and Stress-Regulated Heat Stress Protection Mechanisms in Tomato Male Reproductive Tissues. Plant Physiol **170**: 2461–2477

Fragkostefanakis S, Röth S, Schleiff E, Scharf KD (2015a) Prospects of engineering thermotolerance in crops through modulation of heat stress transcription factor and heat shock protein networks. Plant, Cell Environ **38**: 1881–1895

Fragkostefanakis S, Simm S, Paul P, Bublak D, Scharf KD, Schleiff E (2015b) Chaperone network composition in Solanum lycopersicum explored by transcriptome profiling and microarray meta-analysis. Plant, Cell Environ **38**: 693–709

Frank G, Pressman E, Ophir R, Althan L, Shaked R, Freedman M, Shen S, Firon N (2009) Transcriptional profiling of maturing tomato (Solanum lycopersicum L.) microspores reveals the involvement of heat shock proteins, ROS scavengers, hormones, and sugars in the heat stress response. J Exp Bot **60**: 3891–908

Fujimoto M, Izu H, Seki K, Fukuda K, Nishida T, Yamada S, Kato K, Yonemura S, Inouye S, Nakai A (2004) HSF4 is required for normal cell growth and differentiation during mouse lens development. EMBO J **23**: 4297–4306

Fujimoto M, Takii R, Takaki E, Katiyar A, Nakato R, Shirahige K, Nakai A (2017) The HSF1–PARP13–PARP1 complex facilitates DNA repair and promotes mammary tumorigenesis. Nat Commun **8**: 1638

Gallagher SR (1992) Quantitation of GUS activity by fluorometry. GUS Protocols: using GUS gene as a reporter of gene expression 47–59

Gerland P, Raftery AE, ev ikova H, Li N, Gu D, Spoorenberg T, Alkema L, Fosdick BK, Chunn J, Lalic N, et al (2014) World population stabilization unlikely this century. Science (80-) **346**: 234–237

Gidalevitz T, Prahlad V, Morimoto RI (2011) The Stress of Protein Misfolding: From Single Cells to Multicellular Organisms. Cold Spring Harb Perspect Biol **3**: a009704–a009704

Giese KC, Vierling E (2002) Changes in Oligomerization Are Essential for the Chaperone Activity of a Small Heat Shock Protein in Vivo and in Vitro. J Biol Chem **277**: 46310–46318

Giorno F, Wolters-Arts M, Grillo S, Scharf KD, Vriezen WH, Mariani C (2010) Developmental and heat stress-regulated expression of HsfA2 and small heat shock proteins in tomato anthers. J Exp Bot **61**: 453–462

Goodson ML, Park-Sarge OK, Sarge KD (1995) Tissue-dependent expression of heat shock factor 2 isoforms with distinct transcriptional activities. Mol Cell Biol **15**: 5288–5293

Gragerov AI, Martin ES, Krupenko MA, Kashlev M V, Nikiforov VG (1991) Protein aggregation and inclusion body formation in Escherichia coli rpoH mutant defective in heat shock protein induction. FEBS Lett **291**: 222–4

Gray SB, Brady SM (2016) Plant developmental responses to climate change. Dev Biol **419**: 64–77

Grönroos E, Hellman U, Heldin C-H, Ericsson J (2002) Control of Smad7 stability by competition between acetylation and ubiquitination. Mol Cell **10**: 483–93

Grossman SR, Perez M, Kung AL, Joseph M, Mansur C, Xiao Z-X, Kumar S, Howley PM, Livingston

DM (1998) p300/MDM2 Complexes Participate in MDM2-Mediated p53 Degradation. Mol Cell **2**: 405–415

Guertin MJ, Lis JT (2010) Chromatin Landscape Dictates HSF Binding to Target DNA Elements. PLoS Genet **6**: e1001114

Guo L, Chen S, Liu K, Liu Y, Ni L, Zhang K, Zhang L (2008) Isolation of Heat Shock Factor HsfA1a-Binding Sites in vivo Revealed Variations of Heat Shock Elements in Arabidopsis thaliana. Plant Cell Physiol **49**: 1306–1315

Guo SJ, Zhou HY, Zhang XS, Li XG, Meng QW (2007) Overexpression of CaHSP26 in transgenic tobacco alleviates photoinhibition of PSII and PSI during chilling stress under low irradiance. J Plant Physiol **164**: 126–136

Gutsche I, Essen L-O, Baumeister W (1999) Group II chaperonins: new TRiC(k)s and turns of a protein folding machine. J Mol Biol **293**: 295–312

Hahn A, Bublak D, Schleiff E, Scharf KD (2011) Crosstalk between Hsp90 and Hsp70 Chaperones and Heat Stress Transcription Factors in Tomato. Plant Cell **23**: 741–755

Hansson MD, Rzeznicka K, Rosenbäck M, Hansson M, Sirijovski N (2008) PCR-mediated deletion of plasmid DNA. Anal Biochem **375**: 373–375

Harrison CJ, Bohm AA, Nelson HCM (1994) Crystal structure of the DNA binding domain of the heat shock transcription factor. Sci Pap Ed Guid to Sci Inf **263**: 224–226

Hasanuzzaman M, Nahar K, Alam M, Roychowdhury R, Fujita M (2013) Physiological, Biochemical, and Molecular Mechanisms of Heat Stress Tolerance in Plants. Int J Mol Sci **14**: 9643–9684

Hatfield JL, Boote KJ, Kimball BA, Ziska LH, Al E (2011) Climate impacts on agriculture: implications for crop production. AgronJ **103**: 351-370

Hatfield JL, Prueger JH (2015) Temperature extremes: Effect on plant growth and development. Weather Clim Extrem **10**: 4–10

He Z, Xie R, Zou H, Wang Y, Zhu J, Yu G (2007) Structure and alternative splicing of a heat shock transcription factor gene, MsHSF1, in Medicago sativa. Biochem Biophys Res Commun **364**: 1056–1061

He Z, Zou H, Wang Y, Zhu J, Yu G (2008) Maturation of the nodule-specific transcript MsHSF1c in Medicago sativa may involve interallelic trans-splicing. Genomics **92**: 115–121

Hedhly A (2011) Sensitivity of flowering plant gametophytes to temperature fluctuations. Environ Exp Bot **74**: 9–16

Heerklotz D, Döring P, Bonzelius F, Winkelhaus S, Do P (2001) The Balance of Nuclear Import and Export Determines the Intracellular Distribution and Function of Tomato Heat Stress Transcription Factor HsfA2 The Balance of Nuclear Import and Export Determines the Intracellular Distribution and Function of Tomato Heat. Mol Cell Biol **21**: 1759–1768

Hemmingsen SM, Woolford C, van der Vies SM, Tilly K, Dennis DT, Georgopoulos CP, Hendrix RW, Ellis RJ (1988) Homologous plant and bacterial proteins chaperone oligomeric protein assembly. Nature **333**: 330–334

Holmberg CI (2001) Phosphorylation of serine 230 promotes inducible transcriptional activity of heat shock factor 1. EMBO J **20**: 3800–3810

Honys D, Re D, Twell D (2006) Male Gametophyte Development and Function. Floriculture, ornamental and plant biotechnology: advances and topical issues **1**: 76-87.

Houseley J, Tollervey D (2009) The Many Pathways of RNA Degradation. Cell **136**: 763–776

Hsu PD, Lander ES, Zhang F (2014) Development and Applications of CRISPR-Cas9 for Genome Engineering. Cell **157**: 1262–1278

Hu CD, Chinenov Y, Kerppola TK (2002) Visualization of interactions among bZIP and Rel family proteins in living cells using bimolecular fluorescence complementation. Mol Cell **9**: 789–98

Hu Y (2017) Alternative splicing of HsfA2 mediates thermotolerance in tomato species. PhD thesis, Johann Wolfgang Goethe–Universität, Frankfurt am Main

Huang YC, Niu CY, Yang CR, Jinn TL (2016) The heat-stress factor HSFA6b connects ABA signaling and ABA-mediated heat responses. Plant Physiol **172**: 1182-1199

Ikeda M, Mitsuda N, Ohme-Takagi M (2011) Arabidopsis HsfB1 and HsfB2b Act as Repressors of the Expression of Heat-Inducible Hsfs But Positively Regulate the Acquired Thermotolerance. Plant Physiol **157**: 1243–1254

Ikeda M, Ohme-Takagi M (2009) A Novel Group of Transcriptional Repressors in Arabidopsis. Plant Cell Physiol **50**: 970–975

IPCC (2014) Climate Change 2014: Impacts, Adaptation, and Vulnerability. Summaries, Frequently Asked Questions, and Cross-Chapter Boxes. A Contribution of Working Group II to the Fifth Assessment Report of the Intergovernmental Panel on Climate Change. Cambridge University Press

Ishibashi K, Masuda K, Naito S, Meshi T, Ishikawa M (2007) An inhibitor of viral RNA replication is encoded by a plant resistance gene. Proc Natl Acad Sci **104**: 13833–13838

Iwahori S (1966) High temperature injuries in tomato . Fertilization and development of embryo with special reference to the abnormalities caused by high temperature. J Jpn Soc Hortic Sci. **35**: 55–62

James AB, Syed NH, Bordage S, Marshall J, Nimmo GA, Jenkins GI, Herzyk P, Brown JWS, Nimmo HG (2012) Alternative Splicing Mediates Responses of the Arabidopsis Circadian Clock to Temperature Changes. Plant Cell **24**: 961–981

Jedlicka P, Mortin MA, Wu C (1997) Multiple functions of Drosophila heat shock transcription factor in vivo. EMBO J **16**: 2452–2462

Jefferson RA, Kavanagh TA, Bevan MW (1987) GUS fusions: beta-glucuronidase as a sensitive and versatile gene fusion marker in higher plants. EMBO J **6**: 3901–3907

Jiang C, XU J, Zhang H, Zhang X, Shi J, Li M, Ming F (2009) A cytosolic class I small heat shock protein, RcHSP17.8, of Rosa chinensis confers resistance to a variety of stresses to Escherichia coli , yeast and Arabidopsis thaliana. Plant Cell Environ **32**: 1046–1059

Jolly C, Usson Y, Morimoto RI (1999) Rapid and reversible relocalization of heat shock factor 1 within seconds to nuclear stress granules. Proc Natl Acad Sci **96**: 6769–6774

Kalyna M, Simpson CG, Syed NH, Lewandowska D, Marquez Y, Kusenda B, Marshall J, Fuller J, Cardle L, McNicol J, et al (2012) Alternative splicing and nonsense-mediated decay modulate expression of important regulatory genes in Arabidopsis. Nucleic Acids Res **40**: 2454–69

Kantidze OL, Velichko AK, Razin S V. (2015) Heat stress-induced transcriptional repression. Biochem **80**: 990–993

Karl TR (2009) Global climate change impacts in the United States. Cambridge University Press

Katiyar-Agarwal S, Agarwal M GA (2003) Heat-tolerant basmati rice engineered by over- expression of hsp101. Plant Mol Biol 677–686

Kawasaki F, Koonce NL, Guo L, Fatima S, Qiu C, Moon MT, Zheng Y, Ordway RW (2016) Small heat shock proteins mediate cell-autonomous and -nonautonomous protection in a Drosophila model for environmental-stress-induced degeneration. Dis Model Mech **9**: 953–964

Kazan K (2003) Alternative splicing and proteome diversity in plants: the tip of the iceberg has just emerged. Trends Plant Sci **8**: 468–471

Keller M, Hu Y, Mesihovic A, Fragkostefanakis S, Schleiff E, Simm S (2016) Alternative splicing in tomato pollen in response to heat stress. DNA **24**: 205-217

Kerppola TK (2008) Bimolecular Fluorescence Complementation (BiFC) Analysis as a Probe of Protein Interactions in Living Cells. Annu Rev Biophys **37**: 465–487

Khush GS (2001) Green revolution: the way forward. Nat Rev Genet **2**: 815–822

Kim BH, Schöffl F (2002) Interaction between Arabidopsis heat shock transcription factor 1 and 70 kDa heat shock proteins. J Exp Bot **53**: 371–375

Kim GD, Cho YH, Lee BH, Yoo SD (2017) STABILIZED1 Modulates Pre-mRNA Splicing for Thermotolerance. Plant Physiol **173**: 2370–2382

Kodadek T, Sikder D, Nalley K (2006) Keeping Transcriptional Activators under Control. Cell **127**: 261–264

Kotak S, Larkindale J, Lee U, von Koskull-Döring P, Vierling E, Scharf KD (2007a) Complexity of the heat stress response in plants. Curr Opin Plant Biol **10**: 310–316

Kotak S, Port M, Ganguli A, Bicker F, Von Koskull-Döring P (2004) Characterization of C-terminal domains of Arabidopsis heat stress transcription factors (Hsfs) and identification of a new signature combination of plant class a Hsfs with AHA and NES motifs essential for activator function and intracellular localization. Plant J **39**: 98–112

Kotak S, Vierling E, Baumlein H, Koskull-Doring P v. (2007b) A Novel Transcriptional Cascade Regulating Expression of Heat Stress Proteins during Seed Development of Arabidopsis. PLANT CELL ONLINE **19**: 182–195

Krishna P, Gloor G (2001) The Hsp90 family of proteins in Arabidopsis thaliana. Cell Stress Chaperones **6**: 238–246

Kumar M, Busch W, Birke H, Kemmerling B, Nürnberger T, Schöffl F (2009) Heat Shock Factors HsfB1 and HsfB2b Are Involved in the Regulation of Pdf1.2 Expression and Pathogen Resistance in Arabidopsis. Mol Plant **2**: 152–165

Kumar SV, Wigge PA (2010) H2A.Z-Containing Nucleosomes Mediate the Thermosensory Response in Arabidopsis. Cell **140**: 136–147

Lamke J, Brzezinka K, Altmann S, Baurle I (2016) A hit-and-run heat shock factor governs sustained histone methylation and transcriptional stress memory. EMBO J **35**: 162–175

Lämke J, Bäurle I (2017) Epigenetic and chromatin-based mechanisms in environmental stress adaptation and stress memory in plants. Genome Biol **18**: 124

Laemmli UK (1970) Cleavage of structural proteins during the assembly of the head of bacteriophage T4. Nature **227**: 680–685

Larkindale J, Vierling E (2007) Core Genome Responses Involved in Acclimation to High Temperature. Plant Physiol **146**: 748–761

Laufen T, Mayer MP, Beisel C, Klostermeier D, Mogk A, Reinstein J, Bukau B (1999) Mechanism of regulation of Hsp70 chaperones by DnaJ cochaperones. Proc Natl Acad Sci U S A **96**: 5452–5457

Lee DG, Ahsan N, Lee SH, Kang KY, Bahk JD, Lee IJ, Lee BH (2007) A proteomic approach in analyzing heat-responsive proteins in rice leaves. Proteomics **7**: 3369–3383

Lee DH, Goldberg AL (1998) Proteasome inhibitors: valuable new tools for cell biologists. Trends Cell Biol **8**: 397–403

Lee U, Wie C, Escobar M, Williams B, Hong S, Vierling E (2005) Genetic Analysis Reveals Domain Interactions of Arabidopsis Hsp100 / ClpB and Cooperation with the Small Heat Shock Protein Chaperone System. Plant Cell **17**: 559–571

Li J, Chauve L, Phelps G, Brielmann RM, Morimoto RI (2016) E2F coregulates an essential HSF developmental program that is distinct from the heat-shock response. Genes Dev **30**: 2062–2075

Li J, Labbadia J, Morimoto RI (2017) Rethinking HSF1 in Stress, Development, and Organismal Health. Trends Cell Biol **27**: 895–905

Li Z, Zhang L, Wang A, Xu X, Li J (2013) Ectopic Overexpression of SlHsfA3, a Heat Stress Transcription Factor from Tomato, Confers Increased Thermotolerance and Salt Hypersensitivity in Germination in Transgenic Arabidopsis. PLoS One **8**: e54880

Lin M-y., Chai K-h., Ko S-s., Kuang L-y., Lur HS, Charng Y-y. (2014) A Positive Feedback Loop between HEAT SHOCK PROTEIN101 and HEAT STRESS-ASSOCIATED 32-KD PROTEIN Modulates Long-Term Acquired Thermotolerance Illustrating Diverse Heat Stress Responses in Rice Varieties. Plant Physiol **164**: 2045–2053

Link V, Sinha AK, Vashista P, Hofmann MG, Proels RK, Ehness R, Roitsch T (2002) A heat-activated MAP kinase in tomato: A possible regulator of the heat stress response. FEBS Lett **531**: 179–183

Liu AL, Zou J, Liu CF, Zhou XY, Zhang XW, Luo GY, Chen XB (2013a) Over-expression of OsHsfA7 enhanced salt and drought tolerance in transgenic rice. BMB Rep **46**: 31–6

Liu H-c., Charng Y-y. (2013) Common and Distinct Functions of Arabidopsis Class A1 and A2 Heat Shock Factors in Diverse Abiotic Stress Responses and Development. Plant Physiol **163**: 276–290

Liu HC, Liao HT, Charng YY (2011) The role of class A1 heat shock factors (HSFA1s) in response to heat and other stresses in Arabidopsis. Plant, Cell Environ **34**: 738–751

Liu J, Sun N, Liu M, Liu J, Du B, Wang X, Qi X (2013b) An Autoregulatory Loop Controlling Arabidopsis HsfA2 Expression: Role of Heat Shock-Induced Alternative Splicing. Plant Physiol **162**: 512–521

Liu JG, Qin Q lin, Zhang Z, Peng RH, Xiong A sheng, Chen JM, Yao QH (2009) OsHSF7 gene in rice,

Oryza sativa L., encodes a transcription factor that functions as a high temperature receptive and responsive factor. BMB Rep **42**: 16–21

Livak KJ, Schmittgen TD (2001) Analysis of Relative Gene Expression Data Using Real-Time Quantitative PCR and the 2−ΔΔCT Method. Methods **25**: 402–408

Lobell DB (2014) Climate change adaptation in crop production: Beware of illusions. Glob Food Sec **3**: 72–76

Lobell DB, Schlenker W, Costa-Roberts J (2011) Climate Trends and Global Crop Production Since 1980. Science (80-) **333**: 616–620

Lubben TH, Donaldson GK, Viitanen P V, Gatenby AA (1989) Several proteins imported into chloroplasts form stable complexes with the GroEL-related chloroplast molecular chaperone. Plant Cell **1**: 1223–1230

Lyck R, Harmening U, Hohfeld I, Treuter E, Scharf KD, Nover L (1997) Intracellular distribution and identification of the nuclear localization signals of two plant heat-stress transcription factors. Planta **202**: 117–125

Majoul T, Bancel E, Triboï E, Ben Hamida J, Branlard G (2003) Proteomic analysis of the effect of heat stress on hexaploid wheat grain: Characterization of heat-responsive proteins from total endosperm. Proteomics **3**: 175–183

Le Masson F, Razak Z, Kaigo M, Audouard C, Charry C, Cooke H, Westwood JT, Christians ES (2011) Identification of Heat Shock Factor 1 Molecular and Cellular Targets during Embryonic and Adult Female Meiosis. Mol Cell Biol **31**: 3410–3423

Matsukura S, Mizoi J, Yoshida T, Todaka D, Ito Y, Maruyama K, Shinozaki K, Yamaguchi-Shinozaki K (2010) Comprehensive analysis of rice DREB2-type genes that encode transcription factors involved in the expression of abiotic stress-responsive genes. Mol Genet Genomics **283**: 185–196

Matsushita A, Inoue H, Goto S, Nakayama A, Sugano S, Hayashi N, Takatsuji H (2013) Nuclear ubiquitin proteasome degradation affects WRKY45 function in the rice defense program. Plant J **73**: 302–313

Mccormick S (2004) Control of Male Gametophyte Development. Plant Cell **16**: 142–153

McCormick S (1991) Transformation of tomato with Agrobacterium tumefaciens. Plant Tissue Cult. Man. Springer Netherlands, Dordrecht, pp 311–319

McCormick W, Penman S (1969) Regulation of protein synthesis in HeLa cells: Translation at elevated temperatures. J Mol Biol **39**: 315–333

McLoughlin F, Basha E, Fowler ME, Kim M, Bordowitz J, Katiyar-Agarwal S, Vierling E (2016) Class I and II small heat-shock proteins protect protein translation factors during heat stress. Plant Physiol **172**: 1221-1236

Meehl GA, Stocker TF, Collins WD, Friedlingstein AT, Gaye AT, Gregory JM, Kitoh A, Knutti R, Murphy JM, Noda A (2007) Global climate projections. In: Climate Change 2007: The Physical Science Basis. Contribution of Working Group I to the Fourth Assessment Report of the Intergovernmental Panel on Climate Change. Cambridge University Press

Meiri D, Breiman A (2009) Arabidopsis ROF1 (FKBP62) modulates thermotolerance by interacting

with HSP90.1 and affecting the accumulation of HsfA2-regulated sHSPs. Plant J **59**: 387–399

Meiri D, Tazat K, Cohen-Peer R, Farchi-Pisanty O, Aviezer-Hagai K, Avni A, Breiman A (2009) Involvement of Arabidopsis ROF2 (FKBP65) in thermotolerance. Plant Mol Biol **72**: 191

Merret R, Carpentier M-C, Favory J-J, Picart C, Descombin J, Bousquet-Antonelli C, Tillard P, Lejay L, Deragon J-M, Charng Y (2017) Heat Shock Protein HSP101 Affects the Release of Ribosomal Protein mRNAs for Recovery after Heat Shock. Plant Physiol **174**: 1216–1225

Mesihovic A, Iannacone R, Firon N, Fragkostefanakis S (2016) Heat stress regimes for the investigation of pollen thermotolerance in crop plants. Plant Reprod **29**: 93–105

Metz A (2004) A key role for stress-induced satellite III transcripts in the relocalization of splicing factors into nuclear stress granules. J Cell Sci **117**: 4551–4558

Mirouze M, Paszkowski J (2011) Epigenetic contribution to stress adaptation in plants. Curr Opin Plant Biol **14**: 267–274

Mishra SK, Tripp J, Winkelhaus S, Tschiersch B, Theres K, Nover L, Scharf KD (2002) In the complex family of heat stress transcription factors, HsfA1 has a unique role as master regulator of thermotolerance in tomato. Genes Dev **16**: 1555–1567

Mittler R, Finka A, Goloubinoff P (2012) How do plants feel the heat? Trends Biochem Sci **37**: 118–125

Mittler R, Vanderauwera S, Gollery M, Van Breusegem F (2004) Reactive oxygen gene network of plants. Trends Plant Sci **9**: 490–498

Mogk A, Schlieker C, Friedrich KL, Schönfeld H-J, Vierling E, Bukau B (2003) Refolding of Substrates Bound to Small Hsps Relies on a Disaggregation Reaction Mediated Most Efficiently by ClpB/DnaK. J Biol Chem **278**: 31033–31042

Molinari E, Gilman M, Natesan S (1999) Proteasome-mediated degradation of transcriptional activators correlates with activation domain potency in vivo. EMBO J **18**: 6439–6447

Moore MJ (2005) From Birth to Death: The Complex Lives of Eukaryotic mRNAs. Science (80-) **309**: 1514–1518

Moreno AA, Orellana A (2011) The physiological role of the unfolded protein response in plants. Biol Res **44**: 75–80

Murashige T, Skoog F (1962) A revised medium for rapid growth and bio assays with tobacco tissue cultures. Physiol Plant **15**: 473–497

Murata N, Los DA (1997) Membrane Fluidity and Temperature Perception. Plant Physiol **115**: 875–879

Muratani M, Tansey WP (2003) How the ubiquitin–proteasome system controls transcription. Nat Rev Mol Cell Biol **4**: 192–201

Nakamoto H, Vígh L (2007) The small heat shock proteins and their clients. Cell Mol Life Sci **64**: 294–306

Neta-Sharir I (2005) Dual Role for Tomato Heat Shock Protein 21: Protecting Photosystem II from Oxidative Stress and Promoting Color Changes during Fruit Maturation. Plant Cell Online **17**: 1829–1838

Neudegger T, Verghese J, Hayer-Hartl M, Hartl FU, Bracher A (2016) Structure of human heat-shock transcription factor 1 in complex with DNA. Nat Struct Mol Biol **23**: 140–146

Neueder A, Achilli F, Moussaoui S, Bates GP (2014) Novel isoforms of heat shock transcription factor 1, HSF1γα and HSF1γβ, regulate chaperone protein gene transcription. J Biol Chem **289**: 19894–19906

Nishizawa-Yokoi A, Yoshida E, Yabuta Y, Shigeoka S (2009) Analysis of the Regulation of Target Genes by an Arabidopsis Heat Shock Transcription Factor, HsfA2. Biosci Biotechnol Biochem **73**: 890–895

Nishizawa A, Yabuta Y, Yoshida E, Maruta T, Yoshimura K, Shigeoka S (2006) Arabidopsis heat shock transcription factor A2 as a key regulator in response to several types of environmental stress. Plant J **48**: 535–547

Nollen EA, Brunsting JF, Roelofsen H, Weber LA, Kampinga HH (1999) In vivo chaperone activity of heat shock protein 70 and thermotolerance. Mol Cell Biol **19**: 2069–79

Nover L, Bharti K, Döring P, Mishra SK, Ganguli A, Scharf KD (2001) Arabidopsis and the heat stress transcription factor world: how many heat stress transcription factors do we need? Cell Stress Chaperones **6**: 177–89

Nover L, Scharf KD, Gagliardi D, Vergne P, Czarnecka-Verner E, Gurley WB (1996) The Hsf world: classification and properties of plant heat stress transcription factors. Cell Stress Chaperones **1**: 215–23

Nover L, Scharf KD, Neumann D (1983) Formation of cytoplasmic heat shock granules in tomato cell cultures and leaves. Mol Cell Biol **3**: 1648–55

Nover L, Scharf KD, Neumann D (1989) Cytoplasmic heat shock granules are formed from precursor particles and are associated with a specific set of mRNAs. Mol Cell Biol **9**: 1298–308

Ogawa D, Yamaguchi K, Nishiuchi T (2007) High-level overexpression of the Arabidopsis HsfA2 gene confers not only increased themotolerance but also salt/osmotic stress tolerance and enhanced callus growth. J Exp Bot **58**: 3373–3383

Ohama N, Kusakabe K, Mizoi J, Zhao H, Kidokoro S, Koizumi S, Takahashi F, Ishida T, Yanagisawa S, Shinozaki K, et al (2015) The transcriptional cascade in the heat stress response of Arabidopsis; is strictly regulated at the expression levels of transcription factors. Plant Cell **28**: 181-201

van Oosten-Hawle P, Porter RS, Morimoto RI (2013) Regulation of Organismal Proteostasis by Transcellular Chaperone Signaling. Cell **153**: 1366–1378

Ortiz C, Cardemil L (2001) Heat-shock responses in two leguminous plants: a comparative study. J Exp Bot **52**: 1711–9

Peet MM, Sato S, Gardner RG (1998) Comparing heat stress effects on male-fertile and male-sterile tomatoes. Plant, Cell Environ **21**: 225–231

Peteranderl R, Rabenstein M, Shin YK, Liu CW, Wemmer DE, King DS, Nelson HC (1999) Biochemical and biophysical characterization of the trimerization domain from the heat shock transcription factor. Biochemistry **38**: 3559–69

Pick T, Jaskiewicz M, Peterhansel C, Conrath U (2012) Heat Shock Factor HsfB1 Primes Gene Transcription and Systemic Acquired Resistance in Arabidopsis. Plant Physiol **159**: 52–55

Pirkkala L, Nykanen P, Sistonen L (2001) Roles of the heat shock transcription factors in regulation of the heat shock response and beyond. FASEB J Off Publ Fed Am Soc Exp Biol **15**: 1118–1131

Port M, Tripp J, Zielinski D, Weber C, Heerklotz D, Winkelhaus S, Bublak D, Scharf K-D (2004) Role of Hsp17.4-CII as coregulator and cytoplasmic retention factor of tomato heat stress transcription factor HsfA2. Plant Physiol **135**: 1457–1470

Prasad PVV, Craufurd PQ, Summerfield RJ, Wheeler TR (2000) Effects of short episode of heat stress on flower production and fruit-set of groundnut (Arachis hypogaea L.). J Exp Bot **51**: 777–784

Prieto-Dapena P, Almoguera C, Personat J-M, Merchan F, Jordano J (2017) Seed-specific transcription factor HSFA9 links late embryogenesis and early photomorphogenesis. J Exp Bot **68**: 1097–1108

Prieto-Dapena P, Castano R, Almoguera C, Jordano J (2006) Improved Resistance to Controlled Deterioration in Transgenic Seeds. Plant Physiol **142**: 1102–1112

Qu GQ, Liu X, Zhang YL, Yao D, Ma QM, Yang MY, Zhu WH, Yu S, Luo YB (2009) Evidence for programmed cell death and activation of specific caspase-like enzymes in the tomato fruit heat stress response. Planta **229**: 1269–1279

Queitsch C (2000) Heat Shock Protein 101 Plays a Crucial Role in Thermotolerance in Arabidopsis. Plant Cell Online **12**: 479–492

Rabindran SK, Haroun RI, Clos J, Wisniewski J, Wu C (1993) Regulation of heat shock factor trimer formation: role of a conserved leucine zipper. Science **259**: 230–4

Reddy ASN (2007) Alternative Splicing of Pre-Messenger RNAs in Plants in the Genomic Era. Annu Rev Plant Biol **58**: 267–294

Reddy ASN, Day IS, Göhring J, Barta A (2012) Localization and dynamics of nuclear speckles in plants. Plant Physiol **158**: 67–77

Reddy ASN, Marquez Y, Kalyna M, Barta A (2013) Complexity of the Alternative Splicing Landscape in Plants. Plant Cell **25**: 3657–3683

Rhoads DM, White SJ, Zhou Y, Muralidharan M, Elthon TE (2005) Altered gene expression in plants with constitutive expression of a mitochondrial small heat shock protein suggests the involvement of retrograde regulation in the heat stress response. Physiol Plant **123**: 435–444

Richter K, Haslbeck M, Buchner J (2010) The Heat Shock Response: Life on the Verge of Death. Mol Cell **40**: 253–266

Ristic Z, Wilson K, Nelsen C, Momcilovic I, Kobayashi S, Meeley R, Muszynski M, Habben J (2004) A maize mutant with decreased capacity to accumulate chloroplast protein synthesis elongation factor (EF-Tu) displays reduced tolerance to heat stress. Plant Sci **167**: 1367–1374

Rizhsky L (2002) The Combined Effect of Drought Stress and Heat Shock on Gene Expression in Tobacco. Plant Physiol **130**: 1143–1151

Röth S (2016) Turnover regulation of the heat stress transcription factor HsfB1 in tomato. PhD thesis, Johann Wolfgang Goethe–Universität, Frankfurt am Main

Röth S, Mirus O, Bublak D, Scharf KD, Schleiff E (2017) DNA-binding and repressor function are prerequisites for the turnover of the tomato heat stress transcription factor HsfB1. Plant J **89**: 31–44

Saidi Y, Finka A, Muriset M, Bromberg Z, Weiss YG, Maathuis FJM, Goloubinoff P (2009) The Heat Shock Response in Moss Plants Is Regulated by Specific Calcium-Permeable Channels in the Plasma Membrane. Plant Cell Online **21**: 2829–2843

Saidi Y, Peter M, Finka A, Cicekli C, Vigh L, Goloubinoff P (2010) Membrane lipid composition affects plant heat sensing and modulates Ca^{2+}-dependent heat shock response. Plant Signal Behav **5**: 1530–1533

Sakuma Y (2006) Functional Analysis of an Arabidopsis Transcription Factor, DREB2A, Involved in Drought-Responsive Gene Expression. Plant Cell Online **18**: 1292–1309

Salghetti SE (2001) Regulation of Transcriptional Activation Domain Function by Ubiquitin. Science (80-) **293**: 1651–1653

Sander JD, Joung JK (2014) CRISPR-Cas systems for editing, regulating and targeting genomes. Nat Biotechnol **32**: 347–355

Sandqvist A, Björk JK, Akerfelt M, Chitikova Z, Grichine A, Vourc'h C, Jolly C, Salminen TA, Nymalm Y, Sistonen L (2009) Heterotrimerization of heat-shock factors 1 and 2 provides a transcriptional switch in response to distinct stimuli. Mol Biol Cell **20**: 1340–7

Santoro N, Johansson N, Thiele DJ (1998) Heat Shock Element Architecture Is an Important Determinant in the Temperature and Transactivation Domain Requirements for Heat Shock Transcription Factor. Mol Cell Biol **18**: 6340–6352

Sato S, Peet MM, Thomas JF (2000) Physiological factors limit fruit set of tomato (Lycopersicon esculentum Mill.) under chronic, mild heat stress. Plant, Cell Environ **23**: 719–726

Sato S, Peet MM, Thomas JF (2002) Determining critical pre- and post-anthesis periods and physiological processes in Lycopersicon esculentum Mill. exposed to moderately elevated temperatures. J Exp Bot **53**: 1187–1195

Sato Y, Yokoya S (2008) Enhanced tolerance to drought stress in transgenic rice plants overexpressing a small heat-shock protein, sHSP17.7. Plant Cell Rep **27**: 329–334

Scharf K-D, Berberich T, Ebersberger I, Nover L (2012) The plant heat stress transcription factor (Hsf) family: Structure, function and evolution. Biochim Biophys Acta - Gene Regul Mech **1819**: 104–119

Scharf KD, Heider H, Höhfeld I, Lyck R, Schmidt E, Nover L, Hohfeld I, Lyck R, Schmidt E, Nover L (1998) The tomato Hsf system: HsfA2 needs interaction with HsfA1 for efficient nuclear import and may be localized in cytoplasmic heat stress granules. Mol Cell Biol **18**: 2240–51

Schramm F, Ganguli A, Kiehlmann E, Englich G, Walch D, Von Koskull-Döring P (2006) The heat stress transcription factor HsfA2 serves as a regulatory amplifier of a subset of genes in the heat stress response in Arabidopsis. Plant Mol Biol **60**: 759–772

Schramm F, Larkindale J, Kiehlmann E, Ganguli A, Englich G, Vierling E, Von Koskull-Döring P (2008) A cascade of transcription factor DREB2A and heat stress transcription factor HsfA3 regulates the heat stress response of Arabidopsis. Plant J **53**: 264–274

Seyffer F, Kummer E, Oguchi Y, Winkler J, Kumar M, Zahn R, Sourjik V, Bukau B, Mogk A (2012) Hsp70 proteins bind Hsp100 regulatory M domains to activate AAA+ disaggregase at aggregate surfaces. Nat Struct Mol Biol **19**: 1347–1355

Sharkey TD (2005) Effects of moderate heat stress on photosynthesis: importance of thylakoid reactions, rubisco deactivation, reactive oxygen species, and thermotolerance provided by isoprene. Plant, Cell Environ **28**: 269–277

Shi Y, Mosser DD, Morimoto RI (1998) Molecular chaperones as HSF1-specific transcriptional repressors. Genes Dev **12**: 654–66

Simpson CG, Fuller J, Maronova M, Kalyna M, Davidson D, McNicol J, Barta A, Brown JWS (2007) Monitoring changes in alternative precursor messenger RNA splicing in multiple gene transcripts. Plant J **53**: 1035–1048

Sinha AK, Jaggi M, Raghuram B, Tuteja N (2011) Mitogen-activated protein kinase signaling in plants under abiotic stress. Plant Signal Behav **6**: 196–203

Spoel SH, Mou Z, Tada Y, Spivey NW, Genschik P, Dong X (2009) Proteasome-Mediated Turnover of the Transcription Coactivator NPR1 Plays Dual Roles in Regulating Plant Immunity. Cell **137**: 860–872

Staiger D, Brown JWS (2013) Alternative Splicing at the Intersection of Biological Timing, Development, and Stress Responses. Plant Cell **25**: 3640–3656

Streitner C, Simpson CG, Shaw P, Danisman S, Brown JWS, Staiger D (2013) Small changes in ambient temperature affect alternative splicing in *Arabidopsis thaliana*. Plant Signal Behav **8**: e24638

Sugio A, Dreos R, Aparicio F, Maule AJ (2009) The Cytosolic Protein Response as a Subcomponent of the Wider Heat Shock Response in Arabidopsis. Plant Cell Online **21**: 642–654

Sun W, Bernard C, Van Cotte B De, Van Montagu M, Verbruggen N (2001) At-HSP17.6A, encoding a small heat-shock protein in Arabidopsis, can enhance osmotolerance upon overexpression. Plant J **27**: 407–415

Sundqvist A, Ericsson J (2003) Transcription-dependent degradation controls the stability of the SREBP family of transcription factors. Proc Natl Acad Sci **100**: 13833–13838

Sung DY (2001) Comprehensive Expression Profile Analysis of the Arabidopsis Hsp70 Gene Family. Plant Physiol **126**: 789–800

Sung DY, Guy CL (2003) Physiological and Molecular Assessment of Altered Expression of. Society **132**: 979–987

Suri SS, Dhindsa RS (2008) A heat-activated MAP kinase (HAMK) as a mediator of heat shock response in tobacco cells. Plant, Cell Environ **31**: 218–226

Suzuki N, Bajad S, Shuman J, Shulaev V, Mittler R (2008) The transcriptional co-activator MBF1c is a key regulator of thermotolerance in Arabidopsis thaliana. J Biol Chem **283**: 9269–9275

Tanabe M, Sasai N, Nagata K, Liu XD, Liu PC, Thiele DJ, Nakai A (1999) The mammalian HSF4 gene generates both an activator and a repressor of heat shock genes by alternative splicing. J Biol Chem **274**: 27845–56

Thuerauf DJ, Morrison LE, Hoover H, Glembotski CC (2002) Coordination of ATF6-mediated Transcription and ATF6 Degradation by a Domain That Is Shared with the Viral Transcription Factor, VP16. J Biol Chem **277**: 20734–20739

Tillmann B, Röth S, Bublak D, Sommer M, Stelzer EHK, Scharf K-D, Schleiff E (2015) Hsp90 Is

Involved in the Regulation of Cytosolic Precursor Protein Abundance in Tomato. Mol Plant **8**: 228–241

Töpfer R, Matzeit V, Gronenborn B, Schell J, Steinbiss HH (1987) A set of plant expression vectors for transcriptional and translational fusions. Nucleic Acids Res **15**: 5890

Treuter E, Nover L, Ohme K, Scharf KD (1993) Promoter specificity and deletion analysis of three heat stress transcription factors of tomato. Mol Gen Genet **240**: 113–125

Tripp J, Mishra SK, Scharf KD (2009) Functional dissection of the cytosolic chaperone network in tomato mesophyll protoplasts. Plant, Cell Environ **32**: 123–133

Vanderauwera S, Suzuki N, Miller G, van de Cotte B, Morsa S, Ravanat J-L, Hegie A, Triantaphylides C, Shulaev V, Van Montagu MCE, et al (2011) Extranuclear protection of chromosomal DNA from oxidative stress. Proc Natl Acad Sci **108**: 1711–1716

Vierling E (1991) The Roles of Heat Shock Proteins in Plants. Annu Rev Plant Physiol Plant Mol Biol **42**: 579–620

Wahid A, Close TJ (2007) Expression of dehydrins under heat stress and their relationship with water relations of sugarcane leaves. Biol Plant **51**: 104–109

Wahid A, Gelani S, Ashraf M, Foolad M (2007) Heat tolerance in plants: An overview. Environ Exp Bot **61**: 199–223

Walter P, Ron D (2011) The Unfolded Protein Response: From Stress Pathway to Homeostatic Regulation. Science (80-) **334**: 1081–1086

Wang W, Vinocur B, Shoseyov O, Altman A (2004) Role of plant heat-shock proteins and molecular chaperones in the abiotic stress response. Trends Plant Sci **9**: 244–252

Waters ER, Lee GJ, Vierling E (1996) Evolution, structure and function of the small heat shock proteins in plants. J Exp Bot **47**: 325–338

Weber E, Engler C, Gruetzner R, Werner S, Marillonnet S (2011) A modular cloning system for standardized assembly of multigene constructs. PLoS One**6**: e16765

Westerheide SD, Anckar J, Stevens SM, Sistonen L, Morimoto RI (2009) Stress-Inducible Regulation of Heat Shock Factor 1 by the Deacetylase SIRT1. Science (80-) **323**: 1063–1066

Wiederrecht G, Seto D, Parker CS (1988) Isolation of the gene encoding the S. cerevisiae heat shock transcription factor. Cell **54**: 841–53

Wu C (1995) Heat Shock Transcription Factors: Structure and Regulation. Annu Rev Cell Dev Biol **11**: 441–469

Wu T-y., Juan Y-t., Hsu Y-h., Wu S-h., Liao H-t., Fung RWM, Charng Y-y. (2013) Interplay between Heat Shock Proteins HSP101 and HSA32 Prolongs Heat Acclimation Memory Posttranscriptionally in Arabidopsis. Plant Physiol **161**: 2075–2084

Xu YM, Huang DY, Chiu JF, Lau ATY (2012) Post-Translational Modification of Human Heat Shock Factors and Their Functions: A Recent Update by Proteomic Approach. J Proteome Res **11**: 2625–2634

Xue GP, Drenth J, McIntyre CL (2015) TaHsfA6f is a transcriptional activator that regulates a suite of heat stress protection genes in wheat (Triticum aestivum L.) including previously unknown Hsf

targets. J Exp Bot **66**: 1025–1039

Yamada K, Fukao Y, Hayashi M, Fukazawa M, Suzuki I, Nishimura M (2007) Cytosolic HSP90 Regulates the Heat Shock Response That Is Responsible for Heat Acclimation in Arabidopsis thaliana. J Biol Chem **282**: 37794–37804

Yángüez E, Castro-Sanz AB, Fernández-Bautista N, Oliveros JC, Castellano MM (2013) Analysis of Genome-Wide Changes in the Translatome of Arabidopsis Seedlings Subjected to Heat Stress. PLoS One **8**: e71425

Yoshida T, Ohama N, Nakajima J, Kidokoro S, Mizoi J, Nakashima K, Maruyama K, Kim JM, Seki M, Todaka D, et al (2011) Arabidopsis HsfA1 transcription factors function as the main positive regulators in heat shock-responsive gene expression. Mol Genet Genomics **286**: 321–332

Yuan C-X, Gurley WB (2000) Potential targets for HSF1 within the preinitiation complex. Cell Stress Chaperones **5**: 229

Zhang L, Li Y, Xing D, Gao C (2009) Characterization of mitochondrial dynamics and subcellular localization of ROS reveal that HsfA2 alleviates oxidative damage caused by heat stress in Arabidopsis. J Exp Bot **60**: 2073–2091

Zhang X, Wollenweber B, Jiang D, Liu F, Zhao J (2008) Water deficits and heat shock effects on photosynthesis of a transgenic Arabidopsis thaliana constitutively expressing ABP9, a bZIP transcription factor. J Exp Bot **59**: 839–848

Zhou Y, Chen H, Chu P, Li Y, Tan B, Ding Y, Tsang EWT, Jiang L, Wu K, Huang S (2012) NnHSP17.5, a cytosolic class II small heat shock protein gene from Nelumbo nucifera, contributes to seed germination vigor and seedling thermotolerance in transgenic Arabidopsis. Plant Cell Rep **31**: 379–389

Zhu X, Thalor SK, Takashi Y, Berberich T, Kusano T (2012) An inhibitory effect of the sequence-conserved upstream open-reading frame on the translation of the main open-reading frame of HsfB1 transcripts in Arabidopsis. Plant Cell Environ **35**: 2014–2030

Zinn KE, Tunc-Ozdemir M, Harper JF (2010) Temperature stress and plant sexual reproduction: uncovering the weakest links. J Exp Bot **61**: 1959–68

10 Supplemental data

Supplemental table S1. Primary and secondary antibodies used in this study.

Primary antibody	**Antigen**	**Organism**	**Dilution**	**Reference/Company**
αGFP (mc)	GFP	Mouse	1:5000	Roche
αHA (mc)	HA	Mouse	1:5000	Covance
αactin (mc)	Plant actin	Mouse	1:10000	Sigma
αA1/8HN (pc)	Tomato HsfA1	Rabbit	1:5000	Lyck et al. 1997
αA2/pep6 (pc)	Tomato HsfA2	Rabbit	1:5000	Lyck et al. 1997
αA3 (pc)	Tomato HsfA3	Mouse	1:5000	Bharti et al. 2000
αA7 (pc)	Tomato HsfA7	Rabbit	1:7500	This study
αB1 (pc)	Tomato HsfB1	Rabbit	1:4000	Lyck et al. 1997
α101 (pc)	Plant Hsp101	Rabbit	1:5000	Agrisera
α90 (pc)	Plant Hsp90	Rabbit	1:5000	Agrisera
α70 (pc)	Plant Hsp70	Rabbit	1:10000	Lyck et al. 1997
α17CI (pc)	Tomato Hsp17-CI	Rabbit	1:10000	Port et al. 2004
Secondary antibody				
anti-mouse conjugated to HRP	Mouse IgG heavy chain	Goat	1:10000	Sigma-Aldrich
anti-rabbit conjugated to HRP	Rabbit IgG heavy chain	Goat	1:10000	Sigma-Aldrich

Mc – monoclonal; pc – polyclonal; HRP – Horseradish peroxidase

Supplemental table S2. Plasmid constructs used in this study.

Plasmid construct	**Reference/source**
pRT103 (pRT-Neo)	Töpfer et al., 1987
pRT-HsfA1a	Treuter et al., 1993
pRTdS-GFP-HsfA1a	Heerklotz et al., 2001
pRT-HsfA2	Treuter et al., 1993
pRT-HsfA3(M3) (aa 86-508)	Bharti et al., 2000
PGmhsp17.3B-CI:GUS/PHsp17*-GUS	Treuter et al., 1993
pML94-p21.5ER-AtOEP7-Myc-GFP	Kindly provided by Dr. Sotirios Fragkostefanakis
pML94-pHsfA2-AtOEP7-Myc-GFP	Röth et al., 2017
pRT-Hsp17.4-CII	Port et al., 2004
pRT-mCherry-Hsp17.4-CII	Kindly provided by Dr. Sascha Röth
pRTds-AtEnp1-mCherry	Kindly provided by Dr. Sascha Röth
pML94-GFP-OEP7	Tillmann et al., 2015
pSAT1-cEYFP-C1 1070	TAIR
pSAT1-nEYFP-C1 1074	TAIR

Supplemental table S3. Plasmid constructs generated during this study.

Plasmid name	Template/source	Primer	Primer number and sequence (5' to 3')	Restriction site	Vector
pRT-3HA-HsfA7-I	*S. lycopersicum* cDNA	Fw	7473 - AGTGTCGACAGGTACCATGATGAATCAATTGTATTCTGTTAAAG	SalI	pRT-3HA-HsfA7-II
		Rv	7884 - GGCTCTAGACTAAGGGCTCGAATCC	XbaI	
pRT-3HA-HsfA7-II	*S. lycopersicum* cDNA	Fw	7473	SalI	pRT-3HA-LeHsp70-1
		Rv	7474 - ATATCTAGACTATCCAACGAGTAGCTGGTCG	XbaI	
pRT-3HA-HsfA7-III	pRT3HA-HsfA7-II	Fw	7473	SalI	pRT3HA-HsfA7-II
		Rv	9448 - GGTTCTAGATCATGAATCAACGAGTAGCTGGTCG	XbaI	
pRTdS-GFP-HsfA7-I	*S. lycopersicum* cDNA	Fw	7473	Acc65I	pRTdS-GFP-HsfA7-II
		Rv	7884	XbaI	
pRTdS-GFP-HsfA7-II	*S. lycopersicum* cDNA	Fw	7473	Acc65I	pRT-GFP-LpHsfB1
		Rv	7474	XbaI	
pRTdS-GFP-HsfA7-III	pRT3HA-HsfA7-II	Fw	7473	Acc65I	pRTdsGFP-HsfA6b-II
		Rv	9448	XbaI	
pRT-HsfA7-I	pRT-3HA-HsfA7-I	Fw	9566 - GGCCCATGGATGATGAATCAATTGTATTCTGTTAAAG	NcoI	pRT3HA-HsfA7-I
		Rv	7884	XbaI	
pRT-HsfA7-II	pRT-3HA-HsfA7-II	Fw	9566	NcoI	pRT3HA-HsfA7-I
		Rv	7474	XbaI	
pRT-HsfA7-III	pRTdS-GFP-HsfA7-III	Fw	9566	NcoI	pRT3HA-HsfA7-I
		Rv	9448	XbaI	
pRT-HsfA7-I-mAHA	pRT-3HA-HsfA7-I	Fw	9081- GATAAAGAACTTGATGTGGGCGCCGCCGAAGAGGCAGCGAACA TGAGGACGTGTCTGG	-	-
pRT-HsfA7-II-mAHA	pRT-3HA-HsfA7-II	Fw	9081	-	-
pRT-HsfA7-I-ΔAHA	pRT-3HA-HsfA7-I	Fw	9634 - AAGAACTTGATGAGGACGTGTCTGGAAATGAAGACGG	-	-
		Rv	9635 - GACACGTCCTCATCAAGTTCTTTATCCGTGTTCCC	-	
pRT-HsfA7-II-ΔAHA	pRT-3HA-HsfA7-II	Fw	9634	-	-
		Rv	9635	-	
pRTdS-GFP-HsfA7-I-mNLS	pRTdS-GFP-HsfA7-I	Fw	9417 –GAGAAATTGAAGAGGATATAACCGCAGGAGCTGCAGCACCTAT TGATCCTCAAGGTCCTAGTGCTAC	-	-
pRTdS-GFP-HsfA7-II-mNLS	pRTdS-GFP-HsfA7-II	Fw	9417	-	-

pRTdS-GFP-HsfA7-I-mNES	pRTdS-GFP-HsfA7-I	Fw	7473	Acc65I	pRTdS-GFP-HsfA7-II
		Rv	9409 – GACTCTAGACTAAGGGCTCGAGTCAGCGAACCCGGCCCTCTCT GCCAAG	XbaI	
pRT-HsfA7-I-mNLS	pRTdS-GFP-HsfA7-I-mNLS	-	-	Acc65I/XbaI	pRTdsHsp17.2-CII-mCherry
pRT-HsfA7-II-mNLS	pRTdS-GFP-HsfA7-II-mNLS	-	-	Acc65I/XbaI	pRTdsHsp17.2-CII-mCherry
pRTPHsfA7:HsfA7-I	*S. lycopersicum* gDNA	Fw	10458 - GCCGGTACCCAAGATGATAAACTAAATAACCC	NcoI	pRT-HsfA7-I
		Rv	10459 - CGGCCATGGCTATTAATAGAAAAGAAGAATCAG	Acc65I	
pRTPHsfA7:HsfA7-II	*S. lycopersicum* gDNA	Fw	10458	NcoI	pRT-HsfA7-II
		Rv	10459	Acc65I	
pRTdS-GFP-HsfA3	pRT-HsfA3(M3)	Fw	10195 - CAGGAGCTCAGCGGTACCGAGTGTTTACATGGGATAC	Acc65I	pRTdS-GFP-HsfA7-I
		Rv	10196 - GCCTCTAGACTAGAAACTATCATTCTTG	XbaI	
pSAT1-cEYFP-HsfA1a	pRT-HsfA1a	-	-	XhoI/ XbaI	pSAT1-cYFP-Hsp90
pSAT1-cEYFP-HsfA3	pRT-HsfA3	Fw	10040 - CAGGTCGACGAGTGTTTACATGGGATAC	SalI	pSAT1-cYFP-HsfB1
		Rv	10041 - GGCTCTAGACTAGAAACTATCATTCTTGGGC	XbaI	
pSAT1-NEYFP-HsfA7-I	pRTdS-GFP-HsfA7-I	-	-	Acc65I/XbaI	pSAT1-cYFP-HsfB1
pSAT1-NEYFP-HsfA7-II	pRT-3HA-HsfA7-II	-	-	Acc65I/XbaI	pSAT1-cYFP-HsfB1
pSAT1-NEYFP-HsfA7-I-mNLS	pSAT1-NYFP-HsfA7-I	Fw	9417	-	-
pSAT1-NEYFP-HsfA7-II-mNLS	pSAT1-NYFP-HsfA7-II	Fw	9417	-	-
PHsp21.5-ER:GUS	pML94-p21.5ER-AtOEP7-Myc-GFP	-	-	XhoI/HindIII	PHsp17*-GUS
PHsfA2:GUS	pML94-pHsfA2-AtOEP7-Myc-GFP	-	-	NcoI/HindIII	PHsp17*-GUS

Supplemental table S4. Oligonucleotides used for qRT-PCR.

Amplified gene	Primer	Primer number and sequence (5' to 3')
*Sl*HsfA2	Fw	6576 - GGCGACCATAACTCTATCCTTCCC
	Rv	6577 - GCCTCCTCCACTATTCCAGTATCC
*Sl*HsfA7	Fw	6437 - GCGTGACAAGCAAGTTTTGA
	Rv	6438 - CAAACTCGGGATTTTGCATT
*Sl*Hsp101	Fw	6233 - GTGGCAAGTGTACCATGGAGA
	Rv	6234 - GACTTGCCTCAACTGCTCGT
*Sl*Hsp17.7A-CI	Fw	6263 - ATGGAGAGAAGCAGCGGTAA
	Rv	6264 - ATGTCAATGGCCTTCACCTC
*Sl*APX3	Fw	6259 - CCGCCCTCTAGTCGAGAAAT
	Rv	6260 - AGAACCAGACTGATCTCCAGAGA
*Sl*Hsa32	Fw	6261 - AAGATTGTGGGTCGTCTTGG
	Rv	6262 - CTGAGGCATTCCAGATCCAT

Supplemental table S5. Oligonucleotides used for RT-PCR.

Amplified gene	Primer	Primer number and sequence (5' to 3')
*Sl*HsfA2 (exon2-exon3)	Fw	6026 - AGGCCGGATTCTGTTGTGAC
	Rv	7332 - GAGACCGCCTCAAAGCTTCCTG
*Sl*HsfA7 (exon2-exon5)	Fw	6616 - GACGGCGAAGAGGAAGATGTAG
	Rv	6473 - CCATAAACTTGATCAGGATCTGC
HA-*Sl*HsfA7 (HA-exon1)	Fw	9929 - GGTCTTTTACCCATACGATGTTC
	Rv	7687 - CTTGAACCTGGAAACTCTTC
*Sl*HsfA1a	Fw	6570 - ACAAATGATGTCGTTCCTGGC
	Rv	6571 - GAAAGCTCCCTCAACATTGCC
*Sl*HsfA3	Fw	6443 - GCCAAAGTGCTTCAAAATCCC
	Rv	6444 - TCCACAACTGTATTGAAATCTGGG
*Sl*HsfA7 (exon1)	Fw	9319 - TATCCATGGTGTCCATAAC
	Rv	9320 - TTTAGGAAGTAGTGTAGTCG
*Sl*HsfA2 (promoter-exon1)	Fw	9100 - CTAGACTTCTCCTCTTTCTTCC
	Rv	6091 - TTCCTTGTTGTGCTCCATGA
Cas9	Fw	8794 - CTTCGACCTGGCCGAAGATG
	Rv	8795 - CGTATTTGACCTTGGTGAGC

Erklärung

Ich erkläre hiermit, dass ich mich bisher keiner Doktorprüfung im Mathematisch-Naturwissenschaftlichen Bereich unterzogen habe.

Frankfurt am Main, den …….. ……..

Anida Mesihovic

Versicherung

Ich erkläre hiermit, dass ich die vorgelegte Dissertation über

„**Regulation of the cellular response to elevated temperatures by heat stress transcription factor HsfA7 in *Solanum lycopersicum*"**

Selbständig angefertigt und mich anderer Hilfsmittel als der in ihr angegebenen nicht bedient habe, insbesondere, dass alle Entlehnungen aus anderen Schriften mit Angabe der betreffenden Schrift gekennzeichnet sind.

Ich versichere, die Grundsätze der guten wissenschaftlichen Praxis beachtet, und nicht die Hilfe einer kommerziellen Promotionsvermittlung in Anspruch genommen zu haben.

Frankfurt am Main, den …….. ……..

Anida Mesihovic